ANALYSIS OF THE INTERACTION TRANSCRIPTOME DURING BIOTROPHIC INVASION OF RICE BY THE BLAST FUNGUS, *MAGNAPORTHE ORYZAE*

by

GLORIA MARIA MOSQUERA CIFUENTES

B.S., Universidad Catolica, 1996
M.S., University of Chile, 2001

AN ABSTRACT OF A DISSERTATION

submitted in partial fulfillment of the requirements for the degree

DOCTOR OF PHILOSOPHY

Department of Plant pathology
College of Agriculture

KANSAS STATE UNIVERSITY
Manhattan, Kansas

2007

Abstract

The hemibiotrophic rice blast fungus *Magnaporthe oryzae* undergoes complex morphological development throughout its infection cycle. From 8-20 hours after a fungal spore lands on a leaf surface, the fungus differentiates a complex appressorium that punctures the host cuticle. By ~24 hours post inoculation (hpi), the fungus grows inside an epidermal cell as a primary hypha, and by 36 hpi the fungus has differentiated specialized biotrophic invasive hyphae (IH) that are filling the first-invaded cell and moving into neighbor cells. Throughout its life cycle, IH invade living rice cells although invaded cells appear dead when the fungus moves into the next cell. Biotrophic invasion must be mediated by fungal effectors, proteins that pathogens secrete inside live host cells to control them. However, little is known about blast effectors, and the low fungal biomass in early infection stages complicates identification of effector genes, as well as identification of rice genes controlled by effectors. The characterized *AVR-Pita* effector gene is specifically expressed in planta, but it was not clear how its gene expression pattern changed in different infection stages. We found that *AVR-Pita* is first expressed around the time of penetration. *AVR-Pita* is highly expressed in IH developing in asymptomatic tissue from 36 hpi to as late as 7 days post inoculation when lesions are maturing. Using inoculated rice sheaths, we successfully enriched for infected tissue RNA that contained ~20% IH RNA at 36 hpi. We compared IH gene expression to expression in mycelium from pure culture using a whole-genome *M. oryzae* oligoarray, and we compared infected rice gene expression to expression in mock-inoculated tissue using a rice oligoarray. Rice genes that were induced >50-fold during infection were enriched for genes involved in transferring information from sensors to cellular responses. Fungal genes that were induced >50-fold in IH included known effectors and many IH-specific genes encoding hypothetical secreted proteins that are candidate effectors. Gene knock-out analyses of three putative effector genes failed to show major effects on pathogenicity. Details of the blast interaction transcriptome will provide insights on the mechanisms of biotrophic plant disease.

ANALYSIS OF THE INTERACTION TRANSCRIPTOME DURING BIOTROPHIC INVASION OF RICE BY THE BLAST FUNGUS, *MAGNAPORTHE ORYZAE*

by

GLORIA MOSQUERA CIFUENTES

B.S., Universidad Catolica, 1996
M.S., University of Chile, 2001

A DISSERTATION

submitted in partial fulfillment of the requirements for the degree

DOCTOR OF PHILOSOPHY

Department of Plant Pathology
College of Agriculture

KANSAS STATE UNIVERSITY
Manhattan, Kansas

2007

Approved by:

Major Professor
Barbara Valent

Abstract

The hemibiotrophic rice blast fungus *Magnaporthe oryzae* undergoes complex morphological development throughout its infection cycle. From 8-20 hours after a fungal spore lands on a leaf surface, the fungus differentiates a complex appressorium that punctures the host cuticle. By ~24 hours post inoculation (hpi), the fungus grows inside an epidermal cell as a primary hypha, and by 36 hpi the fungus has differentiated specialized biotrophic invasive hyphae (IH) that are filling the first-invaded cell and moving into neighbor cells. Throughout its life cycle, IH invade living rice cells although invaded cells appear dead when the fungus moves into the next cell. Biotrophic invasion must be mediated by fungal effectors, proteins that pathogens secrete inside living host cells to control them. However, little is known about blast effectors. The low fungal biomass in early infection stages complicates identification of effector genes as well as identification of rice genes controlled by effectors. The characterized *AVR-Pita* effector gene is specifically expressed in planta, but it was not clear how its gene expression pattern changs in different infection stages. We found that *AVR-Pita* is first expressed around the time of penetration. *AVR-Pita* is highly expressed in IH developing in asymptomatic tissue from 36 hpi to as late as 7 days post inoculation when lesions are maturing. Using inoculated rice sheaths, we successfully enriched infected tissue RNA that contained ~20% IH RNA at 36 hpi. We compared IH gene expression with expression in mycelium from pure culture using a whole-genome *M. oryzae* oligoarray, and we compared infected rice gene expression to expression in mock-inoculated tissue using a rice oligoarray. Rice genes that were induced >50-fold during infection were enriched for genes involved in transferring information from sensors to cellular responses. Fungal genes that were induced >50-fold in IH included known effectors and many IH-specific genes encoding hypothetical secreted proteins that are candidate effectors. Gene knock-out analyses of three putative effector genes failed to show major effects on pathogenicity. Details of the blast interaction transcriptome will provide insights into the mechanisms of biotrophic plant disease.

Table of Contents

List of Figures

List of Tables

Acknowledgements

Barbara Valent, my major advisor. All the members of fungal molecular genetics lab. Department of Plant pathology at Kansas State University.

Dedication

This work is dedicated to J. Mosquera and R.M. Cifuentes, the mentors of my life. To all “grillos” that have been on my side no matter what.

CHAPTER 1 - Molecular Analysis of Biotrophic Plant-Microbe Interactions

General Overview

Resistance is the most common response of plants to pathogens and susceptibility is the rare event. Plants have evolved to develop effective mechanisms of defense and resist the attack of microbes that are constantly in contact with their potential host. To establish disease, pathogens need to face and neutralize different obstacles on their way into the plant tissue. The first barrier is the plant cell surface. Penetration could occur through natural openings like stomata, through wounds, or by direct penetration using enzymes and/or mechanical forces. Once pathogens gain access by penetrating the plant cuticle, they face the second obstacle, the plant cell wall. After cell wall penetration, the pathogen is separated from plant cytoplasm just by the plasma membrane (Chisholm et al., 2006). Plasma membranes contain specialized proteins, extracellular surface receptors, which are involved in the detection of pathogen-associated molecular patterns (PAMPs) to trigger immune responses. Chitin is a component of cell walls that is considered one of the major fungal PAMPs.

Plants use different strategies to fight against pathogen attacks, including production of antimicrobial substances or neutralization of the pathogen using resistance (R) protein-mediated defense responses. Effectors have been described as pathogen-derived proteins that are secreted inside the host, to the apoplast or cytoplasm depending on the pathosystem. R proteins have been classified in 5 major groups depending on their structures that are correlated with their role in the recognition of pathogen effectors. Group 1, represented by only one member (*Pto*), corresponds to a protein with a serine/threonine kinase region and a myristylation motif at the N terminus. Group 2, represented by many members, includes proteins with a leucine rich repeat (LRR) region, a putative nucleotide binding site (NBS) domain, and a putative leucine-zipper (LZ) or coiled-coil (CC) sequence. Group 3 members have LRR-NBS domains and a Toll Interleukin 1

Receptor (TIR) region at the N terminus. Group 4 has a transmembrane (TM) domain and an extracellular LRR. Group 5, similarly to the group 1, is represented only by the rice Xa21 gene and has a TM-LRR and a cytoplasmic serine/threonine kinase domain. Members of the first three classes of R proteins are predicted to be limited to the cytoplasmic space (Martin et al., 2003). Recently a new *R* gene cloned from rice has identified a new group (Chen et al., 2006). This new class of *R* gene has a receptor-like kinase domain, a predicted extracellular B-Lectin domain, and an intracellular serine-threonine kinase domain. The finding of *R* genes with new structures represents the increasing divergence of these genes which means that the previous *R* gene classes will continue expanding. It also raises the question about how many types of *R* genes actually exist (Bent and Mackey, 2007). Interestingly, the high level of evolution is not only found in the host side. Only few R proteins interact with their corresponding effectors in a direct way. Indirect interaction (termed the guard hypothesis) has been reported in bacterial systems, which involves the detection of host protein modifications induced by pathogen effectors (Ellis et al., 2007). This strategy shows an active-evolving mechanism from the pathogen to suppress plant defense responses (Van Damme, 2005).

Any particular disease resistance event may occur through diverse mechanisms that could involve components interfering with the pathogen invasion process at different stages. The first plant response to pathogen attacks has been related to perception of PAMPs(Chisholm et al., 2006). If the pathogen suppresses the PAMPs-induced defense, plants can counteract this by activating a more specialized response, an effector-triggered immunity. PAMPs detection involves plant transmembrane receptors and effector recognition involves intracellular NBS-LRR proteins, these two responses represent two different branches of the plant immune response (Jones and Dangl, 2006). Because PAMPs recognition by plants seems to be a very common response, the pathogen needs to develop new strategies to be able to cause disease (Huckenlhoven, 2005) first, by masking PAMPs; second, by circumventing recognition; third, by suppressing defense. As a common feature in a non-specific interaction, susceptible and resistant responses have overlapping components, especially at the beginning of the infection, that are defined as basal defense responses that differ mostly in timing and duration of each event (Birch and Kamoun, 2000).

The molecular basis of plant susceptibility has been less studied because plant response research is focused mainly on incompatible interactions and little is known about the plant components that make them prone to pathogen infection. Nevertheless, studies to identify plant genes required for susceptibility have been published. Mutation of the *PMR6* gene confers resistance to powdery mildew in Arabidopsis, which illustrates an example of a gene required for susceptibility (Vogel, 2002). The *pmr6* mutants contain more pectin in their cell walls than wild type Arabidopsis plant cells. This gene encodes a pectate lyase and presumably interferes with pathogen growth by accumulating pectin in the extrahaustorial matrix, which could interfere with nutrient availability. In the same way, loci required for Arabidopsis susceptibility to the downy mildew pathogen have been identified (Van Damme, 2005). Mutants in DMR loci lost susceptibility and the effect is predicted to be related to impaired signaling, nutrient transport, or membrane biogenesis mechanisms. Interestingly, some host susceptibility factors have been isolated and mutants defective in these genes do not exhibit a constitutive defense response; defenses are only activated after pathogen challenge. For example, a susceptibility gene has also been identified in the rice-*Xanthomonas oryzae pv. oryzae* system (Yang, 2006). The Os8N3 gene encodes a predicted integral membrane protein that is part of the MtN3 gene family with unknown function. Another example involves defense regulators WRKY proteins that are transcriptional regulators of genes involved in different plant biological processes including plant defense. Recently, the *WRKY7* gene in Arabidopsis has been shown to be over-expressed during pathogen infection and loss-of-function mutants exhibited enhanced resistance to *Pseudomonas syringae* (Kim, 2006). The *WRKY7* gene appears to function as a plant defense negative regulator. Thus, gene products that render the host susceptible to the pathogen attack could either be negative regulators of defense responses or substrates specifically used by the pathogen (Huckenlhoven, 2005). The identification of Os8N3, a dominant susceptibility gene supports the hypothesis relating developmentally-regulated genes with disease susceptibility. Both *PMR6* and *Os8N3* are also involved in other cellular processes, cell expansion and pollen viability, respectively. The fact that susceptibility genes can have pleiotropic effects points out the strategy pathogens use to manipulate host genes required for normal plant development. These findings expand the possibilities in the types of genes that expression and functional analyses should focus on, compromising experimental designs such as the use of cDNAs obtained from subtracted libraries or enrichment for incompatible interaction factors. As a take home message

from characterization of susceptibility genes, studies of compatible interactions should not be limited to genes that are repressed during pathogen interactions. Plant genes over-expressed during the compatible interaction could represent potential plant factors involved in susceptibility.

Eukaryotic plant pathogens, fungi and oomycetes, can establish different kinds of interactions with their host. A necrotrophic pathogen kills host cells before colonization. Necrotrophs use toxic molecules and lytic enzymes to destroy host cells and subsequently decompose them, and subsequently use their components as nutrient sources (van Kan, 2006). On the other hand, a biotrophic association is characterized by a tightly controlled infection strategy in which the infected cell is maintained alive to be used as a nutrient source. Plant biotrophic pathogens, especially fungi, are characterized by highly developed infection structures, limited secretion of lytic enzymes, carbohydrate-rich and protein-containing interfacial layers for the separation of the fungal surface from the plant plasma membrane, long-term suppression of host defenses, and haustoria or specialized hyphae for nutrient absorption (Mendgen and Hahn, 2002). Interactions that are initially biotrophic, but later involve cell death are known as hemibiotrophic. Interactions established by this type of pathogen shows characteristics of biotrophy because the pathogen initially develops in living cells, but later switches to a destructive necrotrophic phase (Liu et al., 2007). As is the infection strategy, biotrophic and necrotrophic defense responses are also different. For biotrophic pathogens, the gene-for-gene interaction is an important form of resistance (Glazebrook, 2005). In dicots, it is mainly associated with the salicylic acid-dependent signaling and systemic acquired resistance. On the other hand, the gene-for-gene strategy is not relevant for the resistance to necrotrophs because host cell death will not stop pathogen development.

In a recent report, Van Damme and colleagues (Van Damme, 2005) have listed the main steps that are relevant for the establishment of compatible interactions by biotrophic microorganisms. The first step involves the formation of specialized structures used for host penetration and nutrient acquisition. During this stage the pathogen uses its effector repertoire to initiate the interaction with the host. In the second step the pathogen is inside the host environment and exposed to the host's defense machinery. It is here where the pathogen needs an

efficient strategy to suppress plant defense responses triggered after recognition. In the third step, the establishment of a nutrient acquisition system that assures the pathogen survival is crucial because this is what disease progression depends on.

Biotrophic oomycete and fungal plant pathogens develop intracellular structures called haustoria that are used as feeding structures. In most hemibiotrophs, functionally similar structures, invasive hyphae, are formed. This morphological differentiation has multiple roles in establishing infection because it is critical for effector secretion and establishment of nutrient acquisition. Several studies have been published on the identification of secreted proteins expressed in haustoria. A cDNA library from haustoria formed by the broad bean rust *Uromyces fabae* allowed the isolation of in Planta Induced Genes (PIGs) (Hahn, 1997). Some of these genes were shown to be highly expressed in the haustorium. PIGs sequences showed similarity with amino acid transporters, and genes involved in metabolism such as thiamine biosynthesis. A similar approach in the rust-flax interaction focused on secreted proteins and allowed the identification of 21 haustorially-expressed secreted proteins (HESPs). One of them corresponded to an already characterized avirulence gene, AvrL567 (Catanzariti et al., 2006). Comparison of the genes expressed in these two studies showed the functional diversity of genes expressed in haustoria, on one side, host-interacting genes and on the other, metabolism-related genes.

As part of the host interaction, intracellular pathogen development requires suppression of the plant defense responses. Described pathogenicity determinants often correspond to pathogen-derived molecules that are needed to avoid host defense responses or to counteract their effects. In filamentous fungi, in general, the secretion of degradative enzymes and other proteins is a defining characteristic (Paper et al., 2007). Small secreted proteins representing effectors or others of unknown function are produced to establish host colonization. Some effectors, encoded by avirulence genes, are recognized by plant R proteins to trigger defense responses. Most avirulence gene products are apparently secreted proteins that need to be localized into the host cytoplasm to exert their avirulence function. In plant pathogenic bacteria, effector proteins are scattered along the genome, but there is little evidence suggesting genome location dependency in fungi. *Ustilago maydis* is the only fungal pathogen in which clusters of secreted proteins have been identified (Kamper et al., 2006). Cluster deletion analyses in this

system have shown that proteins in those clusters that are important for virulence range in size between 135 to 799 amino acids (aa). Recently, van der Does and Rep (van der Does, 2007) have reviewed some fungal virulence genes, which encode small secreted proteins involved only in virulence. These examples of virulence genes show the tendency for virulence factors to be small secreted proteins. In *Fusarium graminacearum*, analysis of secreted proteins identified 120 proteins that were produced in planta, from which 49 were not seen under in vitro conditions (Paper et al., 2007). Other pathogenicity determinants include genes that encode proteins involved in protein degradation, cellular detoxification, or transcription factors. Their molecular roles could be somehow simpler to identify because a large effect can be observed in the pathogen when their expression is impaired. On the other hand, other equally important genes, whose function is not directly associated with the ability to produce disease but is important for the pathogen adaptation to the new environment, could also represent interesting genes to be identified. A protein of *Uromyces favae* involved in the maintenance of biotrophic interaction has been identified (Kemen et al., 2005). The 220-aa long Uf-RTP1p protein localizes inside the plant cell and does not exhibit similarity with any other protein in the public databases. Similar proteins could represent important weapons for long-lasting biotrophs, and, why not, hemibiotrophs because host infected cells are maintained alive for certain period of time.

Pathogens can exhibit dynamic changes in metabolism depending on the developmental stage during the infection. In the case of the *Blumeria graminis*-barley interaction, expression analysis of the pathogen shows that the fungus expresses genes involved in building components for the appressorium, in degrading plant cell walls and in penetration during the first 15 hours post infection (hpi). After penetration, pathogen genes involved in metabolism of host are induced (Both et al., 2005). Gene expression analysis in the same patho-system, but using a single-cell transcript profile, also showed the over-expression of nutrition-related sucrose synthase genes HU03P12 and HY10G10 (Gjetting et al., 2007).

Nitrogen starvation stress has been widely correlated with in planta conditions of many fungi. The *Avr9* gene from *Cladosporium fulvum*, which induces a hypersensitive response in *Cf9*-carrying tomato plants, was shown to be expressed after fungal penetration and when the fungus was grown in vitro with limiting nitrogen (Van den Ackerveken, 1994). With this finding,

it was hypothesized that nitrogen starvation could be a key condition regulating expression of pathogenicity-related proteins. However, recent studies demonstrated that *Avr9* is the only avirulence gene from this pathogen whose expression is regulated by nitrogen-limitation conditions. Expression of other pathogenicity genes was not affected when *C. fulvum* was grown in vitro under different nitrogen concentrations (Thomma, 2006).

Unlike bacteria-plant systems, in which secretion of effectors inside host cells is well known to be dependant on the type III secretion system (TTSS), how eukaryotic-derived effectors reach the plant cytoplasm is still unknown. About 17 fungal and oomycete effectors containing signal peptides have been identified, which represents evidence for their secretion from the pathogen. Only oomycete pathogens has an additional motif, the RXLR-DEER motif, associated with secretion into the plant cell's cytoplasm (Whisson, 2007). Nothing is known in any system about the mechanism of secretion inside the host cell. Effector endocytosis involving specialized cell receptors is one hypothesis {Chisholm, 2006 #458}, but this remains to be proven. In this sense, host transmembrane proteins induced during infection could be good candidates.

Rice Blast Disease

Magnaporthe oryzae

Magnaporthe oryzae (Couch and Kuhn) is a filamentous ascomycete fungus that can be grown *in vitro*. This heterotallic fungus occurs in two mating types, *MAT1-1* and *MAT1-2*, which permits genetic studies when fertile strains from opposite mating types are available (Kato and Yamaguchi, 1982; Notteghem and Silue, 1992). The majority of field isolates from rice are infertile, but fertile isolates do occur rarely. The strain GUY11, a *MAT1-2* strain, isolated in French Guiana, is one of these rare fertile rice pathogens (Leung et al., 1988). The genome sequence of *M. oryzae*, laboratory strain 70-15, is available (Dean et al., 2005). The genome is predicted to be around 40 megabases (Mb) in size and to contain about 11,109 genes distributed on 7 chromosomes (Dean et al., 2005). Seventy nine percent of the predicted genes correspond to conserved hypothetical proteins and 20% represent predicted proteins. Genome sequencing also showed that the *M. oryzae* genome is rich in G-protein-coupled receptors (GPCRs), which are

involved in inducing signal transduction pathways, including 61 GPCRs described for the first time. Additional valuable information coming from this whole genome analysis is the prediction of 739 putative secreted proteins (Dean et al., 2005).

Oryza sativa

Rice (*Oryza sativa*) is one of the most important sources of food in the world, especially for developing countries. As the most important disease of rice, rice blast represents a major threat to global food security. The *O. sativa* L. ssp. *japonica* cv. Nipponbare finished genome is predicted to be 389-Mb in size organized into 12 chromosomes with 37,544 protein-encoding sequences {Sequencing, 2005 #296} .

After a genome sequence is available, another important stage, the prediction of coding sequences, begins. Even though rice has been studied for a long time and many genes have already been identified, predicting the structures of the remaining genes is accomplished using automated methods for gene calling. Good evidence for the correct calling of a gene structure is represented by expression data, such as expressed sequence tags (EST) and full-length cDNAs (FL-cDNA). The last one represents valuable information because it provides information about transcription start and stop sites, and also about intron and exon structures. An extensive rice FL-cDNA collection is available, representing expressed genes from ~20 different tissues and stress conditions, including seedlings, calli, germinating seeds, panicles, UVB, UBC, cold, heat, auxin, cytokinin, absicic acid, and cadmium (Kikuchi et al., 2003). Homology searches with FL-cDNAs allowed the assignment of potential functions to 21,596 of these clones. A total of 17,016 rice genes reported in the finished version of the rice genome sequence matched with FL-cDNAs (Kikuchi et al., 2003).

Development of resistant cultivars is considered to be the most effective method to control diseases in many crops including rice blast. The effort to identify and characterize rice blast resistance genes has been very productive, mainly in the last decade. So far, about 37 major blast resistance genes have been identified and 6 have been cloned (*Pib*, *Pi-ta*, *Pi2*, *Pi9*, *Piz-t*,

and *Pi-d2*) (Dai, 2007) and references therein. The availability of plant and fungus genome sequences has made rice blast a good model system for the study of plant-pathogen interactions.

In the specific case of rice, resistance to blast disease imparted by the *Pi-ta* gene (Bryan et al 2000), an NBS-LRR gene, is part of the immune resistance triggered by the fungal effector *AVR-Pita*. The *Pi-ta* gene encodes a cytoplasmic receptor that interacts with the AVR-Pita avirulence protein (Jia et al., 2000) and blocks lesion development. Microscopic studies using leaf inoculation have shown that formation of appressoria at 24 hpi is similar in resistant and susceptible cultivars. At 34 hpi, cell invasion progresses in most of the infection sites in susceptible cultivars and in some sites of the resistant cultivar(Berruyer et al., 2006). Fungal growth stops completely by 48 hpi in the resistant cultivar.

The Pathogenic Process and the Genes Involved

The infection process begins when a three-celled spore lands on the leaf surface and attaches to it by a mucilage produced at the spore tip (Hamer, 1988; Howard and Valent, 1996). After this initial step, a germ tube emerges from the spore and grows on the leaf surface. Recognition of the hard hydrophobic surface by the germ tube is followed by the formation of a penetration-specific structure called an appressorium at ~8 hpi. The melanization of mature appressoria is a critical cellular process for building the enormous turgor pressure used by the penetration peg for breaching the plant cuticle (~20 hpi). Melanized appressoria can be generated in vitro on several artificial surfaces, which facilitates the study of this stage in the absence of the plant host (Hamer, 1988; Bourett and Howard, 1990; Dean, 1997; Talbot, 2003). Once the fungus penetrates the plant cuticle, a thin primary hypha elongates from the penetration peg and is the first intracellular fungal structure that receives all the cytoplasmic components migrating from the appressorium (~24 hpi). At 27 to 30 hpi, this primary hypha differentiates into a more bulbous and branched invasive hypha (IH) that colonizes the first invaded plant cell and later moves to the neighboring cells (>36 hpi). During this period of the infection, the fungus grows within the plant tissue without producing macroscopic symptoms. Symptoms begin to develop only after 4 days, which corresponds to the time that the fungus has established itself

inside the host and is preparing to sporulate and initiate a new infection cycle. Lesions continue expanding until ~ 7 dpi. The entire disease cycle can be defined as pre-penetration growth, biotrophic invasive growth, and mixed biotrophic and necrotrophic growth and sporulation.

Appressorium Formation and Leaf Penetration

The fungus must overcome the hydrophobic host surface barrier to have access to the plant intracellular compartment. To accomplish the invasion process, the fungus attaches to the leaf cuticle, and penetrates it. The *MPG*1 gene, which encodes a fungal hydrophobin, plays an important role in leaf attachment (Talbot et al., 1996). *MPG1* was also highly expressed during appressorium formation and at later colonization stages during symptom development. The *mpg*1 mutants are compromised in mycelial hydrophobicity, hydrophobic spore coat formation and appressorium differentiation on the leaf surface.

The control of cellular developmental stages is very important in pathogens because their success depends upon the formation of the suitable structures at the right moment. Appressorium formation is surprisingly not strictly dependent on perception of host signals, but shows a physical stimulus-dependency instead, which makes this pathogen-associated cellular differentiation very intriguing. Fungal appressorium formation occurs in vitro on hard, hydrophobic surfaces. The transmembrane GPCR protein encoded by the *PTH11* gene has been shown to be important for appressorium differentiation in response to surfaces signals (DeZwaan et al., 1999). It plays a role in activating appressorium formation on highly inductive surfaces and in repressing this morphological differentiation on poorly inductive surfaces.

After spore attachment indicates to the fungus to start forming its penetration arsenal, orchestrated signal transduction pathways play critical roles. Plant stimuli are converted to morphological differentiation through classical signal transduction pathways (Xu, 2000). Appressorium development is known to be regulated by two independent signal transduction pathways, the MAP kinase-dependent pathway involving *PMK1*, and the cAMP-dependent pathway. Although upstream signals for *PMK1*-mediated appressorium formation have been suggested to involve different components, one of them has been identified. *MGB1* is one of the

first components upstream of MAP kinase signaling. It encodes the β-subunit of a G-protein, which has been shown to affect diverse cellular processes such as conidiation, appressorium formation, penetration and invasion (Nishimura et al., 2003). Following recognition, downstream components MST11 and MST7 are the kinases that activate PMK1 MAP kinase. The *MST11* and *MST7* genes are orthologs to the yeast *STE11* and *STE7* MAP kinase kinase kinase and MAP kinase kinase genes , respectively (Zhao et al., 2005), even though it is still unclear what component directly activates MST11. Mutants in *MST11*, *MST7* and *PMK1* are unable to form appressoria and fail to produce disease. *PMK1* functions also include the arrest of germ-tube tip growth, the formation of appressorium-specific cell wall layers, the generation of turgor pressure, and blockage of invasive growth (Xu and Hamer, 1996). A transcription factor, MST12, acting downstream of PMK1 has been identified. Mutants lacking MST12 expression formed appressoria but failed to penetrate and invade plant cells (Park et al., 2002). More recently, Mst50 has been shown to interact with MST11, MST7 and MGB1 and could be the adaptor protein between G-proteins, such as MGB1, and the downstream MAP kinase cascade components (Park, 2006).

Unlike the *PMK*1 kinase pathway, few components of the cAMP pathway have been characterized. cAMP has been shown to activate appressorium formation even on poorly inductive surfaces (Lee and Dean, 1993). Therefore, this is an alternative pathway that the fungus can use to differentiate appressoria. The *MAC1* gene that encodes a membrane-associated protein has been characterized (Choi and Dean, 1997). This protein is an adenylate cyclase involved in the production of cAMP from ATP. On the other hand, a cytoplasmic component *CPKA* , that encodes the catalytic subunit of cAMP-dependent protein kinase A, has been shown to be dispensable for appressorium formation, but not for penetration (Mitchell and Dean, 1995; Xu et al., 1997). Appressoria formed by *CPKA* mutants are melanized but smaller than wild type. This shows that appressorium formation and penetration are genetically independent processes.

The melanization process is accomplished during appressorial maturation, and is critical for plant penetration. The melanin layer is deposited between the appressorial membrane and cell wall, and serves as a permeability barrier that blocks leaking out of glycerol required for

establishing the turgor pressure powering mechanical penetration (Howard and Valent, 1996). This permeability also has been associated with the retention of plant penetration essential components such as degrading enzymes and signaling-related molecules. Poorly or non-melanized appressoria are unable to penetrate the plant cuticle but fungus can infect normally through wounds. The genetics of melanin biosynthesis has been fully characterized. Three unlinked genes have been involved in different steps of the melanin biosynthetic pathway; *ALB* is essential for the initial steps of melanin biosynthesis and has homology with a polyketide synthase of other organisms; *RSY* encodes scytalone dehydratase that functions in the conversion of scytalone into trihydroxynaphthalene; and *BUF* encodes a polyhydroxynaphthalene reductase mainly involved in reduction of trihydroxynaphthalene to vermelone (Chumley and Valent, 1990; Howard and Valent, 1996). Once the fungus has accomplished the penetration process, the cellular pigmentation is not required for invasive growth. Defective mutants in melanin biosynthesis develop normal invasive hyphae when they infect wounded tissues (Kankanala et al., 2007).

Biotrophic Development

Biotrophic interactions involve the strict and complex mode of infection in which living host cells are used by the pathogen as a nutrient supplier (O'Connell and Panstruga, 2006). The pre-penetration steps of infection usually are not critical to determine whether a biotrophic or necrotrophic association occurs. It is the way that plant tissue is colonized after penetration that defines the relationship between the partners.

Rice blast infection is considered as a dynamic hemibiotrophic interaction because the pathogen initially invades as a biotroph; but invaded cells subsequently die. It was recently confirmed that in the initial stage of the infection, *M. oryzae* invades the first epidermal cell using specialized invasive hyphae (IH) that are wrapped in plant-derived membrane called the extra-invasive hyphal membrane, EIHM (Kankanala et al., 2007). Every newly invaded rice cell is initially alive but it dies by the time the fungus moves to the neighboring cells (Kankanala et al., 2007). How the fungus establishes itself inside the host cell without affecting that cell's viability is still unknown. In other systems, the interfacial membrane that divides plant and

pathogen has been associated with bridged communication, for delivery of nutrient supplies from the host to the pathogen and for delivery of effectors from the pathogen to the host (O'Connell and Panstruga, 2006). In the case of hemibiotrophs like *Magnaporthe*, there is no direct evidence that proves that intracellular hyphae are the nourishing organelle.

Cell walls of fungi and oomycetes have polysaccharide components like chitin and β-1-3-glucans that are recognized and targeted by defense machinery that causes hyphal tip destruction. It is unknown if the pathogen modifies its cell wall when growing intracellularly, which might represent a strategy to avoid the recognition by the host basal defense response. Recently studies in *M. oryzae* showed that hyphal tips moving to the second-invaded cells are enclosed in EIHM with distinctive membrane caps at their tips (Kankanala et al., 2007), suggesting that this could be the strategy that the fungus is using to hide from host recognition and protect its invading hyphae.

The haustorium, the pathogen structure representing the closest interaction between the pathogen and its host, is involved in the secretion of effectors into the host and the uptake of nutrients from the host (O'Connell and Panstruga, 2006). In the specific case of *M. oryzae*, biotrophic hyphae could be considered as parallel structures to haustoria in terms of functionality. To exert their role, biotrophic hyphae would need to express a plethora of genes involved in metabolism, membrane component biosynthesis, and cellular transporters. These fungal genes along with components of the host machinery that facilitate pathogen feeding are still unknown. In rice blast, the time point of infection in which IH are already established intracellularly represents an appropriate disease stage to identify not only pathogen effectors, but also fungal components important for nutrient absorption and metabolism. At the same time, host genes that facilitate the pathogen infection process, including nutrient interchange and disease susceptibility can also be identified.

Fungal Avirulence Genes and Putative Effectors

Invasive growth in rice blast disease is defined as the infection stage that follows leaf cuticle penetration and which is initiated by the formation of primary hypha (>24 hpi). Invasive

growth is harder to study than the pre-penetration phase of infection because this stage can not be mimicked on artificial surfaces. So far there are few genes identified to be essential for invasive growth (Fig 1.1), introducing a big gap in the identification of fungal components that are necessary for formation of the plant-fungus interface. Unlike the pre-penetration process the identification of genes involved in invasive growth of infection has been less efficient because these are usually plant specific, even though some could be expressed also under in vitro conditions. Another limitation in the case of avirulence genes is the fact that their functionality can be proven only if the corresponding mutant is inoculated on the appropriate plant background that lacks the matching *R* gene. Most of the mutants lacking avirulence gene function can grow normally under both in vitro and in vivo conditions (Orbach et al., 2000).

M. oryzae avirulence genes include one of the rare cases in which the avirulence activity is not directly accomplished by the gene product or is not a secreted protein. ACE1 (Avirulence Conferring Enzyme1), a cytoplasmic protein recognized by the rice *R* gene product Pi33 has been characterized. *ACE1* encodes a putative hybrid between a polyketide synthase and a nonribosomal peptide synthetase, and is expressed only during the appressorial penetration process (Böhnert et al., 2004). Apparently it is the secondary metabolite produced by this enzyme in mature appressoria that is recognized by the resistance gene product.

As part of the *M. oryzae* infection-related secretome, two avirulence genes encoding secreted proteins have been extensively studied. A telomeric avirulence gene *AVR-Pita* was isolated using a map-based cloning strategy (Orbach et al., 2000). This gene encodes a putative 223-aa metalloprotease that triggers disease resistance by interacting with the rice R protein Pi-ta. The AVR-Pita mature protein (176-aa) interacts directly with the leucine-rich domain of Pi-ta protein in vitro and in vivo (Jia et al., 2000). In the second example, the *PWL2* (Pathogenicity toward Weeping Lovegrass) gene encodes a 145-aa glycine-rich protein with a predicted signal peptide. Strains containing a functional allele of *PWL2* are not able to infect weeping lovegrass, but are pathogenic in other hosts (Sweigard et al., 1995). Rice seems to lack a resistance gene that recognizes *PWL2*. This gene is highly conserved among rice pathogens isolated from the field, which suggests it may have an important role even though *pwl2* $^{-}$ mutants appear to have normal pathogenicity. These few effector examples expose the need to increase effort to identify

more pathogen effectors that can be recognized by rice *R* genes and mediate defense responses, or that induce susceptibility in the absence of a corresponding *R* gene.

So far, few *M. oryzae* genes affecting the development of the invasive hyphae inside host cells have been identified. During interaction with their host, plant pathogenic microorganisms secrete proteins into the plant cell that induce or block defense responses. Genome sequence analysis suggested *M. oryzae* possesses ~739 secreted proteins, which is double the amount predicted for the non-pathogenic saprobe *Neurospora crassa* (Dean et al., 2005). One possible explanation for this difference is the pathogenic nature of *M. oryzae*, raising the possibility that this secretome contains an unexplored arsenal of putative effectors. As a hemibiotrophic fungus, *M. oryzae* needs to avoid recognition by the host defense system, and secreted proteins are good weapons to trick and control the host. Only downstream responses, after the first cell is invaded, will define how successful the fungal development will be. Once the fungus is growing intracellularly, it is the right moment to deliver effector proteins.

Fungal Detoxification and Metabolism in Planta

After penetration, plant colonization takes place and the pathogen needs to overcome different host responses, such as production of toxic compounds that could be very harmful if a good detoxification system is not activated at the right time. An ATP-binding cassette (ABC) transporter *ABC1* was identified in *M. oryzae* and shown to be involved in the efflux of toxic molecules during infection. Mutants with a defect in this gene are not able to survive inside host cells after penetration (Urban et al., 1999). Recently, another ABC transporter, *ABC3*, was also identified and shown to be important in both host penetration and invasive growth. Mutants lacking *ABC*3 expression are nonpathogenic due to defects in penetration that were partially reversed by antioxidant treatment. Once inside the cell, the fungus was unable to survive in the intracellular environment, demonstrating the *ABC3* gene's role in the regulation of fungal response to the oxidative stress inside the host cell (Sun et al., 2006).

Nutrient Availability and Its Role in the Infection Process

Not only detoxification processes are activated in the pathogen as a response to the new environment during infection, other cellular activities like carbohydrate metabolism, are also

activated to respond to stress-related conditions and different nutrient sources. One of these processes is trehalose synthesis and its metabolism. In *M. oryzae*, the *TRE1* gene that encodes a neutral-acid trehalase, has been involved in metabolism and mobilization of the intracellular trehalose (Foster et al., 2003). Activity of this gene was shown to be dispensable for fungal infection because mutants resembled the wild type strain in pathogenicity. In this same study, the *NTH1* gene encoding for a neutral trehalase was shown to be expressed both during sporulation and invasive growth. Strains with a mutation in *NTH1* appeared to be normal in sporulation, but they produced fewer disease lesions. Detailed functional analysis showed that these mutants were able to penetrate the plant cuticle, but the development of IH was slower compared with the wild type strain. Recently, a nuclear localized protein encoded by *MIR1* has been identified and shown to be highly specific for growth in planta (Li et al., 2007). This gene showed no homology with any sequence in GenBank and the only known motif found at the protein level was a nuclear localization signal. Mutation in this gene did not affect appressorium penetration or invasive growth, but it is still intriguing what the function of this protein is, and why it is localized in the nucleus during invasive growth.

In the case of *M. oryzae*, there is not much information about the role of nitrogen in the regulation of virulence genes. The only piece of information available so far is during the pre-penetration stage. *M. oryzae NUT1*, a nitrogen regulator, is essential for expression of *MPG1*, but not for pathogenicity (Froeliger, 1996). It is expected that before penetration the fungus can experience nutrient starvation, which makes nitrogen starvation a relevant condition for gene expression analysis. This assumption might not be true for expression analysis after penetration because plenty of nutrients should be available from the host. A non-overlapping pattern is expected when the nitrogen limitation condition is compared with in planta colonization.

Using global genome analysis, Donofrio et al.(Donofrio et al., 2006) assessed the question of how nitrogen starvation impacts the gene expression pattern and how these changes correlate with in planta conditions. They found that *NUT1* was slightly up-regulated under nitrogen starvation. Meanwhile, *MPG1* was clearly over-expressed after 12 hours of starvation and its expression was reduced after 48 hours. No avirulence genes were shown to be over-

expressed in the studied conditions adding evidence for the theory that these invasive growth specific genes are not regulated by nitrogen limitation.

An important goal in the *M. oryzae*-rice pathosystem is the identification of the entire set of fungal effectors that promote biotrophic invasion of rice cells. There are currently no defining characteristics that would allow one to recognize effectors among the complete *M. oryzae* gene set. We report here progress in two strategies to identify additional fungal effectors. The first (Chapter 2) involves understanding transcriptional regulation of the best characterized blast effector, *AVR-Pita*. Identification of promoter motifs and ultimately of key transcription factors mediating *AVR-Pita* expression could lead to identification of co-expressed effector genes. The second strategy (Chapter 3) uses genome-wide transcriptional profiling to identify all fungal genes that are specifically expressed during biotrophic invasion. Biotrophic IH-specific genes that encode secreted proteins could be excellent candidates for blast effectors. At the same time, a close-up view of changes in rice expression during biotrophic invasion would be expected to provide clues as to what plant genes are being affected by fungal invasion.

Figure 1.1 *M. oryzae* genes discussed in this chapter involved in different infection steps.

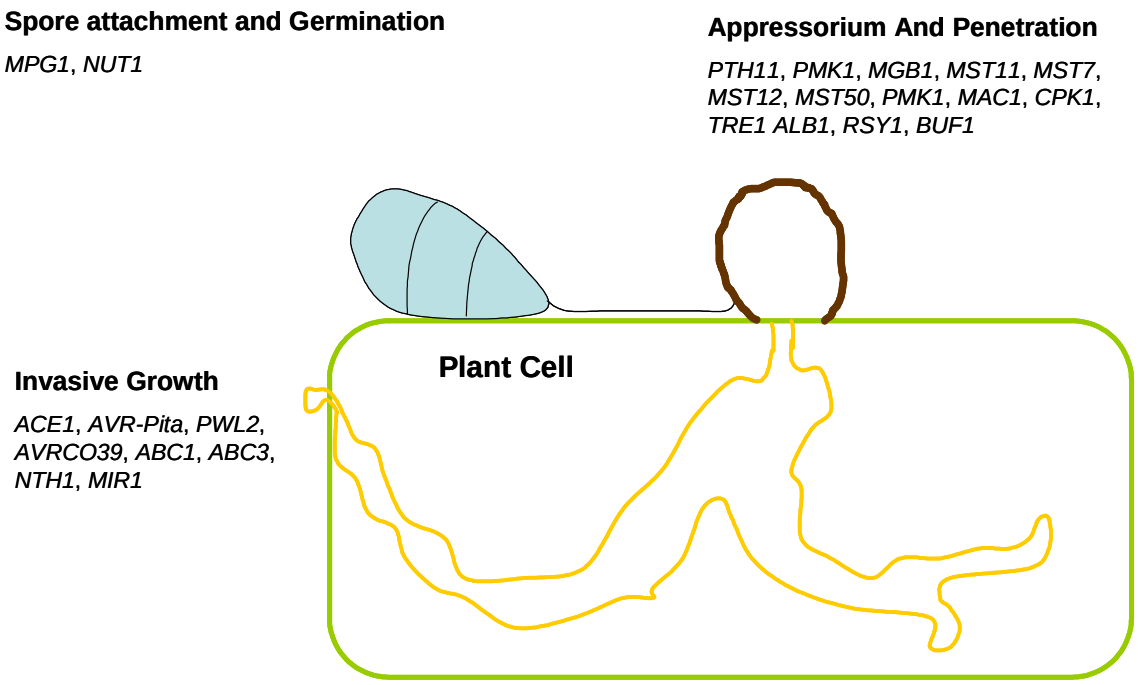

Fungal genes involved in different infection processes. The invasive growth genes correspond to genes that affect or are specifically expressed during invasive growth. Only *ACE1*, *AVR-Pita*, *PWL2* and *AVRCO39* correspond to avirulence genes. For more details see (Talbot, 2003; Ebbole, 2007).

CHAPTER 2 - Promoter Analysis of the Avirulence gene *AVR-Pita*

Abstract

Rice blast disease resistance is governed by a gene-for-gene interaction. Transient expression of *AVR-Pita* inside rice cells triggered *Pi-ta*-mediated resistance, and AVR-Pita interacted directly with Pi-ta in vitro. Therefore, *AVR-Pita* represents a putative effector secreted by biotrophic blast invasive hyphae (IH) into living rice cells. In a previous study, *AVR-Pita* expression was not detected in culture and was difficult to detect during infection. We developed a method to obtain infected rice tissues enriched in IH, and used it to measure the amount of *AVR-Pita* transcript at different infection time points by RT-PCR. No *AVR-Pita* expression was detected at 20 hpi, before penetration had occurred. *AVR-Pita* expression was weak at 24 hpi, when penetration just began, and its expression increased at 36 and 48 hpi when IH were developing inside plant cells. Quantitative real-time PCR showed that there is no *AVR-Pita* expression in spores, but that there is in mature appressoria that are ready to penetrate. Another unexpected finding from our promoter analysis is that the *AVR-Pita* promoter activity as measured using GFP fusion constructs differs from the promoter activity measured by assessing the avirulence phenotype in whole plant infection assays. This suggests that there is a special regulation mechanism of avirulence activity besides transcriptional regulation. One goal of this study was to identify the cis-elements responsible for *AVR-Pita* regulation. Different bioinformatic programs were unable to predict putative regulatory elements specific to *AVR-Pita* and other infection-specific genes. We found that the putative regulatory elements predicted in this in planta specific gene were also found in genes that are known to be repressed during plant colonization, such as the melanin-related genes. Instead, we gained information about *AVR-Pita* expression kinetics. Data obtained in this study can be used in comparative analysis using promoters of other plant-specific fungal genes to identify putative co-expressed genes.

Introduction

A few pathogen genes that are expressed specifically during plant infection have been identified but most of them have not been fully characterized. Even though most research has focused on discovery and dissection of their functionality, understanding how expression of these genes is regulated during the infection process is also an important area of research. This information is critical for the identification of transcription factors that activate the expression of genes that are important for host colonization.

Analysis of fungal infection-related promoters has been used to gain insight into gene regulation mechanisms of important pathogenicity factors. This involves the identification of promoter sequences that are important for the regulation of gene expression during plant infection, and ultimately the identification of transcription factors. This last approach has not been very successful.

The *U. maydis mig1* gene encodes a small secreted protein that is weakly expressed during filamentous growth in vitro. Using a promoter fusion with an enhanced Green Fluorescent Protein (eGFP) , it was shown that *mig1* is not expressed in hyphae growing on maize leaf surface; its expression was first detected after penetration, and it was highly expressed during invasive growth in planta (Basse, 2000). Deletion of different regions of the promoter showed modified patterns of expression compared with that obtained using the larger promoter fragment. In the same pathogen, a 350-bp region was shown to contain all the regulatory elements necessary for the regulation of expression of another gene, *mig2-5*. Mutation analysis performed with the eGFP reporter fusion allowed the identification of promoter elements that are important for *in planta* gene induction (Farfsing et al., 2005). The *AVR9* avirulence gene of the fungal tomato pathogen *C. fulvum* is known to be highly expressed during leaf colonization. Fungus transformed with the *AVR9* promoter fused with the β-glucuronidase (GUS) gene revealed that the expression of this gene is induced after penetration (Van den Ackerveken, 1994). It is also known that this gene is induced in vitro under nitrogen starvation conditions, not only in *C. fulvum* but also in *Aspergillus nidulans*. More recent studies using mutational analysis of the 0.6-kb functional *AVR9* promoter, fused with the GUS reporter gene, has identified two regions that are important for the induction of *AVR9* gene in *A. nidulans* (Snoeijers, 2003). These regions

contain TAGATA consensus sequences that are bound by transcription factors that regulate genes involved in nitrogen metabolism.

In *M. oryzae*, promoter analysis of genes involved in pathogenicity has also been investigated. The *MPG1* gene encodes a small secreted protein that is important for fungal conidiation, appressorium formation, and virulence. Using *sGFP* as the reporter gene, three different regions of the *MPG1* promoter have been identified. One region was important for the gene to be expressed in conidia, in appressoria, and when the fungus is experiencing nutrient limitations; another region was important for the repression when the fungus was grown with sufficient nutrients; and a third region was critical for *MPG1* expression in conidia and appressoria (Soanes et al., 2002). In a second example, the use of a promoter trapping strategy allowed the identification of the *MIR1* gene in *M. oryzae*, wich was highly expressed only during invasive growth. Using an eGFP fusion, a 1.4-kb long promoter sequence of *MIR1* was fully characterized. In this study, a 97-bp region of the promoter that contains two inverted repeat sequences, of TTCCCA and TCCACC, was shown to be critical for *MIR1* gene expression during plant colonization (Li et al., 2007). Similarly, the promoter of the avirulence gene *ACE1* has been studied using an eGFP fusion strategy. Results obtained from this study showed that *ACE1* gene expression is tightly regulated during the penetration process and also that its expression is independent of plant signals (Fudal, 2007).

The *AVR-Pita* avirulence gene from the Chinese field isolate O-137 of *M. oryzae* encodes a putative secreted metalloprotease (Orbach et al., 2000). AVR-Pita protein is different from most other characterized avirulence proteins due to its homology to proteins with a well characterized function. A neutral zinc metalloprotease motif identified in the AVR-Pita carboxy-terminal region was critical for avirulence activity. Expression of the mature protein in *Pi-ta*-containing rice cells triggered HR but not in cells lacking the *R* gene. This finding indicated that AVR-Pita is a fungal effector that is secreted into the plant cytoplasm where it triggers *Pi-ta*-mediated defense responses (Jia et al., 2000).

In strain 0-137, *AVR-Pita* is located within a 1.5-kb region adjacent to one of the telomeres of chromosome 3. A DNA fragment corresponding to the 1531-bp region extending

from the telomere repeat sequence was able to confer avirulence activity when it was transformed into a virulent strain of the fungus. Fragments from *Apa*I and *Hind*III sites to the telomeric repeats failed to confer avirulence activity in similar complementation tests (Fig 2.1) (Orbach et al., 2000). Deletion analysis showed that an 89-bp region extending from 1531-bp site to the *ApaI* site in the *AVR-Pita* promoter was critical for avirulence activity when complementation analyses were done using a virulent fungal strain and whole plant inoculation assays (Orbach et al., 2000). The 475-bp promoter region from 1531 to the translation start site will be referred from here after as the active promoter and the 393-bp fragment starting from the *Apa*I site as inactive promoter (Fig 2.1). In another study, the *AVR-Pita* active promoter fused to a GUS reporter gene showed the specific expression of this gene during later stages of the fungal infection (G.T. Bryan and B. Valent, unpublished results). Besides this *GUS* reporter gene expression, there is no available data showing the kinetics of *AVR-Pita* expression. Detection of mRNA is more difficult when the target gene is expressed specifically in the plant, especially at early stages of the infection, because of the low amount of fungal biomass compared with host tissue. We developed an enrichment protocol for fungal content in infected tissues and detected *AVR-Pita* expression around the time of penetration and during invasive growth when the fungus is developing in the first-and-second invaded cells. We also fused different *AVR-Pita* promoter fragments to a GFP reporter sequence in order to analyze the regulatory regions of *AVR-Pita*.

Results

Identification of the expression kinetics of AVR-Pita

Even though previous expression analysis done during the initial characterization of the *AVR-Pita* gene suggested its infection specificity, it was not clear how its expression pattern changed among the different infection stages. To pursue this objective, we screened early time points of fungal invasion to determine when the expression began. Initial studies to detect *AVR-Pita* mRNAs during infection showed high levels of expression at 36 hpi when biotrophic invasive hyphae were developing inside the first invaded cell and beginning to move to the neighboring cells. Time courses were run and fungal spores were used as time zero; appressoria

formed on plant tissue as a pre-penetration time; appressoria developing primary hyphae as the earliest post-penetration time; and invasive hyphae after 36 and 48 hpi as reference time. RT-PCR analysis showed that *AVR-Pita* was not expressed at 20 hpi in mature appressoria that were ready to penetrate plant cuticle (Fig 2.2). It was just after the fungus had penetrated and formed primary hyphae (24 hpi) that *AVR-Pita* mRNA was weakly detected in the infected samples and mRNA increased substantially after 36 hpi. Other times of infection showed that the expression is also high at 48 hpi and in the surrounding tissue of 7 day-old lesions (data not shown). Lack of amplification in appressoria in this experiment was due only to absence of the specific *AVR-Pita* RNA because an expected band was seen when fungal actin primers were used in the same sample.

Location of the transcriptional start site of AVR-Pita promoter and prediction of cis-regulatory elements

To have more information about the *AVR-Pita* promoter structure, the transcriptional start site was determined by 5'-RACE PCR. Amplification of the *AVR-Pita* 5' cDNA end revealed that the transcription start site is 130-bp upstream from the start codon (Fig. 2.3). Therefore, the *AVR-Pita* active promoter resides between -130 and -475-bp upstream from the translation start site.

Sequence analyses using web-based searches were used to determine whether the previously reported active promoter, in terms of avirulence activity, contains putative regulatory elements that could be responsible for gene regulation. Prediction of cis-elements in the 1.1-kb promoter sequence using a plant promoter program TSSP Softberry (http://softberry.com/berry.phtml?topic=tssp&group=programs&subgroup=promoter**)** identified the repeated sequence RSP00161 (WAAAG where W may represent A or T) once in the active region and four times in the inactive one (Table 2.1). Another repeated sequence RSP00508 (gcaTTTTTatca where lower case letters mean non-conserved nuleotides) was also found to be

present 3 times in the whole promoter of *AVR-Pita* (Table 1.1). We determined if these repeats occurred in the promoter of another *M. oryzae* avirulence gene, *PWL2*. Two RS00161 and eight RSP00508 repeated sequences were found in *PWL2*. To evaluate the significance of the presence of these sequences in the two avirulence genes, other genes known to be highly induced and repressed during infection were also analyzed. This analysis showed a lack of correlation between presence of these repeats and up-regulation in plant. These repeated sequences were also present in the promoters of two genes, AMG01944 and AMG02948, which are significantly down-regulated during infection (see Chapter 3).

We also searched for the potential promoter motifs using the MEME program (http://meme.sdsc.edu/meme/), which is used to discover highly conserved regions in related sequences, using *AVR-Pita* and promoters from other eight genes, including *PWL2*, that are known to be expressed specifically during infection. No conserved motifs in *AVR-Pita* were found to co-localize in the active region of the promoter. Multiple sequence alignment was also done using different sizes of the *AVR-Pita* promoter with others from infection-specific genes. We could not identify conserved sequences among different promoters. The REPFIND program (http://zlab.bu.edu/repfind/form.html), TRANSFACT® and MATCH ™ (http://www.biobase-international.com/pages/index.php?id=transfac) were also used, but no significant results were obtained.

Assessing promoter activity using GFP as reporter gene

Because we failed to identify putative cis-elements in the *AVR-Pita* promoter using computer-based analysis, we decided to analyze the whole promoter fused to a GFP reporter gene. Evaluating promoter activity of different regions would narrow down the sequence that is responsible for infection-specific regulation. The avirulence inactive fragment of the *AVR-Pita* promoter was fused to the GFP reporter gene to evaluate its activity in different *M. oryzae* morphological stages. Ten independent transformants were tested for GFP activity in spores. Surprisingly, a GFP signal was seen in all the transformants, although individual transformants showed different levels of expression (Table 2.2). There were 2 transformants showing low levels, 6 showing intermediate levels, and 2 showing high levels of fluorescence in the spores.

No detectable levels of expression were seen in the wild type spores. Three transformants containing the inactive promoter fragment showing low, intermediate and high levels of GFP expression in spores were chosen for further analysis. Appressoria and invasive hyphae were examined to evaluate the promoter activity during infection. A good correlation was seen between level of expression seen in spores and these other stages; transformants with low levels of expression in spores showed weak expression in appressoria and invasive hyphae. The same results were obtained with the other two transformants. Taken together, the 393 fragment of the *AVR-Pita* promoter is inactive in avirulence assays, but it is still active in expressing the GFP reporter protein. The expression pattern was not substantially different from that obtained from strains transformed with the active (475-bp) promoter. Table 2.1 illustrates the level of expression obtained with each construct; transformants showing high, intermediate, and low levels of expression are numbered as 1, 2, and 3 respectively. Mycelia from transformants containing both the inactive and active promoters did not appear to express any GFP.

Because our previous results showed that *AVR-Pita* gene was not expressed in spores, the GFP signal in spores of all the transformants was unexpected. There are two possible explanations for these results: First, the level of expression of *AVR-Pita* could be very low in spores making it harder to detect the mRNA by RT-PCR in spores; second, the *AVR-Pita* promoter has regulatory sequences upstream of the 475 region that repress its expression in spores. To investigate the second hypothesis, the longer 1.1-kb promoter fragment was fused to GFP. When the longer promoter was used, the expression in 10 transformants was less variable than expression seen when the inactive promoter was used. Eight of them showed low, one intermediate and one high level of expression. Leaf sheath infection assays were performed using transformants showing high, intermediate, and low levels of expression in spores. Contrary to results with other constructs, the transformant showing intermediate expression in spores showed very high expression in invasive hyphae, similar to that obtained with the high-expressing transformant. The transformants from the other two categories, low and high expression in spores, showed the same strength of GFP expression in invasive hyphae. The transformants showing intermediate expression in spores from each construct were used for comparison (Fig 2.3).

Using the larger *AVR-Pita* promoter, there was less of a normal distribution of expression intensities compared to smaller promoters. Because only one of the ten transformants showed very high GFP expression, we hypothesized that this level of expression was due to a positional effect resulting from random ectopic integration of the reporter gene and not to the *AVR-Pita* promoter alone. Surprisingly, this transformant did not show high expression in mycelia so its expression was not constitutive. The expression level of GFP seen in mycelium of this transformant was comparable with wild type lacking GFP expression (data not shown). These results demonstrated that even though this transformant is out of range in GFP expression in spores, it still behaves as the *AVR-Pita* promoter in being in planta specific.

Using mRNA from spores, we were unable to detect *AVR-Pita* mRNAs using a conventional RT-PCR assay. This finding contrasted with the results obtained from the GFP-fused promoter, which showed variable levels of expression in spores with all the promoter fragments analyzed (Fig 2.4). To address the question of whether the expression of AVR-Pita in spores is real but too low to be detected by RT-PCR, we used a more accurate method for quantification of expression. Real-time RT-PCR was performed using RNA from spores, from tissue-developed appressoria (20 hpi) and from invasive hyphae (36 hpi). After normalization of fungal content in infected tissue using actin primers, no expression was obtained in spores using *AVR-Pita* specific primers (Fig 2.5). As expected, this gene was highly expressed in infected tissue when the fungus was growing inside the first-invaded cell. This assay suggested that *AVR-Pita* was also expressed in appressoria, although it is not known if significant numbers of these appressoria had penetrated and begun to form primary hyphae.

Discussion

AVR-Pita gene expression correlates with the biotrophic phase

To understand the precise timing of expression of *AVR-Pita* in planta, we used other time points of infection. Conidiospore mRNA was used as time zero and mature lesions 7 days post inoculation as the final time point. All of our results using RT-PCR and quantitative RT-PCR showed that *AVR-Pita* is not expressed in spores. However, these data showed contrasting results on expression of *AVR-Pita* in appressoria. Although we detected expression of the fungal actin gene in all appressorial samples (infected sheath at 20 hpi), *AVR-Pita* expression was not detected in our RT-PCR experiments and it was detected in our quantitative RT-PCR experiments. One possibility for this inconsistency is the biological variability inherent in pathogen-plant interactions. The infection can develop either quickly or slowly depending on variables in the biological assay that are beyond our control. Using the light microscope, it is not possible for us to see when penetration has occurred until a significant primary hypha is visible. Also, although we scan some samples of our infected tissue to see that appressoria have formed, it is not feasible to scan all tissue for uniform infection development, and some sheath sections processed for RNA extractions may contain infection sites that are further developed. Therefore, the different experiments may have used appressoria that differed in whether or not penetration was actually occurring at the time of RNA extraction. As the current techniques do not allow us to sample appressoria at more precise pre- and post-penetration stages, new techniques are needed to define the precise timing of *AVR-Pita* expression relative to penetration into the plant tissue.

New details on the nature of hemibiotrophy in rice blast disease (Kankanala et al., 2007) suggest that new cell invasions are always biotrophic throughout lesion development, and that newly invaded rice tissue initially lacks any visible symptoms of disease. We found that *AVR-Pita* is still being expressed in asymptomatic tissue immediately surrounding maturing lesions at 7 dpi. These results are consistent with this novel view of hemibiotrophy in rice blast. A major question that remains to be addressed is if the thinner necrotrophic hyphae that develop in leaf tissue after biotrophic invasion also expresses *AVR-Pita*. Gene expression analysis in necrotic tissue in maturing lesions will address this question.

Identification of regulatory regions in the *AVR-Pita Promoter*

Deletion analysis of the *AVR-Pita* promoter identified a region that is essential for avirulence activity in spray-inoculated plants. From these results, it was expected that the promoter region that differentiated the active from the inactive fragment contained the regulatory elements needed for in planta specific expression. Bioinformatic search analyses for cis-elements using this *AVR-Pita* promoter region seemed to be inaccurate after our results showed that inactive fragment still showed promoter activity in IH, when it was fused to GFP. For this reason, instead we used the 1.1-kb upstream region from the start codon. Different programs were unable to predict putative regulatory elements specific to *AVR-Pita* and other infection-specific genes. We found that the putative regulatory elements predicted in this in planta specific gene were also found in genes that are known to be repressed during plant colonization (see Chapter 3) such as the melanin-related genes (Table 2.1).

One commonly used method for defining expression patterns and for promoter functional analysis is fusion of the promoter sequence to reporter genes such as GFP. Surprisingly, the GFP expression patterns we see with all three promoter fragments were inconsistent with all of our RT-PCR results. That is, the AVR-Pita promoter:GFP reporter gene is consistently expressed in conidiospores even though we have never detected the *AVR-Pita* mRNA in these spores. All 20 transformants analyzed from this study (10 from each of the 2 promoter constructs) showed GFP fluorescence in spores, although the levels of fluorescence varied from transformant to transformant. The variation in levels of expression in spores is likely to be due to positional effects resulting from integration of the reporter gene in random genome locations by the non-homologous integration events that predominate in transformation of *M. oryzae*. However, position effects would not account for the uniform inappropriate expression in spores. These results suggest that other factors in addition to the *AVR-Pita* promoter sequence itself may be contributing to regulation of *AVR-Pita* expression in planta. So far, there is only one report of extensive promoter analysis of an avirulence gene in *M. oryzae* (Fudal, 2007), which makes it difficult to interpret our results. We do not know if similar results will be obtained with every avirulence gene of this pathogen or if *AVR-Pita* promoter is very unique in its complexity.

Another unexpected finding from our promoter analysis is that the *AVR-Pita* promoter activity as measured using the GFP fusion construct differs from the promoter activity measured by assessing the avirulence phenotype in whole plant expression assays. The 393-bp promoter fragment that was inactive in the whole plant avirulence assay was active in conferring in planta-specific fluorescence in invasive hyphae. It would be interesting to investigate how much protein is actually produced by the inactive promoter (starting from the *Apa*I site, figure 2.1). This information can reveal if there is a special regulation mechanism of avirulence activity besides the repression of expression. Data obtained in this study can be used in comparison analysis using promoters of other plant-specific fungal genes to identify putative co-expressed genes. Those promoters that exhibit similar patterns of expression to *AVR-Pita* will be potential genes for finding conserved motifs in their promoter regions, and possibly targets of the same transcription factor.

Materials and Methods

Fungal strains and transformation

M. oryzae KV1, a strain that was transformed for constitutive cytoplasmic expression of enhanced Yellow Fluorescence Protein (EYFP) (Kankanala et al., 2007), was used to extract genomic DNA for *AVR-Pita* promoter amplification. The fertile laboratory strain CP987 (Orbach et al., 2000) was used as the recipient for transformation using Agrobacterium strain AGL1. Spore suspensions at $1x10^5$ spores/ml were used for co-cultivation with the induced Agrobacterium strains harboring each construct. Transformants were selected for hygromycin B resistance and single-spored on 4% water agar. Single germinated spores were transferred to oatmeal agar plates and left for growth and sporulation.

Plant material and RNA procedures

Excised leaf sheaths of 3 week old YT-16 plants were inoculated with the KV1 strain using a suspension of $1x10^5$ spores/mL. The inoculated sheaths were incubated for 48 hpi at room temperature and one of them was scanned using fluorescence microscopy to confirm infection. The remaining samples were trimmed (as described in Chapter 3) and placed in 1.5 mL tubes to be stored at -80˚ C until processing. Four pieces of leaf sheath were ground in mortars using liquid nitrogen, and RNA was extracted from the powdered tissue using the SV Total RNA Isolation System (Promega Corporation, Madison, WI). After a washing step, 45 ul of nuclease-free water was applied to each column to elute the RNA. This step was repeated twice, giving a final volume of 90 µl. The concentration of RNA was estimated using a Nanodrop spectrophotometer and 20 to 70 ng were used for cDNA synthesis using a First Strand cDNA Synthesis kit (Promega Corporation, Madison, WI) and 4 µl of random primers. The rest of the protocol was followed as indicated by the kit. Each cDNA sample with its corresponding negative control (without reverse transcriptase) was tested for fungal actin and *AVR-Pita* amplification using MgACTIN328-F 5' TCCCATGTCACCACTTTCAA and MgACTIN328-R 5' TTCGAGATCCACATCTGCTG; AVR-PITA-F 5'GCACCTTTTCACACCCAGTT and AVR-PITA-R 5'CTCGGACGCACGTATAAACA primers respectively. Each PCR reaction was set for a final volume of 25 µl containing 2.5 µl of 10X reaction buffer, 1.5 µl of 25mM $MgCl_2$, 0.5 µl of 20mM of dNTP's, 0.5 µl of 10 µM of each primer, 0.2 µl of 10 u/ml Taq polymerase, and 2 µl of each cDNA. The amplification profile was as follows: 95˚C for 30 seconds (secs), 50˚C for 45 secs, 72˚C for 1 minute (min) repeated 35 cycles and a final step of 72˚C for 1 min. Ten µl of each PCR reaction were run on 2% agarose gels. RNA for detection of *AVR-Pita* at different time points of the infection was extracted using the TRIZOL method (Invitrogen, Carlsbad, CA) to increase the amount of starting material and the yield.

Microscopy

Differential Interference Contrast microscopy (DIC) and epifluorescence microscopy were performed using a Zeiss Axioplan 2 IE Mot microscope. Cells were observed with a 63X C-Apochromat (NA 1.2) water immersion objective lens. Fluorescence of the EYFP protein was observed using a fluoArc lighting system and a YFP-specific filter (excitation 500 ± 20nm,

emission 535 ± 30 nm, filter set 46), both from Zeiss. Images were acquired using a Zeiss AxioCam HRc camera and analyzed with Zeiss Axiovision® Digital Image Processing Software, Version 3.1. Fluorescence was evaluated in spores, at 20 hpi in appressoria and at 28 hpi in invasive hyphae, using 5 sec exposures for fluorescence imaging of each sample.

Quantitative real-time RT-PCR

cDNA was synthesized using 1 to 2 μg of total RNA extracted from spores of the fungus grown for two weeks on oatmeal agar. Infected tissue and spores were processed similarly using the TRIZOL method (Invitrogen, Carlsbad, CA). As a housekeeping gene, the *M. oryzae* actin gene (MGG_03982) was amplified using MgActinF 5'AGC GTG GTA TCC TCA CTT TGC and MgActinR 5' ATC TTC TCT CGG TTG GAC TTG G primers. Primers AVR-PitaF 5' TGC CCT CCT TTC TTC AAC AAC and AVR-PitaR 5' CCC ATT CGT AAC CAT AAT CTT TCC were used to amplify the infection specific *AVR-Pita* gene. Both primers and templates were first tested using a regular RT-PCR assay. Real-time RT-PCR was performed using the following protocol: Cycle 1(1X); step 1, 95.0ºC for 05:00; Cycle 2 (40X); step 1, 95.0ºC for 00:20; step 2, 54.0ºC for 00:30; step 3, 72.0ºC for 00:45. Data collection and real-time analysis were enabled. Cycle 3 (1X); step 1, 95.0ºC for 01:00; Cycle 4(1X); step 1, 55.0ºC for 01:00; Cycle 5, (80X); step 1, 55.0ºC for 00:10. Increase setpoint temperature after cycle 2 by 0.5ºC. Each reaction was set to 25 μl of final volume containing 12.5 μl of 2X iQ™ SYBR Green Supermix, 1 μl of 10 μM of each primer and 10.5 μl of cDNA. Four dilutions of all cDNAs samples were used to test primer efficiency with the housekeeping gene primers. Reactions were run in an iCycler machine (Bio-RAD, Hercules, CA). The sample with the lowest concentration (highest Ct value) was used to adjust the concentration of the other samples using the formula: dilution factor = $2^{-(CtA-CtB)}$, where CtA is the Ct value of sample A and CtB is the Ct value of the sample with the lowest concentration. Two replications of the obtained dilutions were used for the real experiment.

Determination of AVR-Pita transcription start site

Infected tissue RNA samples whose cDNAs were positive for the *Avr-Pita* transcript were used for 5'-RACE PCR analysis. About 180 ng of RNA were used for cDNA synthesis using the BD SMART™ RACE cDNA Amplification kit (BD Biosciences, San Jose, CA) according to the manufacturer instructions. cDNA was used as a template for 5'-end

amplification using a gene specific primer RACEAvr3 5’ GCC CCA CGAGGCGAGCTCGGCACA AC 3’. The amplification profile was as described in the manual instructions using the program 1 recommended for primers with T_m >70 ˚C and a final step with 25 cycles. A band ranging between 300 and 400-bp was isolated from the agarose gel using NucleoTrap® Nucleic Acid Purification kit (BD Biosciences). The purified fragment was ligated into pGEM®T-Vector (Promega Corporation, Madison, CA) as described by the manufacturers, and cloned into NovaBlue competent cells (Novagen, San Diego, CA). Two independent clones were used for plasmid extraction and sequencing analysis using M13F and M13R universal primers.

AVR-Pita promoter constructs

A longer *AVR-Pita* promoter fragment was amplified using 200 ng of genomic DNA from strain KV1. The primers used were Avr-PitaInactiveEcoRI-F primer 5’ GCG AAT TCA TAA TAT GGG CCC AAC TCTTA and Avr-PitaBamHI-5R 5’ GCG GAT CCG CAA AAA TAA TGT TAA TTG TGC (restriction enzyme sites are underlined). The 393-bp fragment was cleaned by using QIAquick® PCR Purification Kit (Qiagen, Valencia, CA), and cloned into the pGEM® T-Vector. Two positive clones from plasmid restriction analysis were used for sequencing with vector-specific T7 and SP6 universal primers. The inactive *Eco*RI /*BamH*I fragment was subcloned into pBV144. The binary plasmid pBV144, containing a 475-bp fragment corresponding to the minimal active AVR-Pita promoter and a hygromycin resistance gene, was used as the backbone to replace the active for the inactive fragment. The new plasmid was introduced into NovaBlue competent cells under selection using kanamicyn resistance. Positive clones were tested by restriction analysis and sequencing to confirm the insert ligation and orientation.

A longer *AVR-Pita* promoter fragment, 1.129-bp long, was amplified and cloned using the same conditions described above for the inactive fragment using WAvr-pita-SacI-F 5’ ATT GAG CTC GGG TAA TAC CTT ATC GA and Avr-PitaBamHI-5R 5’ GCG GAT CCG CAA AAA TAA TGT TAA TTG TGC primers. Because this large promoter fragment has an internal *Eco*RI restriction site, a *SacI* site was used in the forward primer. Blunt ends were created in the *Sac*I ends from the insert and vector for ligating the insert into the vector.

Figure 2.1 Avirulence activity of *AVR-Pita* using different promoter fragments

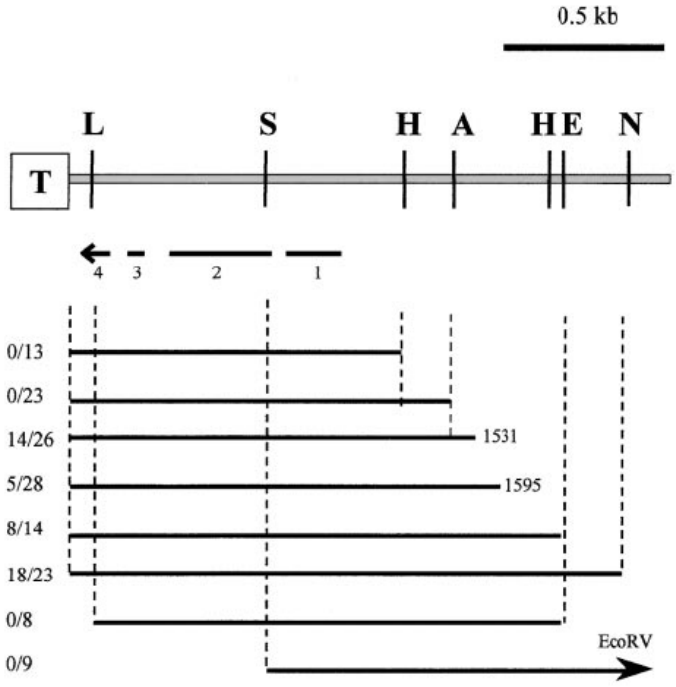

Fragments of *AVR-Pita* used in whole plant infection complementation tests. The 4 exons of *AVR-Pita* are shown. The stop codon is separated from the telomere repeat sequences (Boxed T) by 48-bp. Letters indicate restriction enzyme sites: A, *Apa*I; H, *Hind*III. Only relevant sites mentioned in the text are indicated. Numbers on the left indicate number of avirulent transformants from the total that were tested (Orbach et al., 2000).

Figure 2.2 Expression of *AVR-Pita* at different infection stages of rice blast disease

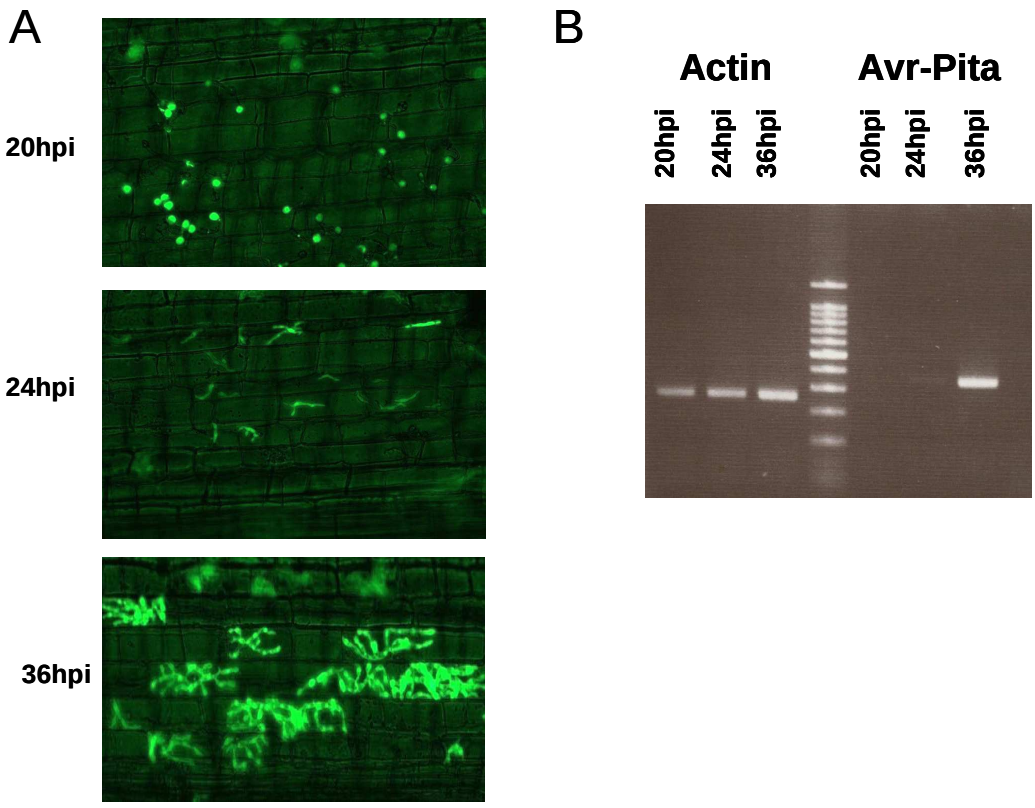

(A) Representative images of samples analyzed for the AVR-Pita transcript. Merged image of DIC and EYFP fluorescence showed the stage of development of strain KV1 expressing constitutive EYFP in rice sheath epidermal cells. Appressoria formed at 20 hpi and primary hyphae were expanding into bulbous IH at 24 hpi. By 36 hpi, the fungus was growing as biotrophic IH. **(B)** RT-PCR using total RNAs extracted from infected sheath samples in (A) showed that the fungal actin mRNA was detected in each sample. *AVR-Pita* mRNA was barely detected at 24 hpi (hard to see in this image) and was relatively abundant at 36 hpi.

Figure 2.3 Sequence of the 1.1-kb *AVR-Pita* promoter used in this study

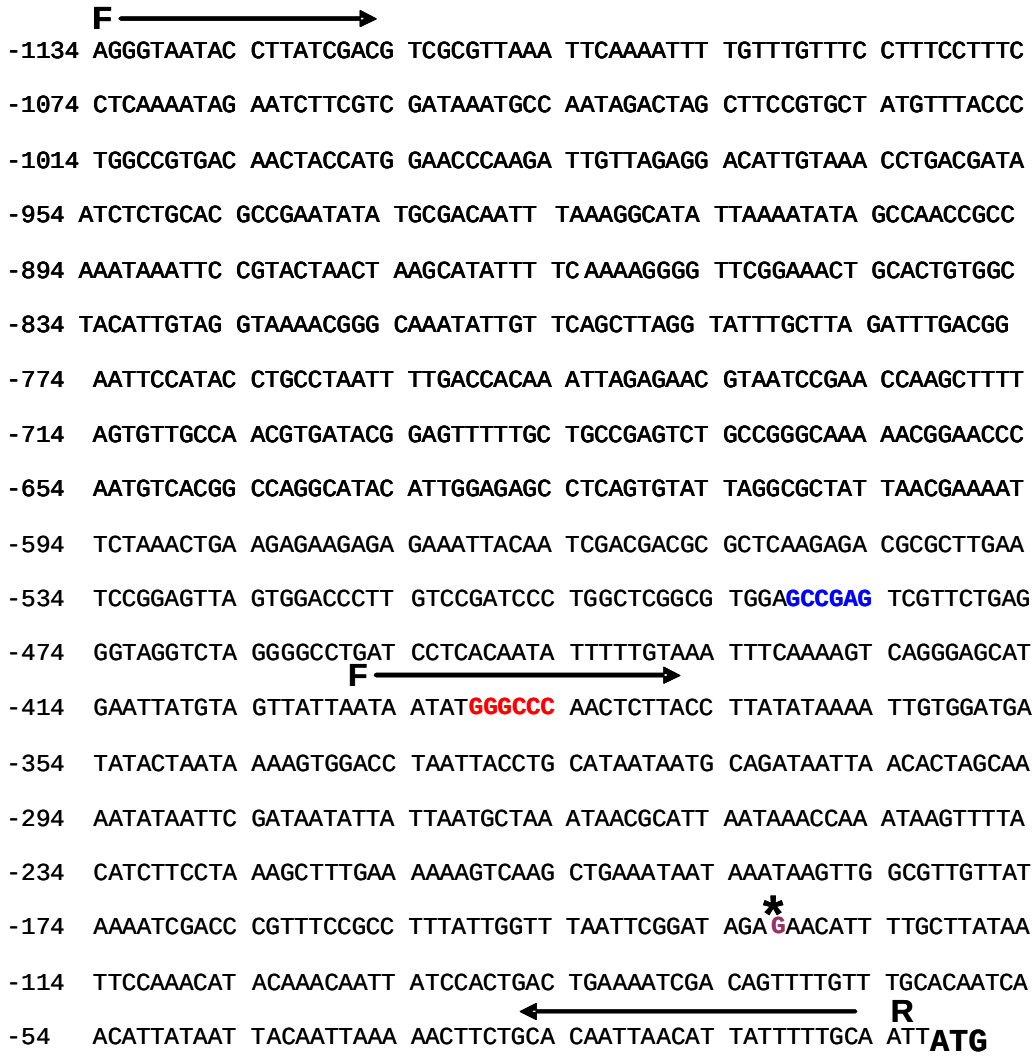

Arrows indicate the location of the primers used to amplify the respective promoter fragments. Letters in blue indicate the start of active promoter, and the letters in red indicate the *Apa*I site that delimits the inactive fragment. The asterisk indicats the transcription start site and the bold ATG corresponds to the translation start site.

Figure 2.4 GFP expression pattern using different *AVR-Pita* promoter fragments

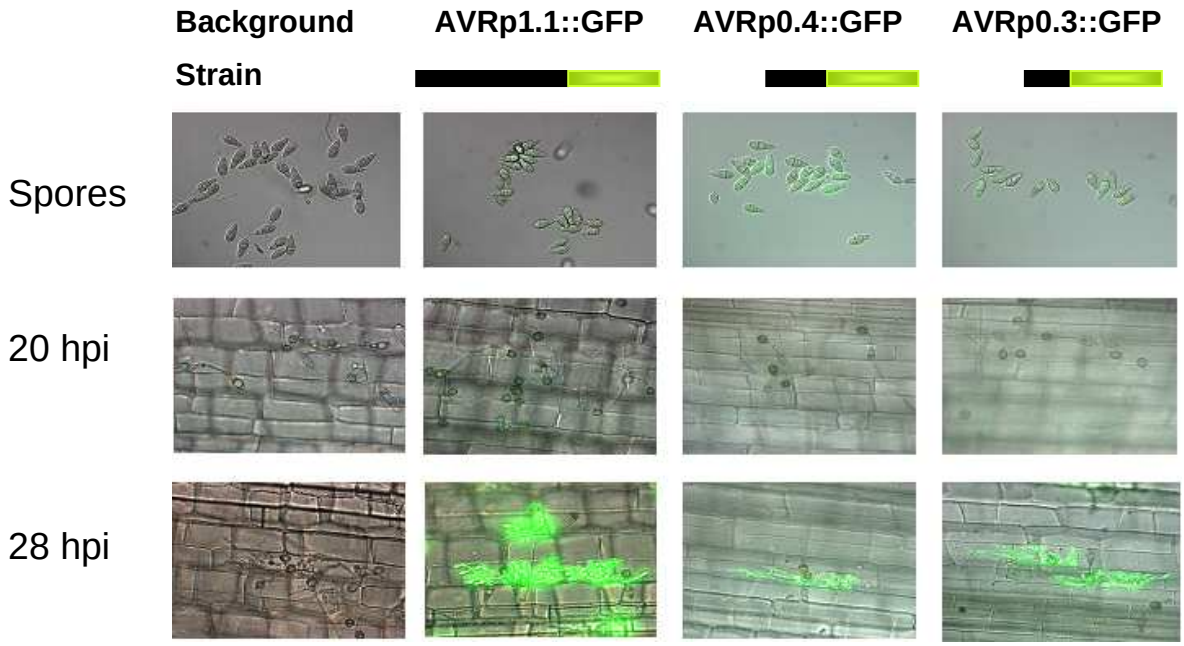

Merged image of DIC and EGFP fluorescence showing promoter activity in spores produced on oatmeal agar plates; and appressoria at 20 hpi, and invasive hyphae at 28 hpi, formed on rice sheath epidermal cells. Due to the high level of variation in the expression of GFP in transformants harboring different constructs, only transformants showing intermediate levels of expression in spores are shown here. The 1.1, 0.4 and 0.3 correspond to the larger, active and inactive promoter, respectively. The background strain is the CP987 without the GFP construct. The excitation light exposure time was fixed to 5 seconds for comparison of the relative levels of fluorescence for each GFP construct..

Figure 2.5 Expression of *AVR-Pita* is not detected in spores using real-time RT-PCR

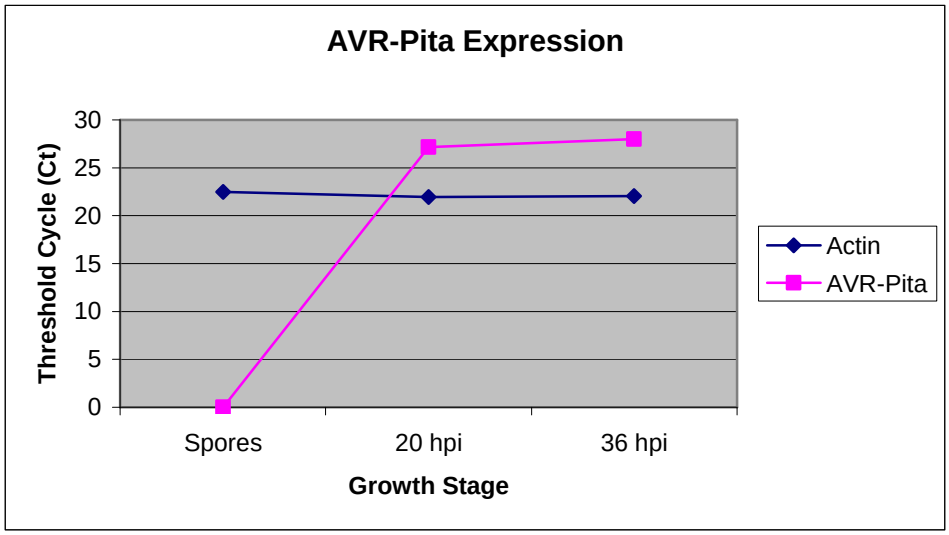

Quantitative analysis of *AVR-Pita* gene expression using RNA from KV1 spores collected from 10 day old oatmeal agar plates. The 20 hpi and 36 hpi samples correspond to leaf sheath infected with KV1. Actin expression was used for template normalization.

Table 2.1 Number of occurrences of repetitive sequences found in thepromoters of *AVR-Pita* and other M. oryzae genes

Gene Name	Fold Change	Number of copies	
		RSP00161	RSP00508
AVR-Pita	3.0	5	3
Pwl2	63.0	2	8
AMG08263	100	5	3
AMG16216	48.0	3	4
AMG08160	58.0	0	1
AMG15980	61.0	6	3
AMG06765	75.0	2	6
PTH11	-5	0	0
AMG01944	-28.1	3	5
AMG02948	-24.9	3	2
AMG06064	-24.6	0	0

Promoter regions corresponding to 1.0-kb of 5'-sequence were analyzed by the Softberry-TSSP program for prediction of plant promoters. The most frequent repetitive sequences are indicated as RPS00161 and RSP00508. Other *M. oryzae* genes used in this analysis and their level of expression (Fold Change as determined in Chapter 3) during infection are also indicated.

Table 2.2 Description of the different fungal transformants obtained from the *AVR-Pita* promoter-GFP analysis

Promoter Size	Transformant	GFP copies	Fluorescence in:		
			Spores	Appressoria	Invasive hyphae
1.1-kb	1	1	+++	+++/-	+++
	2	1	+	+/-	++++
	3	1	+/-	+/-	+
0.48-kb[a]	1	2	+++	+++/-	+++
	2	1?	++	++/-	++
	3	1	++	++/-	++
0.37-kb	1	1	+++	+	++
	2	1	++	+	++
	3	1	+	-	+

Transformants obtained from each construct showed different levels of GFP expression. Size of each promoter is indicated and expression level obtained in each developmental stage in 3 independent transformant is also shown. Number of copies of GFP was determined by Southern blot analysis. Pluses and minus indicate arbitrary measurement of GFP intensity. Measurement in appressoria indicates that some of them were showing fluorescence and others not in the same transformant (indicated by +++/-, or ++/- or +/-). [a] Data were obtained from C. H. Khang and S. Kang (Penn State University).

CHAPTER 3 - Analysis of the Interaction Transcriptome of Biotrophic Invasion by the Rice Blast Fungus, *Magnaporthe oryzae*

Abstract

The hemibiotrophic fungus *Magnaporthe oryzae* produces intracellular invasive hyphae (IH) that alter host cellular processes and defense responses as they successively invade living rice cells. Understanding fungal and rice genes that contribute to biotrophic invasion has been difficult because so few plant cells have encountered IH at the earliest infection stages. We developed a procedure for reproducibly obtaining infected rice sheath RNA that contains ~20% fungal RNA at a point when most IH were still growing in first-invaded cells. The RNAs were analyzed using the whole-genome *M. oryzae* oligoarray and a rice oligoarray. Using a 3-fold differential expression threshold, 1693 fungal genes and 1259 rice genes were induced or repressed during the interaction. Rice genes induced >50-fold during infection were enriched for genes involved in transferring information from sensors to cellular responses. Fungal genes induced >50-fold in IH included the *PWL2* avirulence gene and many genes encoding hypothetical secreted proteins. The IH-specific secreted proteins are candidates for effectors, proteins that pathogens secrete inside live host cells to control cellular processes. Gene knock-out analyses of three putative effector genes failed to show major effects on pathogenicity, underscoring challenges ahead for functional analyses of the genes in the biotrophic interaction transcriptome.

INTRODUCTION

Rice blast is a significant disease that affects one of the most important food sources in the world. Each year rice blast causes losses between 10 and 30% even though diverse cultivars expressing different resistance genes are used for cultivation (Talbot, 2003; Kawasaki, 2004). The causal agent, the hemibiotrophic fungus *Magnaporthe oryzae* (formerly *Magnaporthe grisea*, (Couch and Kohn, 2002), undergoes complex morphological development throughout its infection cycle. Many studies have focused on the process by which fungal spores land on leaves and produce germ tubes that differentiate into appressoria, specialized cells for leaf surface penetration (Howard and Valent, 1996; Talbot, 2003; Dean et al., 2005). After appressorial penetration, the fungus first grows within plant cell lumens as thin, filamentous primary hyphae, which then differentiate into biotrophic invasive hyphae (IH) in susceptible (compatible) interactions. Kankanala et al. (Kankanala et al., 2007) recently reported new cellular details of biotrophic blast invasion. They showed that IH are tightly enclosed in a plant-derived extra-invasive hyphal membrane (EIHM), and that IH stimulate membrane dynamics within invaded rice cells. They suggested that IH co-opt plasmodesmata for cell-to-cell movement and for preparing neighboring cells before invasion. To execute this complicated disease strategy, IH must express specialized genes that, among other things, control rice gene expression. We refer to these pathogen and host genes whose expression directly relates to the biotrophic interaction as the interaction transcriptome (Birch and Kamoun, 2000).

Few fungal genes that are specifically expressed in IH have been identified (Talbot, 2003; Donofrio et al., 2006). Some genes that function in other infection stages also play a role during invasive growth in planta. For example, the mitogen-activated protein kinase (MAPK) PMK1 functions in appressorium formation and in planta growth. PMK1 expression is detectable in various fungal cell types (vegetative mycelium, conidia and IH), but it is induced in appressoria and developing conidia (Bruno et al., 2004). A few genes, such as the efflux pump gene *ABC1* and the neutral trehalase *NTH1*, have their major effect on plant cell colonization. *MIR1* encodes an IH-specific nuclear protein, although gene replacement experiments have not identified its function (Li et al., 2007).

IH-specific genes that encode secreted proteins are of special interest. These genes might encode effectors, proteins that the fungus secretes inside live plant cells to control plant cellular processes. In various pathosystems, effectors have been identified by their avirulence activity in triggering *R* gene mediated hypersensitive resistance. Currently, three blast effector candidates were identified as avirulence (*AVR*) genes. The *PWL* genes (Kang et al., 1995; Sweigard et al., 1995), *AVR-CO39* (Peyyala and Farman, 2006), and *AVR-Pita* (Orbach et al., 2000) all encode IH-specific proteins with secretion signals. The predicted mature AVR-Pita protease functioned to trigger hypersensitive resistance when it was transiently expressed in rice cells with the *R* gene *Pi-ta* (Bryan et al., 2000). Thus, AVR-Pita, and probably PWL2 and AVR-CO39, appear to be rice blast effectors. However, the few, diverse examples of blast AVR/effectors have not provided motifs for identification of additional effectors among the genes predicted in the *M. oryzae* genome (Dean et al., 2005). One strategy for identification of AVR proteins among those secreted by intracellular fungal structures was validated by Catanzariti et al. (Catanzariti et al., 2006)when they showed that proteins secreted by haustoria of the flax rust fungus are enriched in AVR proteins. Therefore, identification of IH-specific secreted proteins represents a reasonable approach for identification of additional blast effectors.

On the host side of the interaction, plant genes encoding enzymes of phytoalexin biosynthesis as well as defense and pathogenesis-related proteins were up-regulated during infection in diverse host pathogen systems (van Loon et al., 2006). The same genes were induced in incompatible (resistant) and compatible interactions, although expression usually occurred later and at lower levels during compatibility (Song and Goodman, 2001; Tao et al., 2003; Vergne et al., 2007). For blast, the jasmonic acid-induced rice transcription factor gene JAMyb (AK069082) represented a rare example of a host gene that was more highly expressed in compatible than in incompatible interactions (Lee et al., 2001).

Several studies have examined gene expression by the blast fungus during axenic growth. For example, >28,000 expressed sequence tags (ESTs) were obtained from cDNA libraries representing fungal cell types that are produced in vitro (mycelia, conidia, appressoria, and perithecia), mycelium from different culture conditions, and a *pmk1*$^{-}$ nonpathogenic mutant lacking PMK1 (Ebbole et al., 2004; Soanes and Talbot, 2005). Expression data available for

appressoria and/or mycelia include serial analysis of gene expression (SAGE), robust-long SAGE, massively parallel signature sequencing (MPSS), and microarray analyses (Irie et al., 2003; Takano et al., 2003; Gowda et al., 2007). Microarray analyses have compared gene expression in germlings growing on inductive surfaces (promoting appressorium formation) and non-inductive surfaces (Dean et al., 2005), and gene expression in mycelium grown in nitrogen-rich and nitrogen-deficient media (Donofrio et al., 2006). All studies showed statistically significant expression differences for the various fungal cell types and growth conditions.

In planta expression analyses have also been performed. Studies performed after macroscopic symptoms developed identified both fungal and rice genes expressed in planta (Kim et al., 2001; Rauyaree et al., 2001; Matsumura et al., 2003). However, infected tissue with visible symptoms probably included filamentous necrotrophic hyphae in addition to IH (Berruyer et al., 2006). Large scale EST analysis (Jantasuriyarat et al., 2005) and microarray analysis (Vergne et al., 2007) performed at early infection stages before appearance of macroscopic symptoms focused on rice gene expression because so little fungus was present in the infected leaf tissue. Expression analysis of early biotrophic invasion, when the fungus occurs predominantly as IH in first-invaded cells, will provide the best opportunity to assess IH gene expression and how IH affect rice gene expression. Since this early colonization stage corresponds to the point when most *AVR/R* gene interactions induce hypersensitive resistance, detailed expression analyses should identify effector/AVR proteins that function in blast disease.

Our goal was to obtain an in depth view of the rice blast interaction transcriptome during biotrophic invasion and to relate this view to the cellular biology of invasion. Using the highly compatible interaction between *AVR-Pita*-containing fungal strain KV1 and susceptible rice leaf sheath lacking *Pi-ta* (Kankanala et al., 2007), we developed a procedure to obtain infected tissue RNAs that were enriched for RNA from IH growing in first-invaded rice cells. After assessing the proportion of IH RNAs in infected samples, we produced balanced control samples containing a similar proportion of RNA from pure mycelium and mock-inoculated rice. An *M. oryzae* microarray was used to compare gene expression in IH to expression in mycelium, and a rice microarray was used to compare expression in the infected tissue to expression in mock-

inoculated tissue. We report the first detailed view of the biotrophic blast interaction transcriptome, and initial functional analyses resulting from this view.

RESULTS

Infected Leaf Sheath Samples Enriched for Biotrophic Invasive Hyphae

A major challenge for expression profiling at early stages of fungal infection is that most plant cells have not yet encountered the fungus. We developed a reproducible procedure to obtain infected tissues enriched for rice cells containing IH and their immediate neighbors. We used sheath tissues at 36 hours post inoculation (hpi) because infection development at this point was relatively synchronous: some IH were growing in first-invaded cells, some had filled first-invaded cells, and some had just moved into neighbor cells (Figure 3.1A). Use of a fungal strain with strong constitutive, cytoplasmic expression of enhanced yellow fluorescent protein (EYFP) allowed visualization of contaminating fungal cell types in the tissue as well as the state of development of IH. Although we confirmed that inoculation of fungal conidia in gelatin solution was important for achieving uniform distribution of appressoria, this practice promoted growth of vegetative mycelium on the sheath surface. The first step in our procedure was to remove vegetative hyphae, appressoria and conidia from this surface. Abundant hyphae that invaded the tissue from cut sheath ends were also discarded. Using the procedure of Kankanala et al. (Kankanala et al., 2007)we next manually dissected the sheath tissue to produce pieces with the inoculated adaxial epidermal layer and ~3 underlying mesophyll cell layers, thus removing many cell layers that had not yet experienced fungal invasion. The last steps were rapid epifluorescence screening for selection of only densely invaded sheath segments and freezing of selected segments in liquid nitrogen. The process was carried to completion with a single sheath

piece at a time, resulting in ~2 min of processing time for each. With this procedure, we obtained infected tissues that were enriched both for fungal RNA content and for the biotrophic IH cell type (Figure 3.1A).

To estimate the ratio of fungal to rice RNAs in the infected sheaths, we compared RT-PCR amplification of the fungal actin gene in infected tissue to amplification in standards produced by mixing pure mycelial RNA and mock-inoculated rice RNA. cDNAs were prepared from both samples, and the actin gene was amplified using specific primers. Presence of IH RNA was confirmed using *AVR-Pita* primers. Using this assay, fungal RNA content in infected tissues was generally ~20% of the infected tissue RNAs (Figure 3.1B). The trimmed sheath procedure provided a significant enrichment of IH RNAs compared to RNAs from leaf samples using spray inoculation (Figure 3.1C).

Identification of the Interaction Transcriptome Using Microarray Hybridization

Samples from three biological replicates of 36 hpi-infected rice sheaths were analyzed using the *M. oryzae* whole genome microarray (Agilent Technologies). This DNA oligoarray contains 60-bp oligonucleotide probes corresponding to 15,170+ predicted *M. oryzae* genes and 6,325 rice genes. Genes represented in this oligoarray are described in the *Magnaporthe grisea Oryza sativa* (MGOS) Database (http://www.mgosdb.org), (Soderlund et al., 2006). The same samples were used with the Agilent rice microarray, which contains oligonucleotides corresponding to ~21,500 expressed rice genes (based on cDNAs from the KOME database; ~60% coverage of the genes in japonica rice; http://cdna01.dna.affrc.go.jp/cDNA/). Complementary RNAs from infected tissues were labeled with Cy3 or Cy5 and hybridized together with control RNA mixtures (20% mycelial RNA and 80% mock-inoculated rice RNA) labeled with the other dye (Hughes et al., 2001). Three biological replications were performed, each with 4 separate microarray hybridizations (2 technical replicates and 2 dye swap experiments). Data were analyzed by Rosetta Resolver® and signature sequences (denoted as significantly different from the diagonal) showed correlations of >80% between biological

replicates. Technical replicates of the same biological samples showed correlations >95%. All 12 data sets were subsequently analyzed together to yield all values reported in this Chapter.

If we were accurate in balancing the fungal to plant RNAs in infected and control samples, we would expect that fungal housekeeping genes would show roughly similar signals in both. The ribosomal protein genes showed expression ratios between +3 and -1 when comparing IH to mycelium. Therefore, either IH are slightly more metabolically active than mycelium in liquid culture, or we underestimated the proportion of IH RNA in the infected tissue. In either case, due to the relative expression levels for housekeeping genes, we focused on the genes that showed at least 3-fold changes in expression levels (Fugure 3.6). Using the 3-fold threshold, 1079 fungal genes were induced and 614 genes were repressed in IH relative to mycelium. For rice, 963 genes were induced and 296 genes repressed in invaded tissue. With noted exceptions, P-values corresponding to differentially expressed genes were highly significant (Figure 3.6).

For validation of microarray results, we performed RT-PCR on a selection of fungal and rice genes with differential expression. cDNAs from four sources including mycelium, 36-hpi mock-inoculated sheaths, 36-hpi inoculated sheaths, and mycelium/mock mixtures were used as templates for amplification. Quality of the cDNA was tested using *M. oryzae* actin primers that spanned an intron to differentiate cDNA from genomic sequences. The expected actin fragment was amplified from mycelium and infected tissue (Figure 3.2A). Amplification was not seen in negative controls in which the reverse transcriptase had been omitted (data not shown). In subsequent experiments, only three samples were included for each gene (Figure 3.2A,B).

First, the 30 fungal sequences having expression levels >50-fold higher in IH were chosen for validation (Figure 3.2A). Among these sequences, 22 were successfully amplified from infected rice. No amplification was seen with mock-inoculated rice or mycelial samples. One predicted gene had two possible transcripts, AMG08417.1 and AMG08417.2. Primers designed to differentiate these transcripts showed that the transcript identified in our microarray analysis corresponded to AMG08417.2, and suggested that AMG08417.1 was incorrectly annotated. For some sequences that failed to amplify, new primers were designed and tested

without success. Maybe genes identified in sequenced laboratory strain 70-15 contain polymorphisms in the primer binding sites in strain KV1.

The same cDNAs were used for amplification of down-regulated fungal genes (Figure 3.2A). A gene homologous to clock-controlled gene-9 from *Neurospora crassa* (AMG12697.1) and the G-protein coupled receptor *PTH11* (AMG05260), both >5-fold down-regulated, were amplified only from the mycelial sample. Melanin biosynthesis genes scytalone reductase (AMG06064, -24.6-fold) and tetrahydroxynaphthalene reductase (AMG01944, -28.1-fold), were amplified only from mycelial RNAs. The hydrophobin *MPG1* (AMG14765, -21.6-fold) was amplified from mycelial RNAs, though a weaker band was amplified from infected tissue (data not shown). This is probably because there is still expression of *MPG1* in IH even though it is significantly down-regulated compared to mycelium.

RNA samples used for validation of fungal genes were also used for validation of up-regulated rice genes (Figure 3.2B). For the eight rice genes we tested with expression levels 26-fold or higher during infection, gene-specific fragments amplified from infected but not from mock-inoculated rice. A gene with 9.5-fold higher expression was only amplified from infected tissue. However, three genes, with 4-, 13-, and 3-fold up-regulation, were amplified from both infected and mock-inoculated tissues. Primers designed for rice genes did not amplify PCR fragments from the mycelial sample.

Up-regulated IH Genes Are Enriched for AVR Genes and Newly-Described Genes

The cRNAs from differentially-labeled 36-hpi infected tissue and control mixtures were hybridized to *M. oryzae* microarrays. The two expected *AVR* genes were among the 1079 fungal genes expressed at >3-fold levels in IH relative to mycelium. *AVR-Pita* (RMG00001) was induced 3-fold in IH, and *PWL2* (AMG11184) was induced 63-fold. In planta specific expression of both *AVR* genes was verified by RT-PCR (Figure 3.2A). The third in planta-specific *AVR* gene, *AVR-CO39* was not represented on the microarray. The appressorium-specific *AVR* gene *ACE1* encodes a cytoplasmic polyketide synthase-nonribosomal peptide synthetase (Böhnert et

al., 2004), and it showed negligible signals in both IH and mycelium. Detection of expression of *AVR* genes suggested that these data represent an in depth view of IH gene expression.

Fungal genes that were highly expressed in IH were more likely to encode secreted proteins and less likely to have previous expression data (Figure 3.6). In the >50-fold group, 50% of encoded proteins had predicted signal peptides and 3% had ESTs. In the 10 to 50-fold group, 19.3% of encoded proteins had predicted signal peptides and 19% had ESTs. In the 3- to 10-fold group, 9.5% of encoded proteins had predicted signal peptides and 38% had ESTs. These results demonstrated that the most abundant IH mRNAs often corresponded to extracellular proteins that are being identified as expressed for the first time. The absence of previously reported expression data for the highly up-regulated genes in IH was consistent with the general lack of early-stage in planta expression data available for the blast fungus. These results validate our hypothesis that IH express many specialized genes during biotrophic invasion of rice.

For the 59 predicted secreted proteins that were >10-fold up-regulated in IH (Table 3.1), only 5 had putative functions based on homology to known proteins. These included *PWL2*, an endochitinase, a laccase, a cellulase, and an endonuclease. None of these genes had corresponding ESTs. Five genes of unknown function had reported ESTs. The remaining sequences corresponded to genes predicted from genome sequencing and annotated as hypothetical proteins. Overall, these results are consistent with the prediction that the fungus induces and subsequently delivers specialized proteins inside the host cell to establish biotrophic infection.

Genes Expressed in Fungal Cell Types Outside the Plant Are Down-Regulated in IH

In infected samples, 614 fungal genes were down-regulated more than 3-fold (Figure 3.7). For this down-regulated gene set, 71% were hypothetical proteins and 9% had predicted signal peptides. While only 17% of the 256 genes that were induced >10-fold in IH had reported expression data, 76% of the 135 genes that were repressed >10-fold had expression data (Figure 3.7). This finding showed that genes that were down-regulated in IH were highly represented in the sequenced cDNA libraries from axenically-grown fungus. Among the 50 most down-

regulated genes (Table 3.2), EST hits were obtained from all cDNA libraries representing the different in vitro growing conditions and cell types (Ebbole et al., 2004).

Known Pathogenicity Genes Were Unchanged or Down-Regulated in IH

We first assessed expression levels for genes involved in appressorium formation (Table 3.3). *PTH11*, the G-protein coupled receptor involved in surface sensing and appressorium formation, was repressed 5.3-fold in IH (relative to mycelium), and *MPG1*, the hydrophobin gene with a major role in appressorium development (Soanes et al., 2002) was repressed 21.6-fold in IH. *PTH11* showed low intensity signals in both channels (317 in mycelium and 78 in IH), whereas *MPG1* showed relatively high signals (169,000 in mycelium and 7,530 in IH). Although probe design has a major impact on hybridization signals, the large differences in signal intensities suggest that *PTH11* has low expression levels in both mycelium and IH and that MPG1 is highly expressed in mycelium and is also expressed in IH, although at a lower level than in mycelium.

Other genes with a role in appressorium formation showed similar expression levels in IH and mycelium (Table 3.3). The adenylate cyclase-interacting protein ACI1, which is involved in signal transduction during appressorium formation, was the only known pathogenicity gene that reached the 3-fold threshold. The *MAGB* and *MGB1* genes, encoding Gα and Gβ subunits, respectively, of heterotrimeric G proteins did not give significant hybridization signals in IH or mycelium. The MAP kinase PMK1 plays a key role in appressorium formation, and is highly expressed in appressoria (Bruno et al., 2004) et al., 2004). Although *PMK1* also plays a role in infectious growth, it shows similar expression levels in IH and mycelium. Genes for calmodulin and the vacuolar serine protease were relatively highly expressed in both tissues.

We also analyzed fungal genes with a role in penetration (Table 3.3). The *MST12* transcription factor is regulated by PMK1, and is required for both penetration and invasive growth. This transcription factor showed similar hybridization signals in both IH and mycelium. The multi-drug resistant efflux pump gene *ABC3*(Sun et al., 2006) is not significantly expressed in either cell type. However, the *RSY*1, *BUF1*, and *4HNR* genes in the melanin biosynthesis pathway showed dramatic down-regulation in IH (>20-fold). This later result is consistent with

demonstrations that melanin-deficient mutants form unpigmented appressoria that can only penetrate abraded cuticle (Howard and Valent, 1996; Kankanala et al., 2007).

Expression levels for pathogenicity genes that function in invasive growth might show differential expression. However, *ABC1* and *MgAPT2* (Gilbert et al., 2006) showed low hybridization signals in IH and mycelium. *NTH1* showed higher expression levels in both cell types. The alternative oxidase gene *MgAOX* was repressed 20-fold during invasive growth, supporting reports that *MgAOX* was repressed during normal invasive growth, and that it may only play a role during oxidative stress conditions generated by respiration inhibitor fungicides (Avilla-Adams and Köller, 2002) and references therein). As one note of caution, the *MIR1* gene is specifically expressed in IH (Li et al., 2007), but our analysis did not detect this differential expression.

In vitro Growth Conditions Do Not Mimic Biotrophic Invasion

The blast fungus produces numerous enzymes that degrade xylans, cellulose and other components of plant cell walls. However, their role during biotrophic invasion is not understood. Plant cell wall degrading enzymes are induced in mycelium grown on nutrient medium containing isolated walls as the major carbon source (Wu et al., 2006), and cDNAs sequenced from mycelium grown on plant cell wall medium have a higher representation of extracellular proteins than cDNAs from other sources (Ebbole et al., 2004). As mentioned, one of the >10-fold up-regulated secreted protein genes (Table 3.1) encodes a putative cellulase. However, out of 5 characterized xylanases (Wu et al., 2006) represented in the microarray, none were up-regulated during biotrophic invasion. ESTs from cell wall-grown mycelium were well represented among transcripts that were repressed in IH (Table 3.2), but none corresponded to the >10-fold induced genes. These results suggest that growth on nutrient medium containing plant cell walls does not mimic the intracellular environment experienced by IH undergoing biotrophic invasion.

Genes required for pathogenicity in several fungal pathogens are induced during growth in media lacking sufficient nitrogen, suggesting that the plant environment might be nitrogen-deficient for the pathogen (Reviewed in (Donofrio et al., 2006). We compared our results on

expression in IH to an expression analysis for mycelium grown under nitrogen starvation conditions, also performed using the *M. oryzae* microarray (Donofrio et al., 2006). Expression profiles for the two conditions are totally different. Of the 5 pathogenicity genes up-regulated by nitrogen starvation, *PTH11*, *MPG1*, *4HNR*, and *AOX* were highly down-regulated in IH (Table 3.3). *NTH1*, the remaining pathogenicity gene induced by nitrogen starvation, was unchanged in its expression level (Table 3.3). Only 3 of the top 55 genes up-regulated by nitrogen starvation were also up-regulated in IH. These were an L-serine dehydratase (AMG03487), an oligonucleotide transporter (AMG11118) and a putative sensor histidine kinase (AMG04824). Neither the global nitrogen regulatory transcription factor *NUT1* (AMG14166), nor a predicted nitrogen regulatory protein *tamA* (AMG09252) (Donofrio et al., 2006) was up-regulated in IH. We conclude that IH were not experiencing nitrogen starvation during biotrophic invasion.

Highly Up-Regulated Rice Genes Encode Signal Transduction Components and Transcription Factors

RNA samples that are enriched for IH genes must also be enriched in rice genes from cells impacted by IH. Using the same IH-enriched RNA samples in experiments with the Agilent rice microarray and a 3-fold cut-off level, 963 genes were induced and 296 were repressed in biotrophically invaded tissue. These genes belonged to multiple categories (Table 3.5).

Seventeen genes showed >50-fold induction (P-values ranged from $3x10^{-15}$ to 0) in infected rice relative to mock-inoculated rice (Table 3.6). Several of these encode unknown proteins, including the most highly induced gene AK071227. Several themes, defined by 3 or more examples, occur in this protein set. Genes for mitogen-activated protein kinase kinase kinases (MAPKKK), for transcription factors, and for cytochrome P450 proteins are represented at least 3 times (Table 3.4). According to PSORT, many genes encode proteins with predicted nuclear or microbody localization.

Three genes showing 96-fold, 86-fold and 77-fold up-regulation in invaded rice (Table 3.4, Figure 3.2B) encoded putative MAPKKKs, the upstream kinases in the MAPK cascades passing signals from receptor/sensor proteins to transcription factors. These particular

MAPKKKs have homology to NPK1-related protein kinase from *Z. mays* (Shou et al., 2004). *NPK1*, originally described from tobacco, encodes a MAPKKK involved in responses to the abiotic stresses drought, cold and high salt (Nakagami et al., 2005). Interestingly, three more NPK-related kinases were up-regulated at moderate levels. These were AK107168 (43.8-fold), AK058518 (28.9-fold) and AK105946 (25.9-fold). In contrast, the better studied rice MAPKKK OsERD1 (AK111595), which plays a role in defense/stress signaling and development, showed low levels of expression in both samples (Nakagami et al., 2005). The MAP kinases that have been characterized for response in blast disease were not highly induced in our study (Reyna and Yang, 2006).

A transcription factor in the OsDREB family (Dehydration Response Element-Binding protein), which regulates genes expressed in response to drought, cold and high salt (Dubouzet et al., 2003), was up-regulated 75-fold in infected tissue (Table 3.4, Figure 3.2B). The transcription factor *OsNAC4* (AK073848), which plays a role in initiation of hypersensitive cell death induced by flagellin recognition in rice (Kaneda et al., 2007), was 64-fold up-regulated (Figure 3.2B). A transcription factor (AK062882) of the APETALA2 (AP2) / Ethylene-Responsive Element Binding Protein (EREBP) family was 58-fold up-regulated. Three additional proteins (Table 3.4), including another putative transcription factor, have predicted nuclear localization according to PSORT. The rice transcription factor JAMyb (AK069082) previously associated with compatibility (Lee et al., 2001) only showed 9.3-fold higher expression levels (P-value of 0), a difference that we validated by RT-PCR (Figure 3.2B). Overall, these results are consistent with extensive reprogramming of rice cell processes during biotrophic invasion.

Rice Resistance and Defense Response Genes Show Low to Moderate Levels of Induction in Infected Tissue

Proteins associated with various types of resistance showed between 3- and 50-fold up-regulation in infected tissue (Table 3.5). AK100135, the rice PDR-type ABC transporter (49-fold) has been suggested to be regulated by abiotic stress in rice roots (Moons, 2003),. Our results demonstrate that it is also induced during blast infection. AK105311, induced 12-fold

during infection, encodes a pleiotropic drug resistance-like protein with homology to NtPDR, an elicitor-responsive gene in tobacco (Sasabe et al., 2002). AK101439, an NBS-LRR resistance protein with homology to a barley resistance protein was up-regulated by 8-fold.

Rice defense genes reported to be highly induced during both compatible and incompatible interactions were induced at low to moderate levels during biotrophic invasion (Table 3.5). Out of 6 phenylalanine ammonia lyases (Lee et al., 2001)represented on the rice array, only two showed slightly enhanced expression (~5-fold) in infected tissue. Fifteen putative peroxidases were induced between 3- and 14-fold. An endo-1,3-beta-glucanase (AK063953) with homology to the pathogenesis-related protein PR-2 of *A. thaliana* (Accession NP_191285,1) was up-regulated 32-fold. Three other glucanases were induced 5-, 14- and 28-fold, seven chitinases were induced from 3- to 20-fold, and two of 6 thaumatin-like genes were induced 4- to 5-fold.

Based on evidence that IH manipulate plasmodesmata (Kankanala et al., 2007), we searched for genes related to plasmodesmatal structure and function. Interestingly, a rice ortholog of the NtNCAPP gene (AK106058, P-value of 2.9E-32) was 8.7-fold up-regulated in infected tissue. In tobacco, NtNCAPP1 appears to play a role in translocation of some non-cell-autonomous proteins across the plasmodesmatal channel (Lee et al., 2003). Plasmodesmatal pore sizes defining the size exclusion limit depend on a dynamic equilibrium between synthesis and degradation of callose, a β-1,3-glucan (Heinlein and Epel, 2004). An endo-1,3-beta-glucanase implicated in plasmodesmatal callose degradation encodes a post-translationally modified glycosylphosphatidylinositol (GPI) lipid-anchored protein (Levy et al., 2007). However, none of the induced glucanases in our data were GPI-anchored proteins. Plasmodesmata structure and plasticity might be impacted by plant cell wall degrading enzymes specific for pit field walls (Heinlein and Epel, 2004), although little is known about these walls in monocots. Annotated rice wall degrading enzymes, pectin methyl esterases, polygalacturonases, and cellulases fell within the +4- to -4-fold range (Table 3.5).

A recent expression analysis used the Agilent rice array to assess impact of wounding rice leaves by similar procedures (incubating cut leaf pieces) to ours (Katou et al., 2007). Comparing our expression results to theirs showed no correlation (Figure 3.8). Additionally, a

mitogen-activated protein kinase phosphatase OsMKP1 (AK105748) that was highly induced by wounding (Katou et al., 2007)showed no change in expression levels in our infected tissue. These results confirmed that our control samples eliminated expression changes due to wounding from consideration. They also showed that plant response to biotrophic blast invasion did not resemble a wounding response.

Unchanged and Down-Regulated Rice Genes in Invaded Tissue

The 7 rice genes that were down-regulated >50-fold in infected tissue differed in properties from >50-fold up-regulated genes. These repressed genes include PSORT-predicted extracellular and cytoplasmic proteins (Table 3.4). Additional down-regulated genes included AK107345 (-43-fold) encoding a putative integral membrane protein (Table 3.5). Although the largest class of up-regulated genes encoded putative protein kinases, only five kinase genes showed down-regulation (-3 to -5-fold) in infected tissue. There were no putative transcription factors among the repressed genes.

Comparison of our results with Vergne et al. (Vergne et al., 2007) showed little overlap with their highest up-regulated genes in the compatible interaction. These researchers investigated rice gene expression in compatible and incompatible interactions in rice leaves at 24 and 48 hpi. A wall-associated kinase (AK067041) that showed the highest level of induction in their study (16-fold at 24 hpi, down again at 48 hpi) was not differentially regulated in ours. Additionally, an LRR-kinase that was induced in their 24-hour compatible data was not differentially regulated in ours.

Mutational Analysis of Highly Up-Regulated Fungal Genes

Genes that encoded IH-specific secreted proteins were candidate effectors with a role in controlling plant cell processes. After RT-PCR validation, 4 such genes were chosen for functional analysis (Table 3.1; Figure 3.2A; P-values = 0). AMG08261 (100-fold up), AMG08541 (84-fold up), AMG12560 (71-fold up), amd AMG08859 (64-fold-up) encode hypothetical and predicted proteins with 115, 102,113, and 135 amino acids, respectively. Other

than signal peptides, no conserved domains were found in these predicted proteins, except for AMG08261, using PSORT (Table 3.6).

Plasmids for producing gene replacement mutants were constructed by cloning the hygromycin resistance gene between ~1-kb fragments of 5'- and 3'- sequences flanking each predicted coding sequence (Figure 3.3). Gene replacement constructs were transformed into strain KV1 using *Agrobacterium tumefaciens*-mediated transformation. Knock-out mutants produced by homologous recombination were identified by PCR and confirmed by Southern analysis. For each gene, two independent gene replacement mutants were compared to the wild type strain, and to an ectopic transformant with the hygromycin resistance gene inserted at some other genomic location. Each ΔAMG08261, ΔAMG08541, ΔAMG12560, and ΔAMG08859 mutant showed normal growth and sporulation on nutrient agar plates. For each mutant, appressorium formation and leaf penetration were similar to the wild type and ectopic transformants in susceptible leaf sheaths (Figure 3.4). Biotrophic colonization of epidermal cells by each mutant in the leaf sheath assay was not noticeably different from the wild-type and ectopic transformant. Finally, there were no reproducible differences in lesion sizes or numbers in the whole plant infection assay, although occasional assays showed some symptom reduction in the mutant strains (Figure 3.5). According to these assays, proteins encoded by these three highly up-regulated genes were dispensable for pathogenicity. We could not replace the gene in AMG15373 and AMG08263 using the same methology. Even though 250 transformants were analyzed for each of these genes, all of them resulted from ectopic insertion of the knock-out cassette.

DISCUSSION

We report rice and fungal gene expression profiles during early stage biotrophic invasion when most IH were colonizing the first-invaded epidermal cell and a few were moving into second cells. We developed a robust procedure to obtain infected tissue RNA with ~20% IH RNA. This ensured that the rice RNA was enriched in RNAs from cells interacting with IH. The same samples were used to compare expression between IH and mycelium, and between infected and mock-inoculated rice. Due to our success in enriching for RNAs in the interaction transcriptome, the numbers of differentially-regulated genes and the transcript abundance ratios we report are much higher than in previous rice blast gene profiling experiments. Detection of mRNAs corresponding to *AVR* genes *AVR-Pita* and *PWL2* in IH-colonized tissue validated our biological samples as a potentially rich source for additional effectors. A broad overview of expression patterns in the biotrophically-invaded rice tissue supported the hypothesis that biotrophic IH secrete effector proteins that reprogram gene expression in rice cells.

Rice genes induced >50-fold included MAP kinase kinase kinases, the first responders of the three component MAP kinase modules that link sensors/receptors to transcription factors and downstream targets. The biological complexity of MAPK cascades is becoming clear (Nakagami et al., 2005). The same MAPK pathway can perform independent cellular functions, and various MAPK components can serve different functions in different biological contexts. The induced MAPKKKs are homologous to the NPK1 kinase from tobacco. NPK1 is associated with heat, cold, hyperosmotic stress, cytokinesis, auxin signaling, pathogen response, drought and freezing tolerance. One NPK1 pathway (NPK1-MEK1-NTF6) is implicated in both cytokinesis and *N*-mediated resistance of tobacco to Tobacco Mosaic Virus. Arabidopsis *NPK* orthologs, *ANP* genes, are involved in response to H_2O_2, in cytokinesis and in auxin signaling (Kovtun et al., 2000). MAPK modules are associated with *AvrPto-Pto* mediated signaling and resistance in tobacco and tomato (Pedley and Martin, 2004), and with flagellin-induced innate immunity in Arabidopsis (Asai et al., 2002). Just how MAPK cascades contribute to biotrophic invasion and compatibility remains an exciting topic for study.

Rice genes highly induced during biotrophic invasion include three transcription factors and unknown nuclear proteins. The transcription factors have been studied in different biological contexts. Five homologs to the Arabidopsis *DREB* transcription factors, considered to be master switches of drought-, cold- and salt- responsive genes, have been characterized in rice (Dubouzet et al., 2003). DREB factors recognize the dehydration responsive element (DRE) binding motif. We report that the *OsDREB1B* gene is 76-fold up-regulated in infected rice. Another transcription factor, AK062882 (58-fold up), belongs to the AP2/EREBP family, which includes members regulating expression of pathogenesis related proteins (http://drtf.cbi.pku.edu.cn/gene_info.php?gn=OsIBCD044038). The 3rd transcription factor, OsNAC4, is induced by 64-fold during biotrophic invasion. In a different study, using both PCR-subtraction and the Agilent rice oligoarray, OsNAC4 was identified as strongly induced during flagellin-mediated hypersensitive cell death in cultured rice cells (Kaneda et al., 2007). These authors suggest that OsNAC4 is a key initiator of plant HR cell death. Interestingly, out of 87 genes with differential expression induced by bacterial flagellin, the only induced genes in common between their study and ours were *OsNAC4*, the *MAPKKK* (AK107168, 44-fold up in our study), and a C2H2 zinc finger protein (AK068861, 42-fold up in our study). This suggests that OsNAC4 is acting in a different context in the two distinct biological processes. Future functional studies for these transcription factors will directly assess a role in biotrophic invasion.

The association of drought-response genes, the NPK1-related MAPKKK and OsDREB genes, with biotrophic invasion should be considered in the context of the field biology of blast disease. That is, drought stress makes rice more susceptible to blast disease. These results are consistent with a report that the rice MAP Kinase *OsMAPK5* positively regulates drought, salt and cold tolerance and negatively regulates PR gene expression and resistance to blast disease (Xiong and Yang, 2003). Understanding the role of the drought-associated MAPKKK and OsDREB during biotrophic blast invasion takes on practical significance, because both classes of genes are being used in transgenic strategies to confer drought resistance in rice and maize (Dubouzet et al., 2003).

We report that rice defense response genes were induced at low to moderate levels (between 3- and 40-fold) during biotrophic invasion. Such genes are generally the most highly

induced genes reported for compatible and incompatible blast interactions (Kim et al., 2001; Rauyaree et al., 2001; Matsumura et al., 2003; Jantasuriyarat et al., 2005; Vergne et al., 2007). Interestingly, Jantasuriyarat et al. (Jantasuriyarat et al., 2005) reported major changes in rice gene expression at 6 and 24 hpi before most of the fungus even had the possibility of penetrating inside the plant, and genes encoding β-1,3-glucanase and phenylalanine ammonia lyase were among the most highly induced. Their results are even more significant due to the extremely low levels of fungal biomass in the tissues (only 4 out of 68,920 ESTs were homologous to known fungal genes). Vergne (Vergne et al., 2007) report similar results. Therefore, it appears that many rice cells that are distant from the invading fungus were expressing basal resistance responses. By enriching for rice cells near to growing IH, we have identified rice genes involved in "effector-triggered susceptibility (ETS)" (Jones and Dangl, 2006). We suggest that different rice cells in our infected sheaths may be expressing different gene sets. Rice cells near to and controlled by IH may express ETS genes and distant rice cells may express basal resistance genes. This hypothesis can best be tested using laser microdissection to achieve purification and analysis of rice cells with specific spatial relationships to IH (Tang et al., 2006).

In addition to sensor response and transcription factor genes, rice ETS genes controlled by IH may impact rice membrane dynamics and plasmodesmatal recognition and function (Kankanala et al., 2007). A putative rice endomembrane protein that is 58.9-fold up-regulated during infection (Table 3.4) may participate in membrane manipulation by IH. The up-regulated rice plasmodesmatal receptor is a putative ortholog of tobacco *NtNCAPP1*, which is involved in translocation of some non-cell-autonomous proteins through plasmodesmata (Lee et al., 2003) . This protein may play a role in sending fungal signals into neighboring cells or even in plasmodesmatal recognition and recruitment for cell-to-cell movement. These rice genes are strong candidates for functional analyses.

Biotrophic IH are morphologically and developmentally distinct from the thin filamentous hyphae that grow in nutrient medium, suggesting that they express different genes. We have clearly shown that this is the case. Many genes previously only predicted by genome sequencing are highly up-regulated in IH (Figure 3.6 & Table 3.1), and many genes previously identified from mycelium were highly down-regulated in IH (Table 3.2).

Our results on IH gene expression are consistent with known blast biology. Melanin biosynthesis genes are not required for biotrophic invasion (Kankanala et al., 2007) and they are highly down-regulated in IH. Lack of induction of plant cell wall degrading enzymes in IH is consistent with biotrophic IH appearing to cross plant cell walls at pit fields using highly constricted IH pegs, and with the general lack of visible degradation of plant cell walls during this early invasion stage (Kankanala et al., 2007).

Our report that the hydophobin gene *MPG1* is significantly down-regulated in IH at 36 hpi is consistent with the report (Talbot et al., 1993) that *MPG1* expression was high at 12 hpi (when appressoria were forming), not detectable at 18, 24 or 48 hpi, and detectable again from 72 to 96 hpi, when macroscopic symptoms occurred. *MPG1* was reported among the most highly expressed genes in a compatible blast interaction in rice leaves at 10 days post inoculation (Matsumura et al., 2003), and in the partially compatible interaction (strain 70-15 in Nipponbare leaves) from 84 to 120 hpi (Kim et al., 2001). Reports of high expression of *MPG1* at 48 hpi by Rauyaree et al. (Rauyaree et al., 2001) might be contradictory. However, in this study of the 70-15/Nipponbare interaction, extensive dark brown hypersensitive spots were clearly visible at 48 hpi (Figure 1 in Rauyaree et al, (Rauyaree et al., 2001)). Thus, the 70-15/Nipponbare interaction differs from our highly compatible interaction, in which visible symptoms do not occur until ~96 hpi. Together, the results are consistent with *MPG1* playing a role as lesions appear and the pathogen prepares to sporulate, and perhaps at earlier stages in less compatible interactions when the fungus is growing but failing to thrive.

Pathogenicity genes *PTH11*, *MPG1* and the melanin biosynthesis genes play important roles during appressorium formation and function (Talbot, 2003), and they are highly induced in nitrogen-starved mycelium (Soanes et al., 2002; Donofrio et al., 2006) and references therein). These genes were highly down-regulated in IH. Thus, it appears that expression in response to nitrogen starvation has relevance to the pre-penetration phase when the fungus is growing on the plant surface, but not to early stages of growth inside the plant. On the other hand, plant cell wall degrading enzymes appear to be highly expressed at later infection stages during macroscopic symptom development (Wu et al., 2006). Thus, growth of fungus in nutrient medium with

isolated rice cell walls as the main carbon source should have relevance to later stages of plant tissue colonization. In general, our analysis has found no evidence that in vitro fungal models can substitute for direct studies of in planta biotrophic growth, confirming the importance of our strategy and the unique insights on IH-specific invasion we report.

As signals exchanged between fungus and plant, secreted proteins are potential players for controlling plant responses. From the *M. oryzae* genome, 739 sequences, 6.6% of ~11,109 predicted proteins (Dean et al., 2005), encode secreted proteins according to the prediction programs SignalP and PROTCOMP (Soderlund et al., 2006). Indeed, *M. oryzae* contains double the number of putative secreted proteins found in the saprobe *Neurospora crassa* (Dean et al., 2005). We showed that ~19% of these secreted proteins are induced >3-fold during early biotrophic infection. Hypothetical secreted proteins comprise nearly half of sequences expressed >50 fold in IH (Figure 3.6). Although it is likely that secreted IH-specific proteins play key roles in biotrophic invasion, targeted gene replacement experiments on 3 of the most highly up-regulated IH genes did not result in clear phenotypes in planta or in vitro. This result is consistent with the general failure to identify phenotypes associated with many known effector/*AVR* genes and the apparent difficulty in identifying genes with IH-specific phenotypes through classical mutational analyses (Talbot, 2003). Further refinement of plant infection assays to reliably detect small changes in pathogen aggressiveness was assessed by extended whole plant inoculation assay (10 pots per strain) but similar results were obtained. In addition, fusion of coding region to a EYFP reporter gene confirmed that some of these genes are invasion specific (Giraldo, M. and Valent, B. unpublished results). In the future assaying double mutants, identifying avirulence activities for IH proteins, and determining if IH-specific proteins interact physically with induced rice proteins will provide clues about possible role of these genes during infection.

The recent finding that intracellular IH are enclosed in plant membrane, the EIHM (Kankanala et al., 2007), has important implications because blast AVR/effector proteins must cross the EIHM to reach the plant cytoplasm. So far, the mechanism of secretion of effector proteins across host membranes is not known for plant pathogenic fungi or oomycetes. Oomycete pathogens secrete their cytoplasmic effectors through an uncharacterized mechanism that requires an RXLR-containing motif following the classical signal peptide (Bhattacharjee et

al., 2006; Birch et al., 2006). In the case of *M. oryzae*, we searched among known AVR/effector proteins and the >50-fold induced secreted proteins for RXLR-like sequences or other potential conserved motifs and found no candidate motifs. We recently showed that blast IH secreted AVR-Pita and PWL proteins, and that they accumulated at predictable locations inside the EIHM (Berruyer et al., Unpublished results). There is no direct evidence that these effectors cross the EIHM, and it is possible that some IH-secreted proteins may be retained in the fungal wall or the interfacial zone between the fungal wall and the EIHM. Proteins secreted outside the fungus but not crossing the EIHM would introduce noise into translocation motif searches. Simple assays to determine delivery of blast effector proteins across the EIHM into the rice cytoplasm will aid in the identification of protein motifs mediating membrane crossing and allow elucidation of the *M. oryzae* effector secretion system.

Assembling a large set of IH-specific genes also permitted bioinformatic searches for promoter cis-elements mediating IH-specific transcription. Such motifs would be valuable for identifying additional co-regulated genes. We predicted that promoters for *AVR-Pita, PWL2* and other putative effector-encoding genes share cis-elements for in planta-specific transcription factors. To discover these, we analyzed the 500 bp up-stream regions of known and putative *AVR*/effector genes using the MEME program. We found no candidate motifs. Promoter analysis can be useful in the identification of co-regulated genes, but confusing results may be obtained when the analyzed sequences are not properly chosen. Our single time point study identified genes that are expressed by IH in planta but not by mycelium grown in vitro. Time course studies during in planta growth might further divide these genes into coordinately expressed clusters, which would provide the best gene groupings for motif searches.

Analysis of the interaction transcriptome of rice blast disease will be an ongoing process. The annotations for *M. oryzae* and for rice are changing rapidly. Our data will be entered on a gene by gene basis in the MGOS database (http://www.mgosdb.org), the site for blast community annotation of the fungus and rice (Soderlund et al., 2006). Therefore, new annotations for the many unknown genes will be immediately associated with the gene's relative expression levels in IH and mycelium. Our analysis will continue to be valuable for genome annotation efforts, especially with the annotation of sequences that encode unknown and

hypothetical proteins. From this data set, many genes remain to be analyzed for their impact on biotrophic blast invasion.

Future work

The data generated in this work opens new perspectives in the study of rice blast disease. Fusion of fungal coding sequences of putative secreted proteins and their native promoters with YFP reporter genes are in progress (M. Giraldo thesis project). This research will confirm their specific expression during infection and also their secretion outside the fungus. Other studies include the generation of a system to test if secreted proteins can induce HR in rice and prove that they are effectors. We also need to generate knock-out mutants in other fungal genes encoding putative secreted proteins. Finally, it will be interesting to see if some of the plant genes that are over-expressed during infection can represent putative susceptibility genes. To prove this, We can generate knock-down lines in specific genes and evaluate their effect in the rice blast infection.

MATERIAL AND METHODS

Fungal Culture

M. oryzae strain KV1 (Kankanala et al., 2007) expressing constitutive EYFP was derived from strain O-137, a highly aggressive field isolate collected from rice in China. The fungus was maintained in frozen storage and cultured on oatmeal agar plates at 24°C under continuous light (Valent et al., 1991). For tissue inoculation, spores were collected in 0.25% gelatin (Cat. # G-6650, Sigma) solution to produce a suspension of 1 x10^5 spores/mL. For growth in liquid medium, a 1 cm square piece of agar containing fungus was excised from the surface of an oatmeal agar plate and blended in 25 ml of 3,3,3 medium (3g/L of glucose, 3g/L of casamino acids, and 3g/L of yeast extract). The blended mycelium was mixed with 225 ml of fresh medium in a 500 ml flask. The culture was incubated at 24°C under continuous rotation at 120 RPM. Mycelium was collected by filtration after 24 h of incubation, and the blending treatment was repeated for 3 rounds of growth. Mycelium was finally collected, dried using paper towels and stored at -80°C for RNA extraction.

Assays for Growth, Sporulation, Appressorium Formation and Plant Infection

Fungal growth and sporulation was observed on oatmeal agar plates (Valent et al., 1991). Appressorium formation, penetration and biotrophic invasion were observed in the leaf sheath assay. Whole plant infection assays were performed by spray inoculations (Berruyer et al., 2006) using three week old YT-16 plants and suspensions of 5×10^4 spores/mL in gelatin solution. Lesion formation in whole plant assays were evaluated at 7 days (Valent et al., 1991).

For sheath inoculations, samples were handled as previously described (Kankanala et al., 2007). Briefly, five cm-long sheath pieces from 3 week old plants were placed in Petri dishes containing wet filter papers to maintain high humidity. Sheaths were placed in wire supports to avoid contact with the wet paper and to hold them horizontally flat for even inoculum distribution over the mid-vein. Spore suspension (1×10^5 spores/mL in gelatin) was injected in one end of the sheath using a 1 mL pipet. At 36 hpi, 0.5 cm pieces were removed from the incubated sheath ends to eliminate fungus that invaded the injured tissue. Each sheath segment was cleaned using a wet sterile swab to remove spores, appressoria and mycelium on the surface, trimmed, and immediately scanned for infection site density using epifluorescence microscopy. Heavily infected samples were frozen in liquid nitrogen and stored at -80°C. For mock-inoculated controls, sheaths were inoculated with gelatin solution, incubated and processed identically to inoculated pieces.

Microscopy

Differential Interference Contrast microscopy (DIC) and epifluorescence microscopy were performed using a Zeiss Axioplan 2 IE Mot microscope. Cells were observed with a 63X C-Apochromat (NA 1.2) water immersion objective lens. Fluorescence of the EYFP protein was observed using a fluoArc lighting system and a YFP-specific filter (excitation 500 ± 20nm, emission 535 ± 30 nm, filter set 46), both from Zeiss. Images were acquired using a Zeiss AxioCam HRc camera and analyzed with Zeiss Axiovision® Digital Image Processing Software, Version 3.1. RNA Extraction, cDNA Preparation, RT-PCR. Total RNAs from mycelium and rice tissues were extracted using a Trizol method (Invitrogen, Carlsbad, CA). Briefly, 100 mg of

tissue was ground using a mortar and pestle with liquid nitrogen, and the resulting powder was suspended in 1mL of trizol. After 5 min of incubation, 0.2 mL of chloroform was added and samples were mixed manually for 15 seconds. After 15 min of centrifugation, the supernatant was recovered and mixed with 0.25 ml of 3 M sodium acetate and 0.25 ml of isopropanol. The pellet was washed twice with 75% ethanol. RNA quantity was measured using a NanoDrop Spectrophotometer (Nano-Drop Technologies, Wilmington,, DE). For microarray hybridizations, RNA quality was determined using an Agilent Bionalyzer (Agilent Technologies, Palo Alto, CA). To obtain control RNAs with similar fungal and plant content, we produced a mixture of 20% mycelial RNA and 80% mock inoculated rice sheath RNA. Five hundred nanograms of total RNA were used for cDNA synthesis reaction using the SuperScript® First Strand kit from Invitrogen according to the manufacturer's instructions. For RT-PCR, two microliters of cDNA were used for PCR amplification. All primers are listed in Table 3.7. When possible, primers were designed to span introns in order to differentiate genomic and cDNA copies. Twenty-seven rounds of PCR amplification were used in all expression validation experiments (Figure 3.2).

Microarray Hybridization and Data Analysis

Total RNA (500 ng) was labeled using a Low RNA Input Fluorescent Linear Amplification Kit (Agilent Technologies, Palo Alto, CA). Typical cRNA yields after one round of amplification were 10-15 ug. The cRNAs were labeled with Cyanine-3 CTP or Cyanine-5 CTP according to the manufacturer's specifications. Fluorescent cRNAs were purified and quantified using a NanoDrop Spectrophotometer (NanoDrop Technologies, Delaware), and 1 µg aliquots of the labeled cRNAs were hybridized to *M. oryzae* microarray slides, version 2 (Cat. # G4137B, Agilent Technologies), and to Rice microarray slides (Cat # G4138A, Agilent Technologies).

For hybridization, the labeled samples (1 ug each Cy3 and Cy5 labeled cRNA) were fragmented by the addition of 25X Agilent Fragmentation buffer and incubated for 30 min at 60°C. The sample was adjusted to a final volume of 450 µl with formamide-containing hybridization buffer(Hughes et al., 2001) and then added to the microarray slides. Slides were incubated for 18 hours with continuous rotation at 40°C. After hybridization, slides were washed in 6X SSPE, 0.005% sarcosyl for 1 min, in 0.06X SSPE for 30 sec, in water for 30 sec, and then

air dried. Slides were scanned on an Agilent G2565BA DNA microarray scanner, and TIFF images were extracted using the Agilent Feature Extraction software (version 8.5). Resultant .xml and .jpeg files were imported into Rosetta Resolver software (Rosetta Biosoftware, Seattle, WA). Data were analyzed separately for each of the three independent biological replicates (four hybridizations for each) for purposes of comparison. Numbers reported in this manuscript resulted from separate analyses of the 12 data sets combined for each microarray. Data sets were plotted as intensity scatter plots (background subtracted/dye normalized Cy3 channel vs background subtracted/dye normalized Cy5 channel). Signature sequences were identified by Resolver and exported to Excel. The P-value range for 3-fold up- and down-regulated fungal genes is shown in Figure 3.6 . P-values for rice genes that were ≥3-fold up-regulated ranged from 0.00841 to 0, and for the rice genes that were ≥3-fold-down-regulated ranged from 0.0067 to 0.

Vector Construction, Fungal Transformation and Southern analysis

Transformation cassettes were constructed by amplifying ~1.0-kb of 5'- and 3'-flanking regions for each predicted coding sequence. The hygromycin gene was cloned between the two flanking region using a fusion PCR strategy. The three pieces together were cloned first into the pGEMT-T® vector (Promega, Madison, WI) for sequence analysis, and later into binary vector pGKO2 (Khang et al., 2005) using a restriction-ligation strategy. KV1 spores were transformed using *Agrobacterium tumefaciens* (Khang et al., 2005). After two rounds of selection in TB3 media containing 250 ug/ml of hygromycin, 50 to 150 independent fungal transformants were analyzed for gene replacement events by PCR amplification. Those that showed no amplification of the coding sequence were further tested for presence of the hygromycin resistance gene using *hph*-specific primers. Gene replacement events were confirmed by Southern blot analysis using the AlkPhos Direct Labeling Kit for non-radioactive labeling of DNA probes (Amersham RPN3690, Piscataway, NJ).

Datasets for the *M. oryzae* and rice microarrays can be accessed through NCBI GEO superSeries accession number GSE8670 (www.ncbi.nlm.nih.gov/geo). This data is available to reviewers at the following link:
http://www.ncbi.nlm.nih.gov/geo/query/acc.cgi?token=lfyvnuqqggoiujm&acc=GSE8670

Figure 3.1 Characterization of infected sheath tissues used for microarray analysis.

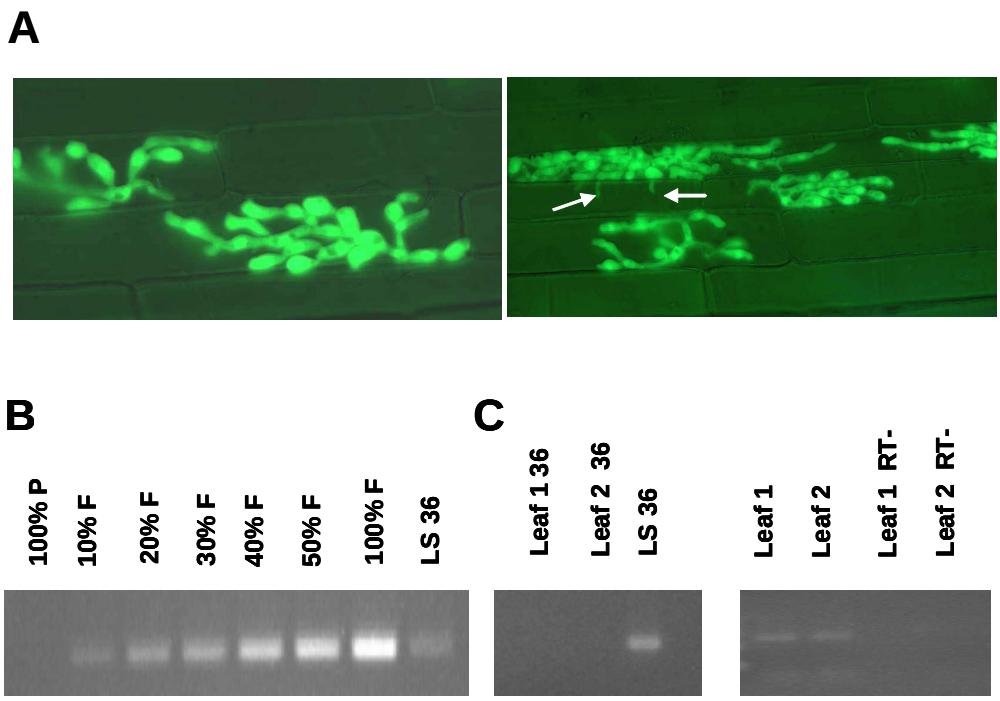

(A) Biotrophic invasive hyphae (IH) in rice sheath epidermal cells at 36 hpi. Typical bulbous IH used for microarray analysis were growing in the first-invaded epidermal cell. In one cell, filamentous IH (arrows) that had not yet enlarged into bulbous IH were growing after crossing the cell wall (Kankanala et al., 2007). Merged DIC and fluorescence channels are shown (size differences due to image cropping).
(B) Relative RT-PCR amplification of fungal actin in 36 hpi infected sheath tissue and control mixtures. RNA mixtures were obtained by combining defined amounts of RNA from fungal mycelium and mock-inoculated sheath. Percentage values (%F) correspond to the fungal RNA content. 100%P is pure plant RNA. For each, 22 cycles of amplification were used.
(C) RT-PCR amplification of fungal actin in infected sheaths and leaves at 36 hpi. A prominent fungal actin band was seen from infected sheath RNAs after 28 cycles, but not from the infected leaf samples. After 35 cycles, faint bands were seen in the infected leaf samples, but not in controls that lacked reverse transcriptase (RT-). For infected leaf tissue, whole plants were inoculated. Samples were collected separately for the most susceptible leaf 1 (the half-extended youngest leaf at the time of inoculation), and the lesser susceptible leaf 2 (the next youngest leaf, fully extended at the time of inoculation). LS36 = Leaf sheath; Leaf 1= youngest leaf; Leaf 2 = older leaf.

Figure 3.2 Validation of microarray data using RT-PCR.

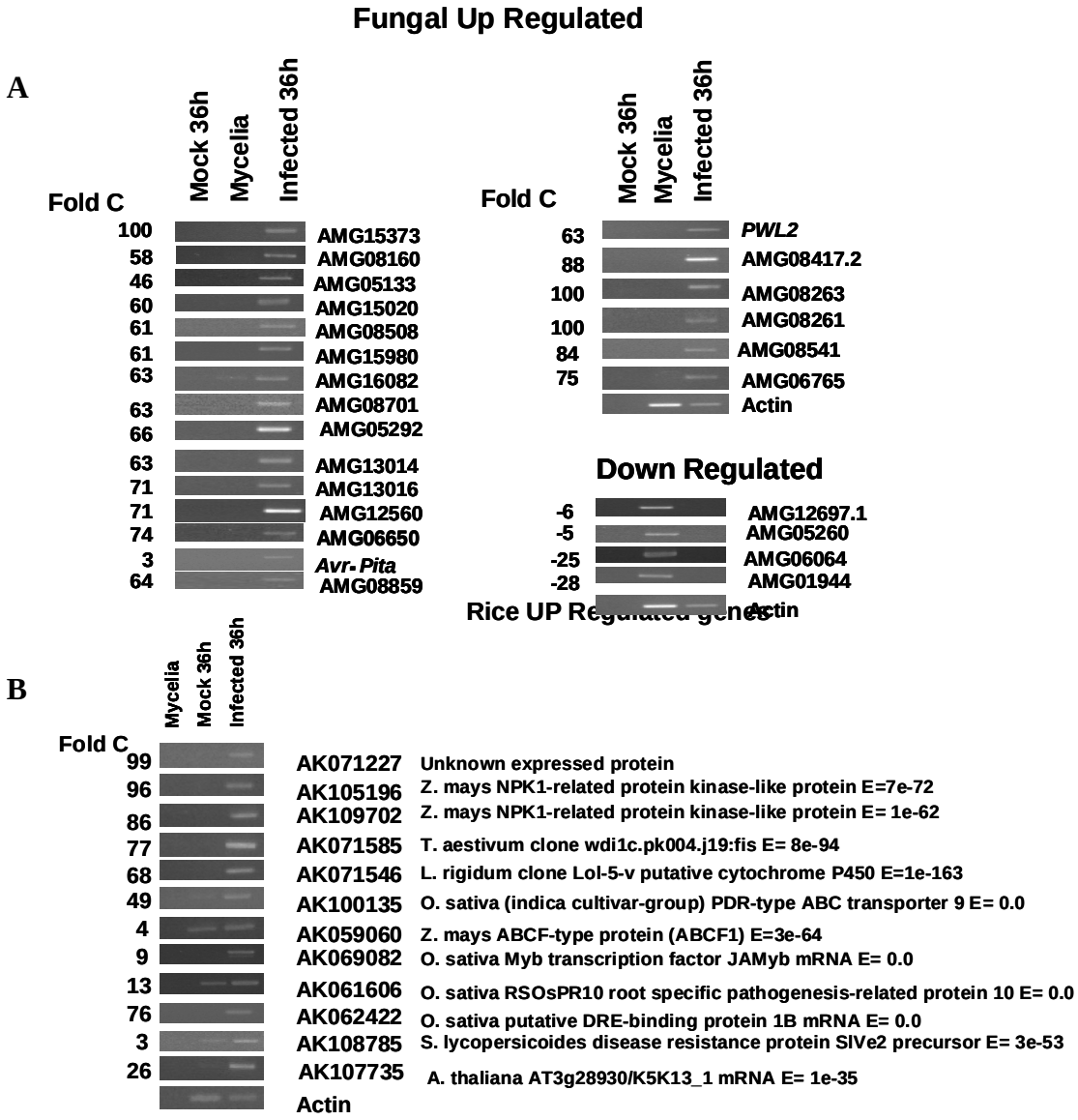

RNAs were produced from mock-inoculated sheath at 36 hpi (Mock 36h), from mycelium (Mycelia), and from infected sheath at 36 hpi (Infected 36h).
(A) Amplification of fungal genes with Mock 36h RNA as the negative control. For each primer pair, 27 rounds of PCR amplification were used. Amplification of the fungal actin gene control reflects the lower amount of fungal RNA in the infected tissue (20%) compared to mycelial RNA, resulting in increased significance for differential amplification of up-regulated genes.
(B) Amplification of rice genes with mycelial RNA as the negative control. Again, 27 cycles of PCR were used. Primers for plant actin were used as controls.

Figure 3.3. Gene replacement analysis of the AMG8541 gene

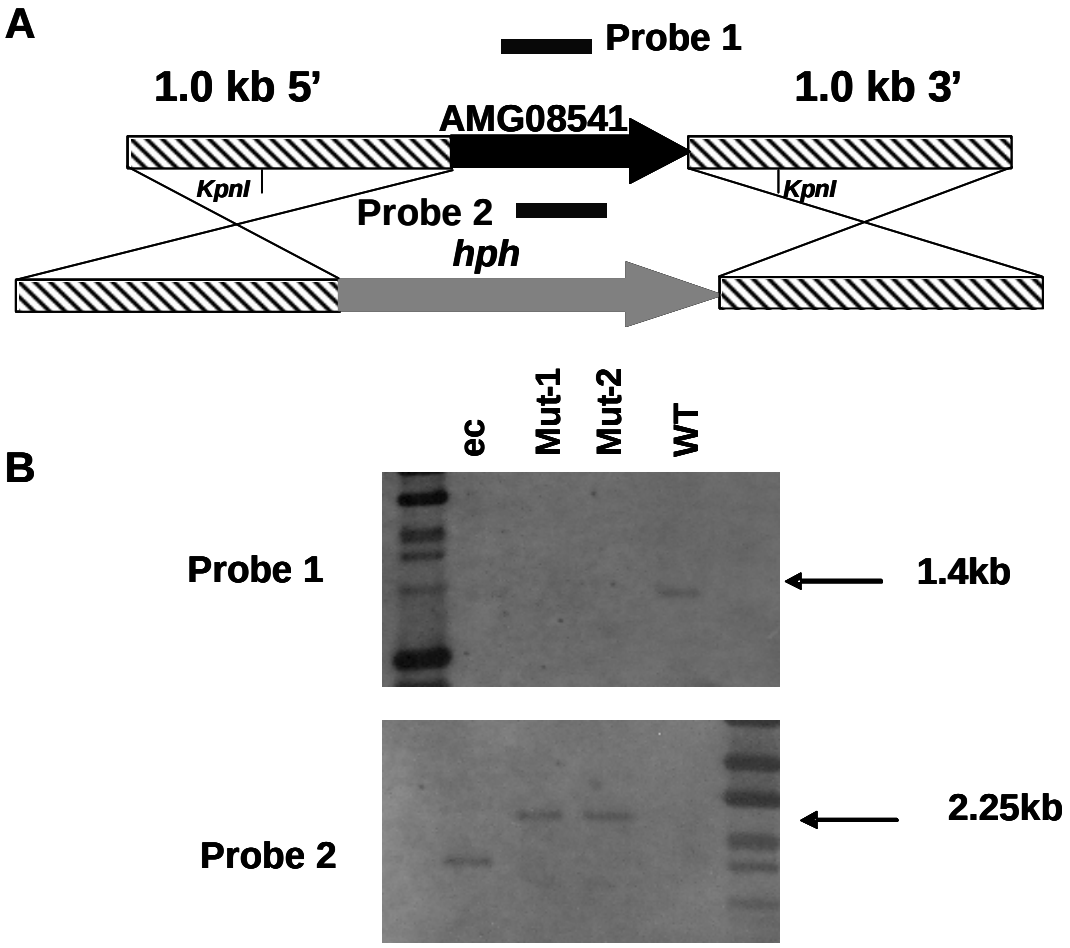

The same methods were used for gene knock-out analyses of AMG08261 and AMG12560.
(A) Schematic diagram of the AMG08541 (black arrow) genomic locus. The gene replacement construct contained the *hph* gene (gray arrow) flanked by ~1000-bp of sequences up-stream and down-stream from the predicted coding sequence.
(B) Southern hybridization analysis was performed using genomic DNAs from an ectopic transformant (ec), two independent knock-out mutants (Mut-1 and Mut-2), and the wild-type strain KV1 (WT). *Kpn* I-digested genomic DNAs were separated by electrophoresis in a 0.8% agarose gel. Probe 1 (wild-type coding sequence) hybridized to the expected 1.4-kb fragment in the wild type strain and ectopic transformant, but not in the mutants. Probe 2 (*hph* coding sequence) hybridized with DNAs from the ectopic transformant and the mutants, but not from wild-type.

Figure 3.4 . Leaf sheath inoculation assay using *M. oryzae amg08261*$^{-}$ knock-out mutants

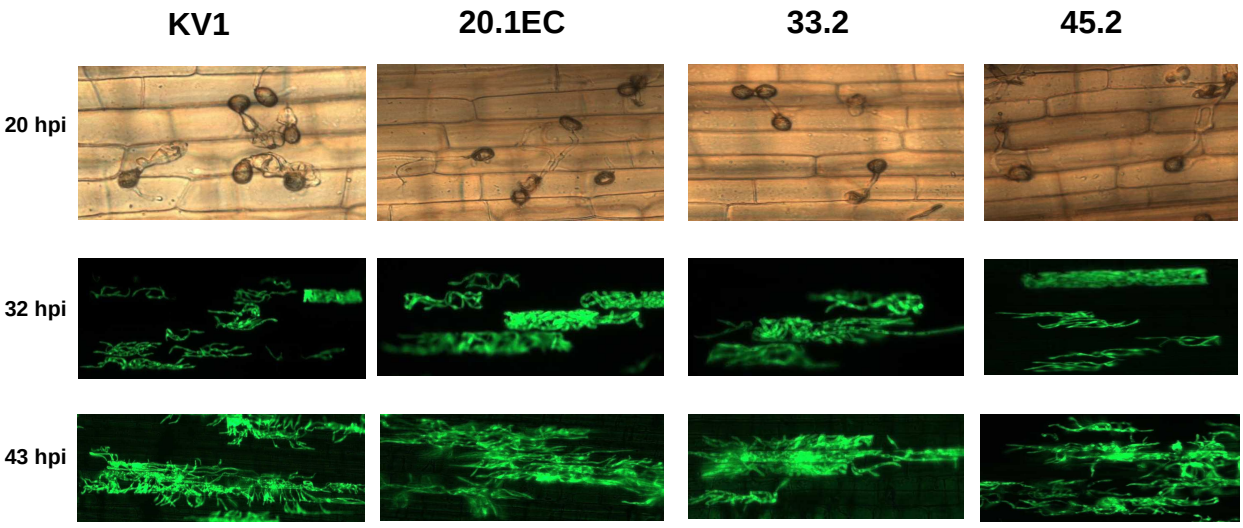

Evaluation of the infection of *amg08261* mutants at early stages on rice leaf sheaths. KV1 indicates the wild type strain; 20.1EC indicates an ectopic transformant; 33.2 and 45.2 indicate two independent mutants. Time points 20 hpi, 32 hpi and 43 hpi correspond to formation of appressoria, infection of the first invaded cell, and movement to the second cell, respectively.

Figure 3.5 Whole plant inoculation assay using *M. oryzae amg08541*$^{-}$ knock-out mutants

Whole plant spray inoculation assays were done and plants were incubated for 7 days. Symptoms are shown for the youngest, most susceptible leaf at the time of inoculation. Leaves were inoculated with: 1, gelatin control; 2, wild-type KV1; 3, ectopic transformant; and 4, and 5, two independent amg08541 knock-out mutants. Assays were repeated at least 3 times.

Figure 3.6 Properties of *M. oryzae* genes that were up-regulated in IH

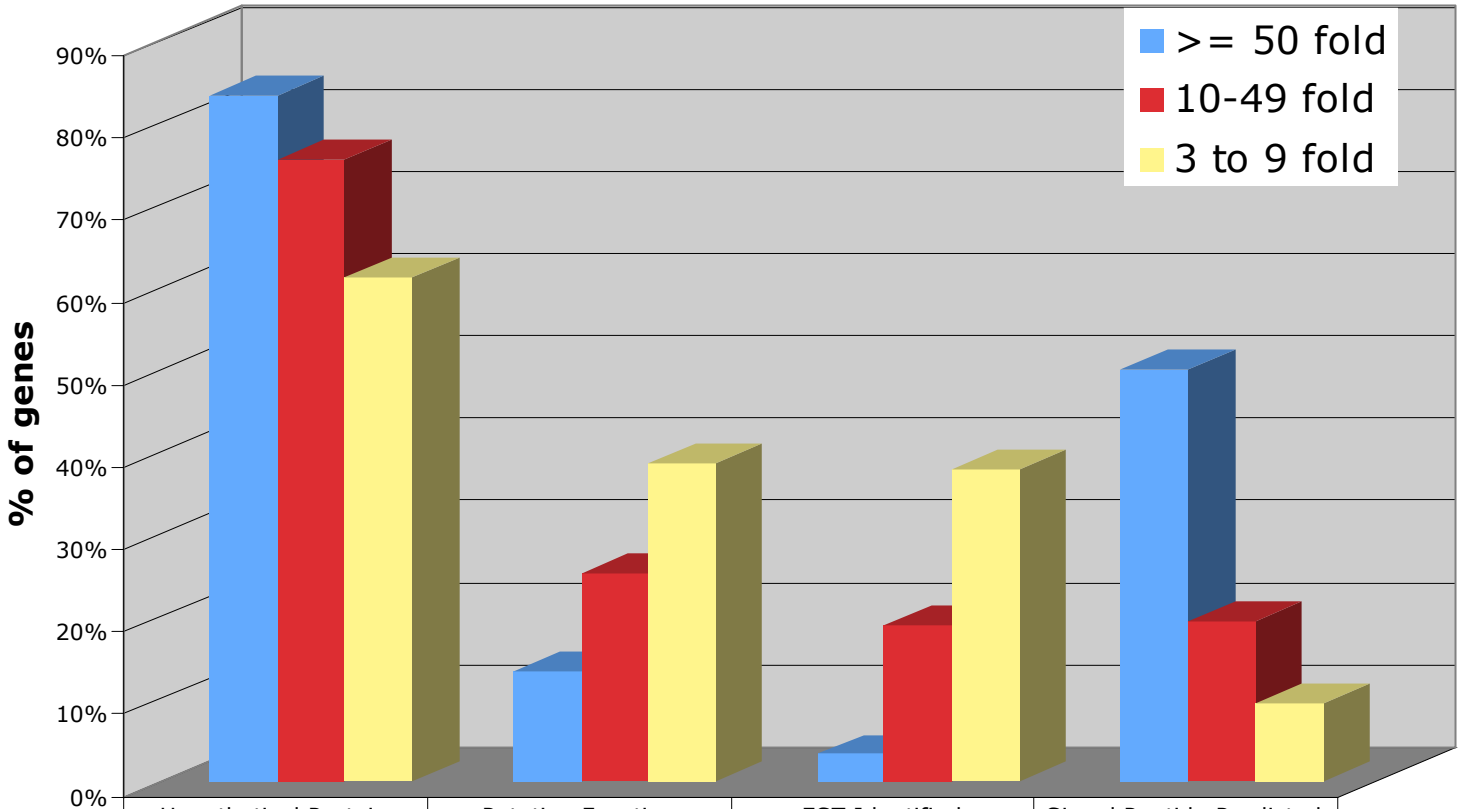

	Hypothetical Protein	Putative Function	EST Identified	Signal Peptide Predicted
>= 50 fold	83%	13%	3%	50%
10-49 fold	76%	25%	19%	19%
3 to 9 fold	61%	39%	38%	9%

Figure 3.7 Properties of *M. oryzae* genes that were down-regulated in IH

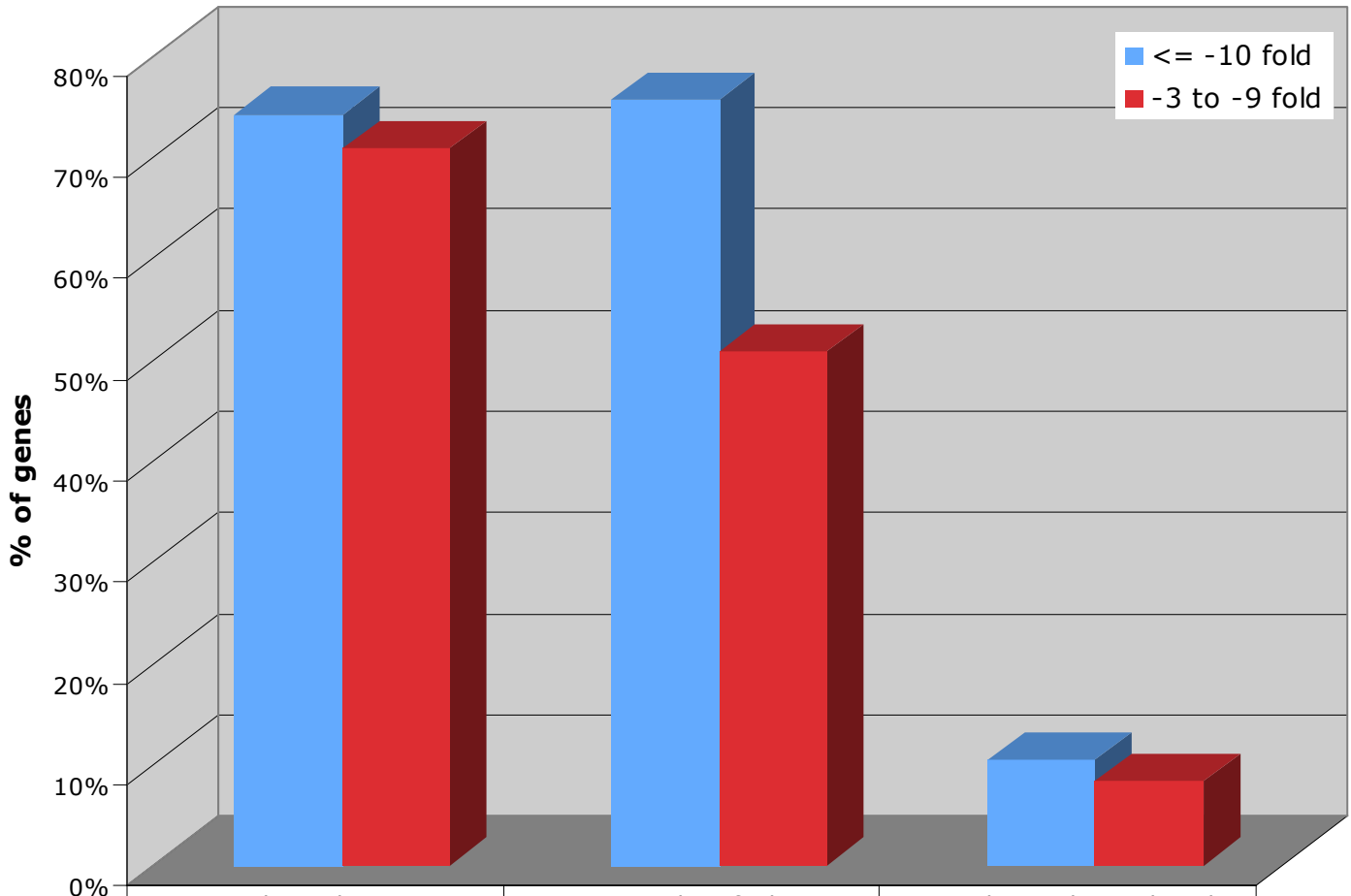

	Hypothetical Protein	EST Identified	Signal Peptide Predicted
<= -10 fold	74%	76%	10%
-3 to -9 fold	71%	51%	8%

Figure 3.8 Comparison of expression of rice genes due to infection and wounding response

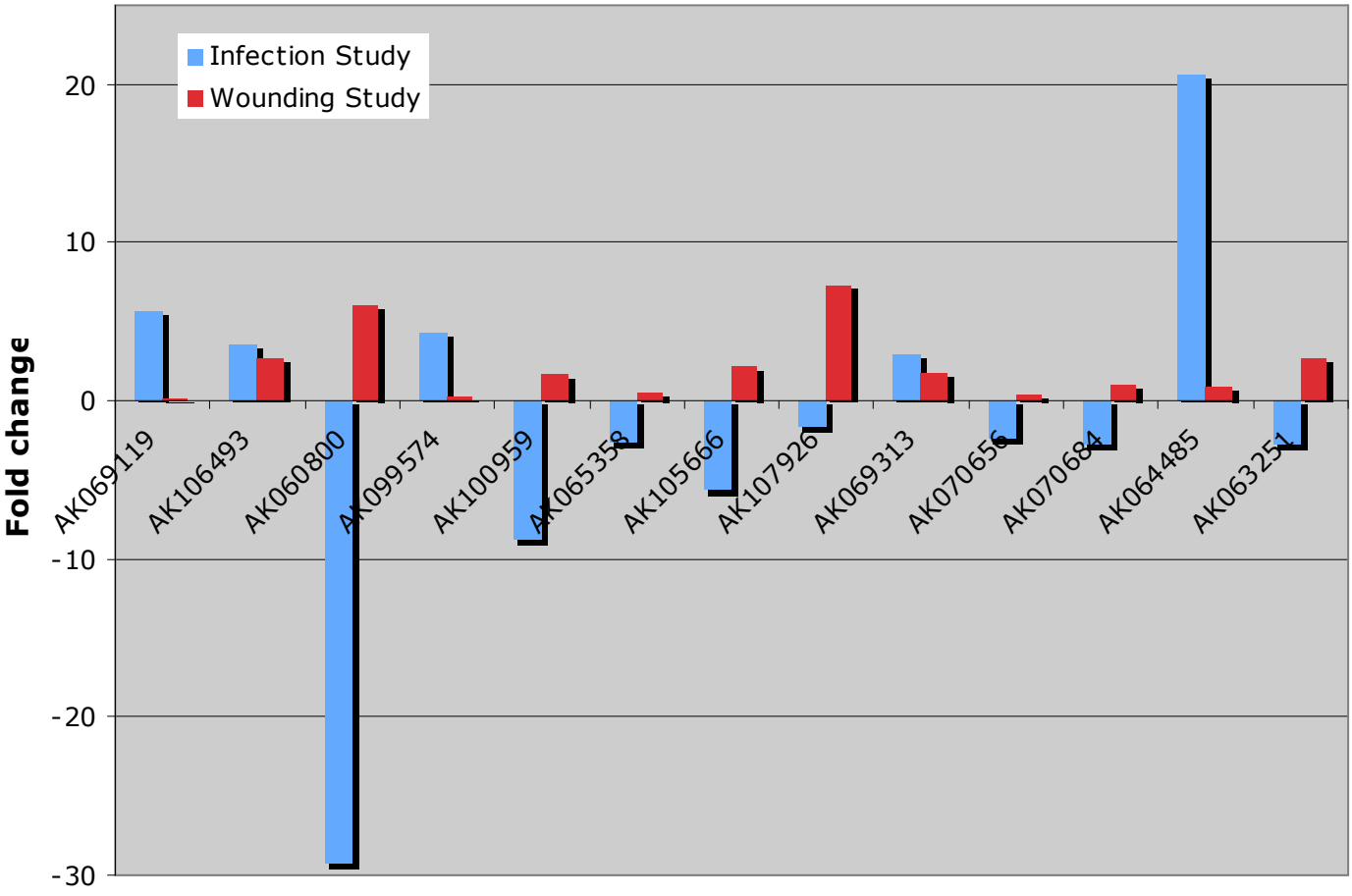

Wounding data taken from Katou et al. 2007. Rice tissue was cut into pieces and incubated by 24 h at 26°C under continuous light.

Table 3.1 Putative secreted proteins expressed >10-fold in IH compared to mycelium

Probe (MGOS name[a])	Fold change	P-value	Putative identity	ES
AMG08263	100	0	Hypothetical protein	
AMG08261[c]	100	0	Hypothetical protein	
AMG08417.2	88	0	Hypothetical protein	
AMG08541[c]	83.8	0	Hypothetical protein	
AMG06765	74.8	0	Hypothetical protein	
AMG06650	73.9	0	Hypothetical protein	
AMG12560[c]	71.3	0	Hypothetical protein	
AMG07384	71.0	0	Hypothetical protein	
AMG08859	64.1	0	Hypothetical protein	
AMG13014	63.4	0	Hypothetical protein	
AMG11184	63.2	0	PWL2, E-value = 0.0	
AMG15980	61.4	0	Hypothetical protein	
AMG08160	57.8	0	endochitinase [*Amanita muscaria*]; E-value = 9e-59	
AMG08787	56.5	0	Hypothetical protein	

AMG08432	51.1	0	Hypothetical protein	
AMG14799	49.2	0	Hypothetical protein	
AMG16216	48.2	0	Hypothetical protein	
AMG05133	46.2	0	laccase [*Gaeumannomyces graminis var. graminis*]; E-value = 0.0	
AMG03019	42.7	0	Hypothetical protein	
AMG16197	36.0	0	Hypothetical protein	n
AMG13593.2	35.7	0	Hypothetical protein	
AMG13918	35.6	2.7 E-24	Hypothetical protein	
AMG02533	35.5	1.29E-29	Hypothetical protein	
AMG05132	35.2	0	Hypothetical protein	
AMG15524	33.4	0	Hypothetical protein	
AMG07601.1	30.1	0	Hypothetical protein	c
AMG12804	28.9	0	Hypothetical protein	
AMG02457	28.2	0	Hypothetical protein	
AMG13251	28.1	0	Hypothetical protein	

AMG01557	27.5	0	Hypothetical protein	
AMG02692	27.0	0	Hypothetical protein	
AMG03089	26.7	0	Hypothetical protein	my
AMG07577	24.8	0	Hypothetical protein	
AMG06843	22.3	0	Hypothetical protein	
AMG11086	21.8	0	Hypothetical protein	
AMG08195	21.2	1.01E-41	Hypothetical protein	
AMG09820	20.3	0	Hypothetical protein	
AMG07137	19.6	0	Hypothetical protein	
AMG12553	19.1	0	Hypothetical protein	
AMG15040	17.7	0	Hypothetical protein	
AMG04878	17.2	0	cellulase CelA [*Clavibacter michiganensis* subsp. *sepedonicus*]; E-value = 1e-18	
AMG13227	17.1	0	Hypothetical protein	
AMG02455	16.1	2.45E-12	Hypothetical protein	
AMG13025	15.4	5.7E-35	Hypothetical protein	

AMG07056	15.3	0	Hypothetical protein	
AMG02439	14.8	5.1E-23	Hypothetical protein	
AMG06036	13.9	0	Endonuclease/Exonuclease/Phosphatase [*Candida albicans* SC5314] gb|EAL00625.1|; E-value = 5e-21	
AMG08482	13.6	3.41E-28	Hypothetical protein	
AMG02914	13.4	3.39E-30	Hypothetical protein	
AMG12924	13.3	0	Hypothetical protein	
AMG02925	13.2	0	Hypothetical protein	
AMG13855	13.1	8.01E-41	Hypothetical protein	
AMG00035	13.0	1.40E-45	Hypothetical protein	
AMG07561	12.8	0	Hypothetical protein	c
AMG02702	11.6	0	Hypothetical protein	
AMG04075	11.4	3.71E-42	Hypothetical protein	
AMG08865	10.4	0	Hypothetical protein	
AMG08416.1	10.3	0	Hypothetical protein	c

AMG06620	10.2	2.60E-29	Hypothetical protein	

[a]MGOS gene names correspond to the probes used in version 2 of the Agilent *M. oryzae* microarray. They will not change with new releases of the genome sequence. MGOS names can be converted to Broad Database gene names at www.mgosdb.org.

[b] "–" indicates no EST hits. Hits are labeled according to the library in which they occurred. Library abbreviations: ap = appressorium, cm = mycelium from complete medium, cs = conidiospores, my = mycelium from minimal medium, (Ebbole et al., 2004).

[c]These genes were used for gene replacement experiments.

Table 3.2 The 50 most down-regulated fungal genes during biotrophic infection

Probe	Fold change	P-value	Putative identity	Predicted Signal Peptide	cDNA Libraries[a]
AMG06063.1	-82.9	0	Hypothetical protein		cs cw my
AMG13759.1	-77.1	0	Hypothetical protein		cm
AMG06063.2	-59.6	2.14E-40	Hypothetical protein		cs cw my
AMG11634.1	-55.2	0	Hypothetical protein		cs mk mt
AMG09784.1	-53.6	2.91E-41	Hypothetical protein		mt ap cs
AMG00941.1	-46.3	0	Hypothetical protein		mt ns cs
AMG14000.1	-43.2	0	Hypothetical protein	SP	ap cs mk mt ns su
AMG15966	-39.3	0	Hypothetical protein		cm mt
AMG09317	-38.7	0	Hypothetical protein		cm cs cw
AMG01344.2	-38.4	0	Hypothetical protein		cm cs cw ns
AMG12371.1	-38.3	5.76E-22	Hypothetical protein		
AMG09954	-37.8	0	Hypothetical protein		cs cw
AMG08367	-37.4	0	expressed protein [*A. thaliana*] ref|NP_974838.1|		mk mt
AMG04896.2	-37.2	0	Hypothetical protein	SP	my ns
AMG01490	-36.6	0	Hypothetical protein		cm ns
AMG01344.1	-35.8	0	Hypothetical protein		cw su my

AMG10496	-35.7	0	metalloprotease 1 precursor [*Coccidioides posadasii*]	SP	cm
AMG05375	-35.2	0	Hypothetical protein		cm
AMG07022	-34.3	0	Hypothetical protein		
AMG05270	-33.7	0	Hypothetical protein		cm cs cw mt my ns su
AMG04953	-33.5	2.09E-34	acidic amino acid permease [*Penicillium chrysogenum*]		cm cw mt
AMG10872	-33.3	0	Hypothetical protein		cs ns
AMG14477	-32.8	0	Hypothetical protein	SP	ns
AMG13759.2	-32.7	0	Hypothetical protein		cw
AMG07762	-31.6	0	Hypothetical protein		cm cs cw
AMG11366	-31.3	3.54E-16	Hypothetical protein		cm
AMG12878.2	-31.0	0	Hypothetical protein		cm su ns
AMG01944	-28.1	0	1,3,6,8-Tetrahydroxynaphthalene Reductase		mk cm
AMG04981	-27.8	0	cytochrome P450 monooxygenase [*Botryotinia fuckeliana*]		cm ns su
AMG05178	-27.8	4.13E-07	Hypothetical protein		cm
AMG05092.2	-27.4	1.84E-10	Hypothetical protein		cm
AMG13068.2	-27.3	0	Hypothetical protein		ns

AMG06334	-26.5	1.74E-31	IgE-binding protein [*Aspergillus fumigatus*]	SP	cm cw
AMG06993.1	-26.3	0	Hypothetical protein		
AMG06707	-26.2	0	Dipeptidyl-peptidase V precursor –[*Aspergillus fumigatus*] gb|AAB67282.1|	SP	ns su
AMG01829.1	-25.1	8.91E-34	Hypothetical protein		cm cw my ns
AMG02948	-24.9	1.19E-21	*BUF1*, trihydroxynaphthalene reductase		ap cm cs cw mk mt ns su
AMG08668.3	-24.8	0	Hypothetical protein		
AMG06064	-24.6	1.39E-37	scytalone dehydratase (EC 4.2.1.94) - *Magnaporthe oryzae*		ap cm mt su
AMG00656	-24.3	5.82E-41	Hypothetical protein		cm cw mt
AMG02248	-24.2	0	Hypothetical protein		
AMG07563	-24.2	1.64E-10	Hypothetical protein		
AMG14788	-24.2	0	Hypothetical protein		ns
AMG06740	-24.1	5.06E-42	Hypothetical protein		mt
AMG06595	-23.8	0	Hypothetical protein		cm cw mt my
AMG11066	-23.7	0	Hypothetical protein		
AMG07092	-23.6	0	Hypothetical protein		
AMG06010	-23.1	0	Hypothetical protein		

AMG01617	-23.1	0	related to beta-1, 3 exoglucanase precursor [*Neurospora crassa*]	SP	
AMG04610.2	-22.4	0	Hypothetical protein		cm cw

[a]Library abbreviations: ap = appressorium, cm = mycelium from complete medium, cs = conidiospores, cw = mycelium grown on rice cell walls, mk = *pmk1*$^{-}$ mutant, mt = mating type, my = mycelium from minimal medium, ns = nitrogen-starved mycelium, and su = subtracted library (Ebbole et al., 2004).

Table 3.3 Expression levels of pathogenicity genes in IH relative to mycelium

Probe	Fold Change	P-value	Gene Identity	*E*-value, Accession #
AMG04255	3.0	0.00048	*ACI1*, MAC1 (adenylate cyclase)-interacting protein 1	4e-45, AY166602
AMG05982	2.0	4.96E-09	*MST12*, transcription factor downsteam of *PMK1*	7e-37, AF432913
AMG02428	1.7[a]	0.07995	*ACE1*, Appressorium-specific PK-NRPS enzyme	0.0 AJ704622
AMG03578.1	1.5	0.00435	*CALM*, Calmodulin	7e-74, AF103729
AMG06876	1.5	0.00056	*NTH1 (PTH9)*, neutral trehalase	0.0, AAN46743
AMG14183	1.5[a]	0.08556	*MgAPT2*, P-type ATPase	0.0, XM_366691
AMG10289	1.4	0.02549	*SPM1*, vacuolar subtilisin-like serine proteinase	0.0, AB070268
AMG07015	1.3[a]	0.1	*PMK1*, pathogenicity MAP kinase	0.0, U70134
AMG12418.1	1.2[a]	0.47419	*MAGB*, Gα subunit of a heterotrimeric G protein	1e-98, AF011341
AMG06279	1.1 [a]	0.72849	*MGB1*, G_{β} subunit of a heterotrimeric G protein	0.0, AB086901
AMG08776	1.1[a]	075067	*ABC1*, ATP-driven efflux pump protein	0.0, AF032443
AMG08216	-1.1[a]	0.60706	*ABC3*, MDR efflux pump	0.0 DQ156556
AMG05260	-5.3	1.39E-08	*PTH11*, integral membrane protein AF119670	0.0, AF119670
AMG06174	-20.5	0	*AOX*, alternative oxidase	1e-66, AB005144
AMG14765	-21.6	3.11E-40	*MPG1*, hydrophobin	6e-54, L20685
AMG06064	-24.6	1.39E-37	*RSY1*, scytalone dehydratase	0.0, AB004741
AMG02948	-24.9	1.19E-21	*BUF1*, trihydroxynaphthlene reductase	0.0, AY846878
AMG01944	-28.1	0	*4HNR*, tetrahydroxy-naphthalene reductase	0.0, XM_365550

[a]P-value >0.05.

[b]Pathogenicity trait affected: C=conidiation, A=appressorium formation, P=penetration, INF=infectious growth (usually defined as inability to infect wounded tissue), AVR=avirulence activity in rice with corresponding *R* gene

Table 3.4 Rice genes up-regulated or down-regulated >50-fold in infected tissue

Sequence Id[a]	Annotation (E-value)	Fold change (P-value)	Comments[b]
Up-Regulated			
AK071227	Unknown expressed protein	99.1 (0)	Chr. 8; not predicted; none
AK105196	*Zea mays* NPK1-related protein kinase (mapkkk1) mRNA (E-value=7e-72)	95.7 (0)	Chr. 1; microbody
AK109702	*Z. mays* NPK1-related protein kinase-like (mapkkk1) mRNA.(E-value=1e-62).	86.2 (0)	Chr. 5; nucleus
AK061237	*Arabidopsis thaliana* mRNA, clone RAFL25-06-N10.(E-value=4e-79).	82.9 (0)	Chr. 1; cytoplasmic; phosphatase
AK071585	*Triticum aestivum* mRNA wdi1c.pk004.j19:fis, (E-value=8e-94).	77.4 (0)	Chr. 1; nucleus; (Related to NPK1 mapkkk)
AK100808	*Z. mays* inward rectifying shaker K+ channel mRNA, complete cds (E-value=0)	76.9 (2.8E-15)	Chr. 2; microbody
AK062422	*Oryza sativa* putative DRE-binding protein 1B mRNA (E-value=0)	75.9 (0)	Chr. 9; microbody
AK106404	*Z. mays* clone EL01N0511B03.d mRNA sequence (E-value=0)	70.3 (0)	Chr.11; mitochondrial inner membrane; cytochrome P450
AK071546	*Lolium rigidum* Lol-5-v putative cytochrome P450 mRNA (E-value=1e-163)	68.2 (0)	Chr. 4; mitochondrial inner membrane
AK111076	Unknown expressed protein	66.0 (2.6E-25)	Chr. 4; nucleus; none

AK073848	*O. sativa* mRNA for OsNAC4 transcription factor (E-value=1e-174)	63.8 (0)	Chr. 1; microbody
AK064287	*Z. mays* clone EL01N0511B03.d mRNA sequence (E-value=1e-163)	59.2 (0)	Chr. 12; ER; cytochrome P450
AK101957	*A. thaliana* At2g46890 mRNA for unknown protein, clone: RAFL17-06-H20 (E-value=1e-100)	58.9 (5.4E-19)	Chr. 4; ER; endomembrane system, integral to membrane
AK062882	*O. sativa* AP2 domain-containing protein AP29 mRNA (E-value=2e-16)	58.1 (0)	Chr. 8; nucleus; ethylene responsive element binding factor (1E-12)
AK067516	Unknown expressed protein	57.7 (1.1E-20)	Chr. 1; nucleus; none
AK063042	Unknown expressed protein	57.7 (0)	Chr. 3; nucleus; transcription factor
AK111091	Unknown expressed protein	56.7 (0)	Chr. 1; chloroplast stroma; none
Down-Regulated			
AK107088	A. thaliana At2g46930/F14M4.24 mRNA (E-value=1e-134)	-50.5 (8.5E-10)	Chr. 1; extracellular; pectin acetyl esterase
AK072459	*Malus domestica* unknown mRNA (E-value=0)	-58.9 (8.9E-11)	Chr. 10; extracellular; methyl transferase
AK105875	Unknown expressed protein	-68.5 (8.7E-19)	Chr. 1; nucleus; disease resistance kinase
AK065689	*A. thaliana* chloroplast carotenoid epsilon-ring hydroxylase (*LUT1*) mRNA, nuclear gene for chloroplast product (E-value=0)	-69.9 (2.2E-12)	Chr. 10; plasma membrane; cytochrome P450
AK067229	*O. sativa* alkaline alpha-galactosidase mRNA (E-value=0)	-71.7 (1.5E-8)	Chr. 8; ER

AK105369	Unknown expressed protein	-72.0 (1.6E-10)	Chr. 7; cytoplasm; none
AK107138	*M. truncatula* triacylglycerol/steryl ester lipase-like protein mRNA (E-value=1e-107)	-74.7 (1.7E-14)	Chr. 8; extracellular

[a]Rice gene names are from the KOME database (http://cdna01.dna.affrc.go.jp/cDNA/).

[b]Chromosome #; PSORT localization prediction; function predicted by protein homology or GO annotation designations in the KOME database.

Table 3.5 Rice gene categories with members that were up- or down-regulated more than 3-fold

Gene Id	Annotation	Fold change	P-value	E- value
WRKY				
AK106282	*Oryza sativa* (indica cultivar-group) transcription factor WRKY09 (WRKY09) mRNA, complete cds.	18.6	0	5.0E-80
AK102093	*O. sativa* (indica cultivar-group) WRKY DNA-binding protein (WRKY89) mRNA, complete cds.|PLN	11.7	0	1.0E-121
AK066255	*O. sativa* (japonica cultivar-group) WRKY45 mRNA, complete cds.	11.0	0	0.0
AK108860	*Solanum tuberosum* StWRKY mRNA for WRKY-type DNA binding protein, complete cds.|PLN	9.6	0	5.0E-42
AK108555	*Arabidopsis thaliana* WRKY transcription factor 51 (WRKY51) mRNA, complete cds.|PLN	8.0	0	8.0E-29
AK065265	*O. sativa* (indica cultivar-group) transcription factor WRKY31 (WRKY31) mRNA, complete cds.	4.6	3.03E-11	1.0E-164
AK101653	*A. thaliana* putative WRKY-type DNA binding protein (At2g46400) mRNA, complete cds.|PLN	4.0	0	5.0E-14
AK108389	*O. sativa* (indica cultivar-group) transcription factor WRKY08 (WRKY08) mRNA, complete cds.	3.3	4.48E-09	2.0E-50
AK109568	*O. sativa* (japonica cultivar-group) WRKY17 mRNA, complete cds.	3.3	8.72E-21	0.0
AK107199	*O. sativa* (japonica cultivar-group) WRKY24 mRNA, complete cds.	3.0	8.65E--13	0.0
Defense				
AK063248	*Hordeum vulgare* HvPR-1a mRNA for a basic PR-1-type pathogenesis-related protein.|PLN	28.3	0	2.0E-34
AK060005	*H. vulgare* HvPR-1a mRNA for a basic PR-1-type pathogenesis-related protein.|PLN	14.4	0	1.0E-32
AK066825	*O. sativa* lipoxygenase (CM-LOX2) mRNA, partial cds.|PLN	13.9	0	0.0
AK061606	*O. sativa* (japonica cultivar-group) RSOsPR10 mRNA for root specific pathogenesis-related protein 10, complete cds.	13.0	0	0.0

AK101439	*H. vulgare* mRNA for NBS-LRR disease resistance protein homologue (rga S-9202 gene).	8.0	4.83E-26	1.0E-51
AK064985	*A. thaliana* RPT2 (RPT2) mRNA, complete cds.|PLN	6.1	0	1.0E-100
AK060057	*O. sativa* (japonica cultivar-group) Prb1 mRNA, complete cds.	5.3	0	0.0
AK101496	*H. vulgare* partial mRNA for NBS-LRR disease resistance protein homologue (rga S-9203 gene).	2.9	0.00418	7.0E-90
AK073881	*Prunus persica* putative NBS-LRR type disease resistance protein (RPM1) mRNA, complete cds.	2.9	0.00004	2.0E-47
AK108785	*Solanum lycopersicoides* disease resistance protein SlVe2 precursor, mRNA, complete cds.	2.5	0.00058	3.0E-53
AK070856	*H. vulgare* partial mRNA for NBS-LRR disease resistance protein homologue (rga S-9203 gene).	2.1	0.00105	1.0E-162
AK072959	*Triticum aestivum* stripe rust resistance protein Yr10 (Yr10) mRNA, complete cds.|PLN	-2.0	4.54E-08	8.0E-41
AK111610	resistance to *Pseudomonas syringae* protein 5 [imported] - *A. thaliana*	-3.0	4.54E-11	2.0E-86
Peroxidases				
AK102307	*O. sativa* cationic peroxidase (OsCPX1) mRNA, complete cds.|PLN	13.7	1.77E-28	0.0
AK104277	*H. vulgare* peroxidase BP 1 (Prx5) mRNA, complete cds.|PLN	13.3	0	6.0E-99
AK072761	*Gossypium hirsutum* bacterial-induced peroxidase mRNA, complete cds.|PLN	9.0	0	1.0E-62
AK064918	*A. thaliana* mRNA for peroxidase ATP22a.|PLN	8.8	0	1.0E-84
AK109480	*H. vulgare* peroxidase BP 1 (Prx5) mRNA, complete cds.	8.5	0	1.0E-101
AK069456	*Asparagus officinalis* mRNA for peroxidase (prx3 gene).	7.6	0	1.0E-125
AK065893	*A. thaliana* At4g32320 mRNA for putative L-ascorbate peroxidase, complete cds	6.8	0.00162	1.0E-85
AK065090	*Z. mays* mRNA for anionic peroxidase.|PLN	6.5	1.82E-18	4.0E-71
AK070715	*Triticum monococcum* peroxidase 8 (POX8) mRNA, complete cds.	5.3	7.71E-44	1.0E-120
AK067667	*Z. mays* mRNA for anionic peroxidase.|PLN	5.0	0	9.0E-73
AK067416	*Z. mays* partial mRNA for peroxidase (pox3 gene).|PLN	4.3	2.81E-07	1.0E-123
AK058883	*Z. mays* mRNA for peroxidase (pox1 gene).|PLN	4.1	0	4.0E-84
AK104633	*Ipomoea batatas* mRNA for peroxidase (pod gene).|PLN	3.2	3.02E-38	7.0E-94

AK106200	*Spinacia oleracea* peroxidase prx12 precursor, mRNA, complete cds.|PLN	3.1	0.00158	3.0E-72
AK103558	*Z. mays* mRNA for anionic peroxidase.|PLN	3.0	4.19E-07	1.0E-79
AK109551	*Nicotiana tabacum* mRNA for cationic peroxidase isozyme 40K, complete cds.|PLN	2.9	1.14E-19	2.0E-70
AK073202	*O. sativa* peroxidase (POX22.3) mRNA, complete cds.|PLN	2.8	0	0.0
AK060007	*S.oleracea* mRNA for peroxidase, clone PC55.|PLN	2.6	0	3.0E-92
AK073978	*S. tuberosum* mRNA for putative peroxidase (prx2 gene).|PLN	2.2	0.00857	6.0E-98
AK061809	*Z. mays* mRNA for peroxidase (pox2 gene).|PLN	2.0	1.07E-06	7.0E-17
AK101508	*Nicotiana tabacum* mRNA for cationic peroxidase isozyme 40K, complete cds.|PLN	-3.2	0.00009	1.0E-72
AK069281	*Triticum monococcum* peroxidase 7 (POX7) mRNA, complete cds.	-3.3	1.94E-08	0.0
Kinases				
AK105196	*Z. mays* NPK1-related protein kinase-like protein (mapkkk1) mRNA, partial cds.|PLN	95.7	0	7.0E-72
AK109702	*Z. mays* NPK1-related protein kinase-like protein (mapkkk1) mRNA, partial cds.|PLN	86.2	0	1.0E-62
AK071585	NPK1-related protein kinase homolog T26B15.7 - *A. thaliana*	77.4	0	1.0E-58
AK107168	*Z. mays* NPK1-related protein kinase-like protein (mapkkk1) mRNA, partial cds.|PLN	43.8	0	3.0E-93
AK111977	*Z. mays* Avr9/Cf-9 induced kinase 1 (ACIK1) mRNA, complete cds.	34.8	1.71E-07	1.0E-124
AK058518	NPK1-related protein kinase homolog F10M23.230 - *A. thaliana*	28.9	0	6.0E-64
AK105946	*Z. mays* NPK1-related protein kinase-like protein (mapkkk1) mRNA, partial cds.|PLN	25.9	0	2.0E-70
AK107566	*O. sativa* (japonica cultivar-group) clone OsJalk8 putative leucine-rich repeat receptor-like kinase mRNA, complete cds.	12.2	0	0.0
AK099582	wall-associated serine/threonine kinase (EC 2.7.1.-) 2 [imported] - *A. thaliana*	13.1	0	6.0E-89

AK100906	probable diacylglycerol kinase [imported] - *A. thaliana*	10.4	0	0.0
AK102590	*Lycopersicon esculentum* diacylglycerol kinase (DGK1) mRNA, complete cds.|PLN	9.5	0	0.0
AK072014	*A. thaliana* WNK3 mRNA for protein kinase, complete cds.|PLN	8.1	1.38E-20	1.0E-63
AK069094	*A. thaliana* protein kinase-like protein (At3g25840) mRNA, complete cds.|PLN	7.7	0.00038	5.0E-94
AK068330	*Nicotiana tabacum* Avr9/Cf-9 induced kinase 1 (ACIK1) mRNA, complete cds.	6.0	0	1.0E-133
AK105337	*A. thaliana* At5g47070 mRNA for putative protein serine/threonine kinase, complete cds, clone: RAFL17-20-O04.|PLN	6.0	0	2.0E-95
AK106447	receptor-protein kinase-like protein - *A. thaliana*	5.9	3.66E-07	2.0E-98
AK069157	*O. sativa* subsp. indica pyruvate dehydrogenase kinase 1 mRNA, complete cds.|PLN	5.7	0	0.0
AK110253	*Z. mays* mRNA for putative protein kinase.|PLN	5.6	4.25E-23	0.0
AK109607	*A. thaliana* putative protein kinase (At2g05940) mRNA, complete cds.|PLN	5.6	0	1.0E-119
AK100357	*A. thaliana* putative casein kinase (At3g13670) mRNA, complete cds.|PLN	5.5	0	0.0
AK100082	*A. thaliana* putative receptor protein kinase (At1g28440) mRNA, complete cds.|PLN	5.0	2.21E-21	0.0
AK068025	*O. sativa* (japonica cultivar-group) mRNA for orthophosphate dikinase, complete cds.|PLN	4.7	0	0.0
AK102758	*Z. mays* KI domain interacting kinase 1 (KIK1) mRNA, complete cds.|PLN	4.5	0	0.0
AK072243	*O. sativa* fructose-6-phosphate-2-kinase/fructose-2,6-bisphosphatase mRNA, complete cds.|PLN	4.5	7.20E-23	0.0
AK106421	*A. thaliana* Columbia protein kinase mRNA, complete cds.|PLN	4.0	1.10E-06	7.0E-97
AK100389	*O. sativa* (japonica cultivar-group) MAPK6 mRNA, complete cds.	4.0	4.03E-40	0.0
AK066978	*Lycopersicon esculentum* auxin-regulated dual specificity cytosolic kinase mRNA, complete cds	3.7	0	2.0E-50
AK061645	*O. sativa* (japonica cultivar-group) MAPK6 mRNA, complete cds.	3.5	2.03E-35	0.0

AK108455	*A. thaliana* putative protein kinase (At1g67580; F12B7.13) mRNA, complete cds.|PLN	3.5	6.30E-16	5.0E-40
AK110482	*A. thaliana* putative receptor serine/threonine kinase PR5K (PR5K) mRNA, complete cds.|PLN	3.4	5.05E-33	1.0E-93
AK071798	*Prunus armeniaca* pyrophosphate-dependent phosphofructo-1-kinase mRNA, partial cds.|PLN	3.4	0	1.0E-109
AK111550	*A. thaliana* At4g23180 mRNA for putative receptor-like protein kinase 4 (RLK4), complete cds.|PLN	3.4	0	1.0E-110
AK105151	*O. sativa* (indica cultivar-group) choline kinase (CK) mRNA, complete cds.	3.4	0	0.0
AK071968	*O. sativa* (indica cultivar-group) choline kinase (CK) mRNA, complete cds.	3.2	0	0.0
AK103306	*A. thaliana* calcium-dependent protein kinase (At3g51850) mRNA, complete cds.|PLN	3.1	3.04E-06	1.0E-162
AK067266	*A. thaliana* ATPK64 mRNA for protein kinase, complete cds.	3.1	1.40E-45	3.0E-47
AK109954	*Nicotiana tabacum* cytokinin-regulated kinase 1 (CRK1) mRNA, complete cds.|PLN	3.1	5.23E-15	4.0E-78
AK101080	*Z. mays* phosphoenolpyruvate carboxylase kinase 1 (PPCK1) mRNA, complete cds.	3.0	0	1.0E-149
AK111842	leucine-rich repeat transmembrane protein kinase 1 - *Z. mays* (fragment)	3.0	2.54E-08	1.0E-170
AK061220	serine/threonine protein kinase-like protein - *A. thaliana*	2.9	0	1.0E-138
AK065374	*A. thaliana* SOS2-like protein kinase PKS8 mRNA, complete cds.	2.9	1.46E-22	1.0E-121
AK064359	*A. thaliana* putative receptor protein kinase (At5g53890) mRNA, complete cds.|PLN	-2.9	4.16E-13	0.0
AK067238	*A. thaliana* clone RAFL15-23-F05 (R20566) putative cell division-related protein (At1g53050) mRNA, complete cds.	-3.2	1.40E-45	1.0E-162
AK067723	*A. thaliana* putative receptor protein kinase (At1g28440) mRNA, complete cds.|PLN	-3.4	0	0.0
AK103166	*A. thaliana* putative receptor protein kinase (At5g53890) mRNA, complete cds.|PLN	-4.3	0	0.0
AK073574	*Saccharum* hybrid cultivar SP70-1143 SHR5-receptor-like kinase mRNA, partial cds.	-4.8	2.06E-32	1.0E-142

Chitinases				
AK059767	*Tulipa bakeri* tbc1 mRNA for bulb chitinase-1, complete cds.|PLN	19.8	5.91E-37	1.0E-74
AK071453	*O. sativa* (japonica cultivar-group) class III chitinase RCB4 (Rcb4) mRNA, complete cds.|PLN	10.6	0	1.0E-150
AK100973	*O. sativa* (japonica cultivar-group) mRNA for acidic class III chitinase OsChib3a, complete cds.|PLN	8.5	1.10E-11	0.0
AK102505	*O. sativa* (japonica cultivar-group) mRNA for chitinase, complete cds.|PLN	6.8	1.40E-45	8.0E-69
AK108949	*O. sativa* mRNA for endochitinase.|PLN	4.5	3.49E-11	0.0
AK073843	*O. sativa* (japonica cultivar-group) mRNA for chitinase, complete cds.|PLN	4.3	4.72E-15	2.0E-87
AK064180	*O. sativa* (japonica cultivar-group) mRNA for chitinase, complete cds.|PLN	3.1	5.39E-08	2.0E-58
AK061042	*O. sativa* mRNA for endochitinase.|PLN	2.9	3.14E-21	0.0
Membrane Proteins				
AK107700	*Z. mays* plasma membrane integral protein ZmPIP2-6 mRNA, complete cds.|PLN	25.8	0	1.0E-127
AK072632	*Z. mays* plasma membrane integral protein ZmPIP2-6 mRNA, complete cds.|PLN	6.4	0	0.0
AK061898	*O. sativa* (japonica cultivar-group) mRNA for membrane related protein (mrp1 gene).	4.9	0	0.0
AK065035	*O. sativa* (japonica cultivar-group) mRNA for membrane related protein (mrp1 gene).	4.8	0	0.0
AK061782	*Triticum aestivum* plasma membrane intrinsic protein 2 (PIP2) mRNA, complete cds.|PLN	4.7	0	0.0
AK102174	*Z. mays* plasma membrane integral protein ZmPIP1-5 mRNA, complete cds.|PLN	3.8	0	0.0
AK058648	*Saccharum* hybrid cultivar H65-7052 membrane protein mRNA, complete cds.|PLN	3.5	7.62E-12	2.0E-80
AK102748	*Gossypium hirsutum* membrane-anchored endo-1,4-beta-glucanase (CEL) mRNA, complete cds.	3.0	0	0.0
AK066134	(O49621) MLO-like protein 1 (AtMlo1) (MLO protein homolog 1) (AtMLO-H1)	3.0	1.18E-18	1.0E-101

AK107345	*A. thaliana* integral membrane protein, putative (At3g21690) mRNA, complete cds.|PLN	-42.9	8.77E-10	1.0E-126
Heat Shock proteins				
AK100412	*O. sativa* (japonica cultivar-group) Spl7 mRNA for heat stress transcription factor Spl7, complete cds.	5.0	0	0.0
AK064271	*A. thaliana* At2g26150 mRNA for putative heat shock transcription factor, complete cds.|PLN	4.9	4.79E-07	5.0E-54
AK101934	*Lycopersicon peruvianum* heat stress transcription factor A3 (HSFA3) mRNA, complete cds.|PLN	4.4	0	1.0E-68
AK101824	*O. sativa* (japonica cultivar-group) heat shock factor RHSF5 mRNA, complete cds.	3.5	6.60E-06	0.0
AK066844	*O. sativa* (japonica cultivar-group) heat shock factor RHSF7 mRNA, complete cds.	3.2	3.39E-36	1.0E-149
AK062091	*Fragaria x ananassa* LMW heat shock protein mRNA, complete cds.|PLN	3.0	0	2.0E-24
Cellulose Synthesis or Degradation				
AK073561	*Bambusa oldhamii* cellulose synthase BoCesA6 mRNA, partial cds.	2.4	1.30E-19	0.0
AK111344	*Nicotiana tabacum* cellulose synthase-like protein CslE mRNA, complete cds.	2.4	0.0002	3.0E-15
Plasmodesma Receptor				
AK106058	*Nicotiana tabacum* non-cell-autonomous protein pathway2 (NCAPP2) mRNA, complete cds.	8.7	2.94E-32	3.0E-88
Glucanases				
AK063953	*O. sativa* endo-1,3-beta-glucanase mRNA, complete cds.|PLN	32.4	0	0.0
AK058891	Sorghum bicolor beta-1,3-glucanase mRNA, partial cds.|PLN	4.2	2.13E-18	5.0E-89
AK069096	*O. sativa* endo-1,3-beta-glucanase mRNA, complete cds.|PLN	2.9	3.88E-29	0.0

AK104139	*O. sativa* endo-1,3-beta-glucanase mRNA, complete cds.|PLN	-3.6	0	0.0
AK103072	*A. thaliana* putative beta-1,3-glucanase (At2g27500) mRNA, complete cds.|PLN	-4.0	3.92E-33	1.0E-122
Pectin-Degrading Enzymes				
AK100257	*Z. mays* mRNA for pectin methylesterase-like protein.|PLN	-3.3	3.03E-08	1.0E-126
AK101962	*A. thaliana* clone U11512 putative pectin methylesterase (At5g09760) mRNA, complete cds.	-4.7	0	1.0E-135
AK073853	*A. thaliana* putative polygalacturonase (At1g60590/F8A5_12) mRNA, complete cds.|PLN	3.6	3.43E-10	1.0E-139
AK105858	*Lycopersicon esculentum* polygalacturonase (XOPG1) mRNA, complete cds.|PLN	-4.1	0	1.0E-112
AK106049	*Lycopersicon esculentum* polygalacturonase (XOPG1) mRNA, complete cds.|PLN	-4.3	0	1.0E-108
PALs				
AK068993	*Bambusa oldhamii* phenylalanine ammonia-lyase (PAL1) mRNA, complete cds.	5.2	0	0.0
AK067801	*Bambusa oldhamii* phenylalanine ammonia-lyase (PAL1) mRNA, complete cds.	4.9	3.28E-06	0.0
Expansins				
AK060313	*O. sativa* expansin Os-EXP3 (Os-EXP3) mRNA, complete cds.|PLN	3.3	0.00054	0.0
AK064012	*O. sativa* beta-expansin (EXPB4) mRNA, complete cds.|PLN	3.1	2.82E-15	0.0
AK099870	*O. sativa* (japonica cultivar-group) expansin-like protein mRNA, partial cds.|PLN	2.1	1.77E-24	0.0
AK061423	*O. sativa* beta-expansin (EXPB7) mRNA, complete cds.|PLN	-2.2	3.48E-29	0.0
AK059638	*O. sativa* beta-expansin (EXPB11) mRNA, partial cds.|PLN	-2.3	3.87E-12	0.0
AK062225	*O. sativa* alpha-expansin OsEXP10 mRNA, complete cds.|PLN	-2.6	4.20E-30	0.0
AK061068	*O. sativa* beta-expansin (EXPB2) mRNA, complete cds.|PLN	-5.0	0	1.0E-155

AK100959	*O. sativa* beta-expansin (EXPB3) mRNA, complete cds.|PLN	-8.8	0	0.0

Table 3.6 Description of *M. oryzae* genes used for gene knock-out analysis

Gene	Annotation	Features	Homology[a]	Score
AMG08261	Hypothetical protein	Glycosyl hydrolase family 76	Hypothetical protein of *Gibberella zeae*	9e-128
AMG08541	Predicted protein		Predicted protein *Pheosphaeria nodorum*	3e-14
AMG12560	Predicted protein		Cysteine desulphurase, SufS *Mycobacterium smegmatis*	0.99
AMG08859	Predicted protein		Disease resistance protein Aig2, putative *Aspergillus fumigatus*	0.58

[a] Homology based on BLASTP search (http://www.ncbi.nlm.nih.gov/BLAST/Blast.cgi?PAGE=Proteins&PROGRAM=blastp&BLAST_PROGRAMS=blastp&PAGE_TYPE=BlastSearch&SHOW_DEFAULTS=on).

Table 3.7 List of primers used in this study

Primer Name	Sequence 5'-3'	Comment
Fungal Primers		
AMG15373-3-F	**CGCCGTCTACGCCATCCTGG**	
AMG15373-4-R	**CCGCCTGGTGATGACGTCGG**	
AMG08263-F	**AAATCAATCAAACGCGGGACTGGC**	
AMG08263-R	**ACATGGCGTCCTCATCATCGGAAT**	
AMG08261-F	**TTTACGGTGCTTGCCACCTTTACC**	
AMG08261-R	**GCCTTCCATTGCTCGAATCTGCTT**	
AMG08541-F	**AAGAACGTCGGCACAGGTAACGG**	
AMG08541-R	**CTTAACGGTCTGGGCCTTGTTGG**	
AMG06765-F	**GAAGGCGACCGTGCTTGCATATTT**	
AMG06765-R	**TTGCATCCCTCTCCTTCAGAGCAA**	
AMG06650-F	**GCAGCTCCACAACGTCTGTTCAAT**	
AMG06650-R	**AGTCACAGTAGCCGCACGAGTATT**	
AMG12560-F	**AGACTTCCCCGGTGCCAAAGC**	
AMG12560-R	**AGATGCAGGGGTTGTCCCCG**	
AMG13016-F	**TTTCGCTACTGTTGCCACCTTGG**	
AMG13016-R	**TTAGTTAAGCTGGGTACCCTCCGC**	
AMG05292-F	**AGCACCTCGACCAAAGTCAAGCTA**	
AMG05292-R	**TGGCAAGTGTAGCCGTTGATAAGC**	
AMG13014-F	**GGACAACTTTACGCCGCTCAACAA**	
AMG13014-R	**TATCATCCCTCAACCAGCCCAACA**	
AMG08701-F	**CCGTGGGCTACGGCTATGAAATTA**	
AMG08701-R	**ATGGAACCTGCATGTGACGCGTAT**	
AMG15980-F	**AGCTCTCATTCTCAGCAATCGCCA**	
AMG15980-R	**TCATTTCCGTCCAGAGACTTGGCA**	
AMG08508-F	**TGTTACCATGTTCGCCGTTGGT**	
AMG08508-R	**CATAGTCCGAGAACTTTGCTTGGC**	
AMG08160-2-F	**ATGTCACTCGTTAACCTCTCCAGG**	

AMG08160-3-R	**AACGAGATGAAGTTGGCCGTGT**	
AMG05133-F	**TGGCATCCGACAGAACTACACCAA**	
AMG05133-R	**TCAAGCGAGAACTTCCAGTGCGTA**	
AMG08859-F	**GCGATGTTCACCTGACCTGGG**	
AMG08859-R	**AGCCGTACTGTAGCTGGTGCG**	
AMG08417.2-F	**AAAGATCCTGCACTCGCTCATCGT**	
AMG08417.2-R	**ACCTGGTCCCAATACTCAGTGCAA**	
AMG16082-F	**CGCAAGCAGTTCCATCGAAGCTTTAC**	
AMG16082-R	**ATTGCTCCACTTCTTCGAATCGGG**	
AMG15020-F	**TGACCAATGGCAACAAGCGCGA**	
AMG15020-R	**TCTTGGAGCCAGTCTTGGTGCTA**	
PWL2-F	**GTGGCGGGTGGACTAACAAACAAT**	
PWL2-R	**AAACTCGCCTGGCGGTCCATAATA**	
AVR-PITA-F	**GCACCTTTTCACACCCAGTT**	
AVR-PITA-R	**CTCGGACGCACGTATAAACA**	
AMG12697.1-F	**ATTTCCGACAATGCACAGCCGCTAC**	
AMG12697.1-R	**CATGTCGGCACCTTTGATGTTGCT**	
AMG05260-F	**AATCCGACTCTTTCAGTAGCGGCA**	
AMG05260-R	**CTCCATGCATTTGCCTTCGATGCT**	
AMG06064-F	**ATGACTTGCGTCTATGAGTGGGCA**	
AMG06064-R	**TATTTGTCGCCAAAGGTCTCCCGT**	
AMG01994-F	**CTTTGTCATGTCCAACAGCGGCAT**	
AMG01944-R	**CAAATGCACGGCAGAAACCCTCAA**	
MgACTIN328-F	**TCCCATGTCACCACTTTCAA**	
MgACTIN328-R	**TTCGAGATCCACATCTGCTG**	
RICE PRIMERS		
OsACTIN-F	**GAAGATCACTGCCTTGCTCC**	
OsACTIN-R	**CGATAACAGCTCCTCTTGGC**	
MOS41902-F	**ATCTTGGCCGAGTGTTGACGAGAT**	**AK071227**

MOS41902-R	**TCAAAGTTGTTTGCTCGCCGAAGG**	
MOS04462-F	**TACTGGAGCACCCATTTCTCGCAT**	**AK105196**
MOS04462-R	**TCCGAAACTTCAGATGGGTCGCTT**	
MOS28016-F	**ATTGGGAATCAGACGATGGCTGGA**	**AK109702**
MOS28016-R	**TTGGCGGAGCTGTTCATCCACAAA**	
MOS04461-F	**AAGGACTTCCTGGATGGCTGCTT**	**AK071585**
MOS04461-R	**TGGAGGATTCGATCGCTTCTGCTT**	
MOS45375-F	**ACATGCCGCTCTGGAGCTACTAAT**	**AK062422**
MOS45375-R	**AGCTCTTTGGAGAGGAGAAGTAAA**	
MOS19247-F	**AGCATCAGGGTGATTCCCTTGTCA**	**AK071546**
MOS19247-R	**TCAATCAGGCCCTCATGGTCTTGT**	
MOS03724-F	**CAGTGGAGCTTGTTGCAAACCCTT**	**AK100135**
MOS03724-R	**TCACCACCTCGCTTCATCAGGAAA**	
MOS52342-F	**GCTTGCCTTCGTCAAGTTCTTGGT**	**AK059060**
MOS52342-R	**TCTCACTTCCACCTCTTCGCGTTT**	
MOS56011-F	**ATGAAGCTCAACCCTGCTGTGGAT**	**AK061606**
MOS56011-R	**AGGAAGCAGCAATACGGAGATGGA**	
MOS52906-F	**CGACCATCGGCAATTTCATTCGGT**	**AK069082**
MOS52906-R	**ACCGTTAAGCTGGTTGGTCCTGAA**	
MOS00599-F	**TGGAGCTCCTGGATGCTGGAAATA**	**AK108785**
MOS00599-R	**AGGAGCTGATGCACTTGGAGATGT**	
AK107735-F	**AGCAAGAAAGTTGCTGGCAAGGTC**	
AK107735-R	**TCAAATCTCAACCTGGGTCGTCGT**	

References

Asai, T., Tena, G., Plotnikova, J., Willmann, M.R., Chiu, W.-L., Gomez-Gomez, L., Boller, T., Ausubel, F.M., and Sheen, J. (2002). MAP kinase signalling cascade in Arabidopsis innate immunity. Nature 415, 977-983.

Avilla-Adams, C., and Köller, W. (2002). Disruption of the alternative oxidase gene in *Magnaporthe grisea* and its impact on host infection. Molecular Plant-Microbe Interactions 15, 493-500.

Basse, C.W., Stumpferl, S., and Kahmann, R. (2000). Characterization of a *Ustilago maydis* Gene Specially induced during the Biotrophic Phase: Evidence for negative as Well as Positive Regulation. Molecular and Cellular Biology 20, 329-339.

Bent, A.F., and Mackey, D. (2007). Elicitors, Effectors, and R Genes: The New Paradigm and a Lifetime Supply of Questions, pp. 399-436.

Berruyer, R., Poussier, S., Kankanala, P., Mosquera, G., and Valent, B. (2006). Quantitative and qualitative influence of inoculation methods on *in planta* growth of rice blast fungus. Phytopathology 96, 346-355.

Berruyer, R., Khang, C.H., Kankanala, P., Kang, S., and Valent, B. (Unpublished results).

Bhattacharjee, S., Hiller, N.L., Liolios, K., Win, J., Kanneganti, T.-D., Young, C., Kamoun, S., and Haldar, K. (2006). The malarial host-targeting signal is conserved in the Irish potato famine pathogen. PLOS Pathogens 2, e50.

Birch, P.R.J., and Kamoun, S. (2000). Studying interaction transcriptomes: coordinated analyses of gene expression during plant-microorganism interactions. In New Technologies for Life Sciences: A Trends Guide, R. Wood, ed (New York: Elsevier Science), pp. 77-82.

Birch, P.R.J., Rehmany, A.P., Pritchard, L., Kamoun, S., and Beynon, J.L. (2006). Trafficking arms: oomycete effectors enter host plant cells. Trends in Microbiology 14, 8-11.

Böhnert, H.U., Fudal, I., Dioh, W., Tharreau, D., Notteghem, J.-L., and Lebrun, M.-H. (2004). A Putative Polyketide Synthase/Peptide Synthetase from Magnaporthe grisea Signals Pathogen Attack to Resistant Rice. Plant Cell 16, 2499-2513.

Both, M., Csukai, M., Stumpf, M.P.H., and Spanu, P.D. (2005). Gene Expression Profiles of *Blumeria graminis* Indicate Dynamic Changes to Primary Metablism during Development of an Obligate Biotrophic Pathogen The Plant Cell 17, 2107-2122.

Bourett, T.M., and Howard, R.J. (1990). *In vitro* development of penetration structures in the rice blast fungus *Magnaporthe grisea*. Canadian Journal of Botany 68, 329-342.

Bruno, K.S., Tenjo, F., Li, L., Hamer, J.E., and Xu, J.-R. (2004). Cellular localization and role of kinase activity of *PMK1* in *Magnaporthe grisea*. Eukaryotic Cell 3, 1525-1532.

Bryan, G.T., Wu, K., Farrall, L., Jia, Y., Hershey, H.P., McAdams, S.A., Faulk, K.N., Donaldson, G.K., Tarchini, R., and Valent, B. (2000). A single amino acid difference distinguishes resistant and susceptible alleles of the rice blast resistance gene *Pi-ta*. Plant Cell 12, 2033-2045.

Catanzariti, A.-M., Dodds, P.N., Lawrence, G.J., Ayliffe, M.A., and Ellis, J.G. (2006). Haustorially Expressed Secreted Proteins from Flax Rust Are Highly Enriched for Avirulence Elicitors. Plant Cell 18, 243-256.

Chen, X., Shang, J., Chen, D., Lei, C., Zou, Y., Zhai, W., Liu, G., Xu, J., Ling, Z., Cao, G., Ma, B., Wang, Y., Zhao, X., Li, S., and Zhu, L. (2006). A B-lectin receptor kinase gene conferring rice blast resistance. The Plant Journal 46, 794-804.

Chisholm, S.T., Coaker, G., Day, B., and Staskawicz, B.J. (2006). Host-microbe interactions: shaping the evolution of the plant immune response. Cell 124, 803-814.

Choi, W., and Dean, R.A. (1997). The Adenylate Cyclase Gene MAC1 of Magnaporthe grisea Controls Appressorium Formation and Other Aspects of Growth and Development. The Plant Cell 9, 1973-1983.

Chumley, F.G., and Valent, B. (1990). Genetic analysis of melanin-deficient, nonpathogenic mutants of Magnaporthe grisea. Mol. Plant-Microbe Interact. 3, 135-143.

Couch, B.C., and Kohn, L.M. (2002). A multilocus gene genealogy concordant with host preference indicates segregation of a new species, *Magnaporthe oryzae*, from *M. grisea*. Mycologia 94, 683-693.

Dai, L.-Y., Liu, X-L., Xiao, Y-H., and Wang, G-L. (2007). Recent Advances in Clonning and Characterization of Disease Resistance Genes in Rice. Journal of Integrative Plant Biology 49.

Dean, R.A. (1997). Signal pathways and appressorium morphogenesis. Annu. Rev. Phytophatol. 35, 211-234.

Dean, R.A., Talbot, N.J., Ebbole, D.J., Farman, M.L., Mitchell, T.K., Orbach, M.J., Thon, M., Kulkarni, R., Xu, J.-R., Pan, H., Read, N.D., Lee, Y.-H., Carbone, I., Brown, D., Oh, Y.Y., Donofrio, N., Jeong, J.S., Soanes, D.M., Djonovic, S., Kolomiets, E., Renmeyer, C., Li, W., Harding, M., Kim, S., Lebrun, M.H., Bohnert, H., Coughlan, S., Butler, J., Calvo, S., Li-Jun, M., Nicol, R., Purcell, S., Nusbaum, C., Galagan, J.E., and Birren, B.W. (2005). The genome sequence of the rice blast fungus *Magnaporthe grisea*. Nature 434, 980-986.

DeZwaan, T.M., Carroll, A.M., Valent, B., and Sweigard, J.A. (1999). *Magnaporthe grisea* Pth11p is a novel plasma membrane protein that mediates appressorium differentiation in response to inductive substrate cues. The Plant Cell 11, 2013-2030.

Donofrio, N.M., Oh, Y., Lundy, R., Pan, H., Brown, D.E., Jeong, J.S., Coughlan, S., Mitchell, T.K., and Dean, R.A. (2006). Global gene expression during nitrogen starvation in the rice blast fungus, *Magnaporthe grisea*. Fungal Genetics and Biology 43, 605-617.

Dubouzet, J.G., Sakuma, Y., Ito, Y., Kasuga, M., Dubouzet, E.G., Miura, S., Seki, M., Shinozaki, K., and Yamaguchi-Shinozaki, K. (2003). Os*DREB* genes in rice, *Oryza sativa* L., encode transcription activatiors that function in drought-, high-salt- and cold-responsive gene expression. The Plant Journal 33, 751-763.

Ebbole, D.J. (2007). Magnaporthe as a Model for Understanding Host-Pathogen Interactions. The Annual Review of Phytopathology 45, 437-456.

Ebbole, D.J., Jin, Y., Thon, M., Pan, H., Bhattarai, E., Thomas, T., and Dean, R. (2004). Gene Discovery and Gene Expression in the Rice Blast Fungus, Magnaporthe grisea: Analysis of Expressed Sequence Tags. Molecular Plant-Microbe Interactions 17, 1337-1347.

Ellis, J.G., Dodds, P.N., and Lawrence, G.J. (2007). Flax Rust Resistance Gene Specificity is Based on Direct Resistance-Avirulence Protein Interactions. Annu. Rev. Phytopathol. 45, 289-306.

Farfsing, J.W., Auffarth, K., and Basse, C.W. (2005). Identification of cis-Active Elements in *Ustilago maydis mig2* Promoters Conferring High-Level Activity During Pathogenic Growth in Maize. Molecular Plant-Microbe Interactions 18, 75-87.

Foster, A.J., Jenkinson, J.M., and Talbot, N.J. (2003). Trehalose synthesis and metabolism are required at different stages of plant infection by *Magnaporthe grisea*. The EMBO Journal 22, 225-235.

Froeliger, E.H., Carpenter, B.E. (1996). *NUT1*, a major nitogen regulatory gene in *Magnaporthe grisea*, is dispensable for pathogenicity. . Mol. Gen. Genet. 251, 647-656.

Fudal, I., Collemare, J., Böhnert, H.U., Melayah, D., and Lebrun, M-H. . (2007). Expression of *Magnaporthe grisea* Avirulence Gene *ACE1* Is Connected to the Initiation of Appressorium-Mediated Penetration. Eukaryotic cell 6, 546-554.

Gilbert, M.J., Thornton, C.R., Wakley, G.E., and Talbot, N.J. (2006). A P-type ATPase required for rice blast disease and induction of host resistance. Nature 440, 535-539.

Gjetting, T., Hagedorn, P.H., Schweizer, P., Thordal-Christensen, H., Carver, T.L.W., and Lyngkjr, M.F. (2007). Single-Cell Transcript Profiling of Barley Attacked by the Powdery Mildew Fungus. Molecular Plant-Microbe Interactions 20, 235-246.

Glazebrook, J. (2005). Contrasting mechanisms of defense against biotrophic and necrotrophic pathogens. Annual Review of Phytopathology 43, 205-227.

Gowda, M., Venu, R.C., Li, H., Jantasuriyarat, C., Chen, S., Bellizzi, M., Pampanwar, V., Kim, H., Dean, R.A., Stahlberg, E., Wing, R., Soderlund, C., and Wang, G.-L. (2007). Magnaporthe grisea Infection Triggers RNA Variation and Antisense Transcript Expression in Rice. Plant Physiology 144, 524-533.

Hahn, M., and Mendgen, K. (1997). Characterization of in planta-induced rust genes isolated from a haustorium-specific cDNA library. Molecular Plant-Microbe Interactions 10, 427-437.

Hamer, J.E., Howard, R.J., Chumley, F.G., and Valent, B. . (1988). A mechanism for surface attachment in spores of a plant pathogenic fungus. Science 239, 288-290.

Heinlein, M., and Epel, B.L. (2004). Macromolecular transport and signaling through plasmodesmata. In International Review of Cytology: A Survey of Cell Biology, W.J. Kwang, ed (Oxford: Elsevier), pp. 93-164.

Howard, R.J., and Valent, B. (1996). Breaking and Entering: Host penetration by the fungal rice blast pathogen *Magnaporthe grisea*. Annual Review of Microbiology 50, 491-512.

Huckenlhoven, P. (2005). Powdery mildew susceptibility and the biotrophic infection strategies. FEMS Microbiology letters 245, 9-17.

Hughes, T.R., Mao, M., Jones, A.R., Burchard, J., Marton, M.J., Shannon, K.W., Lefkowitz, S.M., Ziman, M., Schelter, J.M., Meyer, M.R., Kobayashi, S., Davis, C., Dai, H., He, Y.D., Stephaniants, S.B., Cavet, G., Walker, W.L., West, A., Coffey, E., Shoemaker, D.D., Stoughton, R., Blanchard, A.P., Friend, S.H., and Linsley, P.S. (2001). Expression profiling using microarrays fabricated by an ink-jet oligonucleotide synthesizer. Nat Biotech 19, 342-347.

Irie, T., Matsumura, H., Terauchi, R., and Saitoh, H. (2003). Serial Analysis of Gene Expression (SAGE) of *Magnaporthe grisea*: genes involved in appressorium formation. Molecular Genetics and Genomics 270, 181-189.

Jantasuriyarat, C., Gowda, M., Haller, K., Hatfield, J., Lu, G., Stahlberg, E., Zhou, B., Li, H., Kim, H., Yu, Y., Dean, R.A., Wing, R.A., Soderlund, C., and Wang, G.-L. (2005). Large-Scale Identification of Expressed Sequence Tags Involved in Rice and Rice Blast Fungus Interaction. Plant Physiol. 138, 105-115.

Jia, Y., McAdams, S.A., Bryan, G.T., Hershey, H.P., and Valent, B. (2000). Direct interaction of resistance gene and avirulence gene products confers rice blast resistance. The EMBO Journal 19, 4004-4014.

Jones, J.D.G., and Dangl, J.L. (2006). The plant immune system. Nature 444, 323-329.

Kamper, J., Kahmann, R., Bolker, M., Ma, L.-J., Brefort, T., Saville, B.J., Banuett, F., Kronstad, J.W., Gold, S.E., Muller, O., Perlin, M.H., Wosten, H.A.B., de Vries, R., Ruiz-Herrera, J., Reynaga-Pena, C.G., Snetselaar, K., McCann, M., Perez-Martin, J., Feldbrugge, M., Basse, C.W., Steinberg, G., Ibeas, J.I., Holloman, W., Guzman, P., Farman, M., Stajich, J.E., Sentandreu, R., Gonzalez-Prieto, J.M., Kennell, J.C., Molina, L., Schirawski, J., Mendoza-Mendoza, A., Greilinger, D., Munch, K., Rossel, N., Scherer, M., Vranes, M., Ladendorf, O., Vincon, V., Fuchs, U., Sandrock, B., Meng, S., Ho, E.C.H., Cahill, M.J., Boyce, K.J., Klose, J., Klosterman, S.J., Deelstra, H.J., Ortiz-Castellanos, L., Li, W., Sanchez-Alonso, P., Schreier, P.H., Hauser-Hahn, I., Vaupel, M., Koopmann, E., Friedrich, G., Voss, H., Schluter, T., Margolis, J., Platt, D., Swimmer, C., Gnirke, A., Chen, F., Vysotskaia, V., Mannhaupt, G., Guldener, U., Munsterkotter, M., Haase, D., Oesterheld, M., Mewes, H.-W., Mauceli, E.W., DeCaprio, D., Wade, C.M., Butler, J., Young, S., Jaffe, D.B., Calvo, S., Nusbaum, C., Galagan, J., and Birren, B.W. (2006). Insights from the genome of the biotrophic fungal plant pathogen Ustilago maydis. Nature 444, 97-101.

Kaneda, T., Fujiwara, S., Takai, R., Takayama, S., Isogai, A., and Che, F.-S. (2007). Identification of genes involved in induction of plant hypersensitive cell death. Plant Biotechnology 24, 191-200.

Kang, S., Sweigard, J.A., and Valent, B. (1995). The *PWL* host specificity gene family in the blast fungus *Magnaporthe grisea*. Molecular Plant-Microbe Interactions 8, 939-948.

Kankanala, P., Czymmek, K., and Valent, B. (2007). Roles for rice membrane dynamics and plasmodesmata during biotrophic invasion by the blast fungus. The Plant Cell 19, 706-724.

Kato, H., and Yamaguchi, T. (1982). The perfect state of *Pyricularia oryzae* Cav. from rice plants in culture. Ann. Phytopathol. Soc. Jpn 42, 507-510.

Katou, S., Kuroda, K., Seo, S., Yanagawa, Y., Tsuge, T., Yamazaki, M., Miyao, A., Hirochika, H., and Ohashi, Y. (2007). A calmodulin-binding mitogen-activated protein kinase phosphatase is induced by wounding and regulates the activities of stress-related mitogen-activated protein kinases in rice. Plant Cell Physiol. 46, 332-344.

Kawasaki, S. (2004). Proceedings of the 3rd International Rice Blast Conference:
Rice Blast: Interaction with rice and control. (Dordrecht, The Netherlands: Kluwer Academic Publishers).

Kemen, E., Kemen, A.C., Rafiqi, M., Hempel, U., Mendgen, K., Hahn, M., and Voegele, R.T. (2005). Identification of a protein from rust fungi transferred from haustoria into infected plant cells. Molecular Plant Microbe Interactions 18, 1130-1139.

Khang, C.H., Park, S.-Y., Lee, Y.-H., and Kang, S. (2005). A dual selection based, targeted gene replacement tool for *Magnaporthe grisea* and *Fusarium oxysporum*. Fungal Genetics and Biology 42, 483-492.

Kikuchi, S., Satoh, K., Nagata, T., Kawagashira, N., Doi, K., Kishimoto, N., Yazaki, J., Ishikawa, M., Yamada, H., Ooka, H., Hotta, I., Kojima, K., Namiki, T., Ohneda, E., Yahagi, W., Suzuki, K., Li, C.J., Ohtsuki, K., Shishiki, T., Otomo, Y., Murakami, K., Iida, Y., Sugano, S., Fujimura, T., Suzuki, Y., Tsunoda, Y., Kurosaki, T., Kodama, T., Masuda, H., Kobayashi, M., Xie, Q., Lu, M., Narikawa, R., Sugiyama, A., Mizuno, K., Yokomizo, S., Niikura, J., Ikeda, R., Ishibiki, J., Kawamata, M., Yoshimura, A., Miura, J., Kusumegi, T., Oka, M., Ryu, R., Ueda, M., Matsubara, K., Kawai, J., Carninci, P., Adachi, J., Aizawa, K., Arakawa, T., Fukuda, S., Hara, A., Hashidume, W., Hayatsu, N., Imotani, K., Ishii, Y., Itoh, M., Kagawa, I., Kondo, S., Konno, H., Miyazaki, A., Osato, N., Ota, Y., Saito, R., Sasaki, D., Sato, K., Shibata, K., Shinagawa, A., Shiraki, T., Yoshino, M., and Hayashizaki, Y. (2003). Collection, Mapping, and Annotation of Over 28,000 cDNA Clones from japonica Rice. Science 301, 376-379.

Kim, K.-C., Fan, B., and Chen, Z. (2006). Pathogen-Induced Arabidopsis WRKY7 Is a Transcriptional Repressor and Enhances Plant Susceptibility to *Pseudomonas syringae*. Plant Physiology 142, 1180-1192.

Kim, S., Il-Pyung, A., and Lee, Y.-H. (2001). Analysis of Genes Expressed During Rice-*Magnaporthe grisea* Interactions. Molecular Plant-Microbe Interactions 14, 1340-1346.

Kovtun, Y., Chiu, W.L., Tena, G., and Sheen, J. (2000). Functional analysis of oxidative stress-activated protein kinase cascade in plants. Proceedings of the National Academy of Scineces U.S.A. 97, 2940-2945.

Lee, J.-Y., Yoo, B.-C., Rojas, M.R., Gomez-Ospina, N., Staehelin, L.A., and Lucas, W.J. (2003). Selective Trafficking of Non-Cell-Autonomous Proteins Mediated by NtNCAPP1. Science 299, 392-396.

Lee, M.-W., Qi, M., and Yang, Y. (2001). A novel jasmonic acid-inducible rice myb gene associates with fungal infection and host cell death. Molecular Plant-Microbe Interactions 14, 527-535.

Lee, Y.H., and Dean, R.A. (1993). cAMP Regulates Infection Structure Formation in the Plant Pathogenic Fungus Magnaporthe grisea. The Plant Cell 5, 693-700.

Leung, H., Borromeo, E.S., Bernardo, M.A., and Notteghem, J.L. (1988). Genetic analysis of virulence in the rice blast fungus *Magnaporthe grisea*. Phytopathology 78, 1227-1233.

Levy, A., Erlanger, M., Rosenthal, M., and Epel, B.L. (2007). A plasmodesmata-associated beta-1,3-glucanase in Arabidopsis. The Plant Journal 49, 669-682.

Li, L., Ding, S.-L., Sharon, A., Orbach, M., and Xu, J.-R. (2007). Mir1 is highly upregulated and localized to nuclei during infectious hyphal growth in the rice blast fungus. Molecular Plant-Microbe Interactions 20, 448-458.

Liu, G., Kennedy, R., Greenshields, D.L., Peng, G., Forseille, L., Selvaraj, G., and Wei, Y. (2007). Detached and Attached Arabidopsis Leaf Assays Reveal Distinctive Defense Responses Against Hemibiotrophic Colletotrichum spp. Molecular Plant-Microbe Interactions 20, 1308-1319.

Martin, G.B., Bogdanove, A.J., and Sessa, G. (2003). Understanding the functions of plant disease resistance proteins. Annual Review of Plant Biology 54, 23-61.

Matsumura, H., Reich, S., Ito, A., Saitoh, H., Kamoun, S., Winter, P., Kahl, G., Reuter, M., Kruger, D.H., and Terauchi, R. (2003). Gene expression analysis of plant host-pathogen interactions by SuperSAGE. PNAS 100, 15718-15723.

Mendgen, K., and Hahn, M. (2002). Plant infection and the establishment of fungal biotrophy. Trends in Plant Science.

Mitchell, T.K., and Dean, R.A. (1995). The cAMP-Dependent Protein Kinase Catalytic Subunit Is Required for Appressorium Formation and Pathogenesis by the Rice Blast Pathogen Magnaporthe grisea. The Plant Cell 7, 1869-1878.

Moons, A. (2003). Ospdr9, which encodes a PDR-type ABC transporter, is induced by heavy metals, hypoxic stress and redox perturbations in rice roots. FEBS Letters 553, 370-376.

Nakagami, H., Pitzschke, A., and Hirt, H. (2005). Emerging MAP kinase pathways in plant stress signalling. Trends in Plant Science 10, 339-346.

Nishimura, M., Park, G., and Xu, J.-R. (2003). The G-beta subunit *MGB1* is involved in regulating multiple steps of infection-related morphogenesis in *Magnaporthe grisea*. Molecular Microbiology 50, 231-243.

Notteghem, J., and Silue, D. (1992). Distribution of mating type alleles in *Magnaporthe grisea* populations pathogenic on rice. Phytopathology 82, 421-424.

O'Connell, R.J., and Panstruga, R. (2006). Tête à tête inside a plant cell: establishing compatibility between plants and biotrophic fungi and oomycetes. New Phytologist 171, 699-718.

Orbach, M.J., Farrall, L., Sweigard, J.A., Chumley, F.G., and Valent, B. (2000). The fungal avirulence gene *AVR-Pita* determines efficacy for the rice blast resistance gene *Pi-ta*. Plant Cell 12, 2019-2032.

Paper, J.P., Scott-Craig, J.S., Adhikari, N.D., Cuomo, C.A., and Walton, J.A. (2007). Comparative proteomics of extracellular proteins in vitro and in planta from the pathogenic fungus *Fusarium graminearum*. Proteomics 7, 3171-3183.

Park, G., Xue, C., Zheng, L., Lam, S., and Xu, J.-R. (2002). MST12 Regulates Infectious Growth But Not Appressorium Formation in the Rice Blast Fungus *Magnaporthe grisea*. Molecular Plant-Microbe Interactions 15, 183-192.

Park, G., Xue, C., Zhao, X., Kim, Y., Orbach, M., and Xu, J-R. (2006). Multiple Upstream Signals Convergence on the Adaptor Protein Mst50 in Magnaporthe grisea. The Plant Cell 18, 2822-2835.

Pedley, K.F., and Martin, G.B. (2004). Identification of MAPKs and Their Possible MAPK Kinase Activators Involved in the Pto-mediated Defense Response of Tomato. Journal of Biological Chemistry 279, 49229-49235.

Peyyala, R., and Farman, M.L. (2006). Magnaporthe oryzae isolates causing gray leaf spot of perennial ryegrass possess a functional copy of the AVR1-CO39 avirulence gene. Molecular Plant Pathology 7, 157-165.

Project, T.I.R.G.S. {Sequencing, 2005 #296} (2005). The map-based sequence of the rice genome. Nature 436, 793-800.

Rauyaree, P., Choi, W., Fang, E., Blackmon, B., and Dean, R. (2001). Genes expressed during early stages of rice infection with the rice blast fungus Magnaporthe grisea. Molecular Plant Pathology 2, 347-354.

Reyna, N.S., and Yang, Y. (2006). Molecular analysis of the rice MAP kinase gene family in relation to *Magnaporthe grisea* infection. Molecular Plant-Microbe Interactions 19, 530-540.

Sasabe, M., Toyoda, K., Shiraishi, T., Inagaki, Y., and Ichinose, Y. (2002). cDNA cloning and characterization of tobacco ABC transporter: NtPDR1 is a novel elicitor-responsive gene. FEBS Letters 518, 164-168.

Shou, H., Bordallo, P., and Wang, K. (2004). Expression of the Nicotiana protein kinase NPK1 enhanced drought tolerance in transgenic maize. Journal of Experimental Botany 55, 1013-1019.

Snoeijers, S.S., Perez-Garcia, A., Goosen, T., De Wit, P.J. G.M. (2003). Promoter analysis of the avirulence gene *Avr9* of the fungal tomato pathogen *Cladosporium fulvum* in the model filamentous fungus *Aspergillus nidulans*. Current Genetics 43, 96-102.

Soanes, D.M., and Talbot, N.J. (2005). A bioinformatic tool for analysis of EST transcript abundance during infection-related development by *Magnporthe grisea*. Molecular Plant Pathology 6, 503-512.

Soanes, D.M., Kershaw, M.J., Cooley, R.N., and Talbot, N.J. (2002). Regulation of the *MPG1* hydrophobin gene in the rice blast fungus *Magnaporthe grisea*. Molecular Plant Microbe Interactions 15, 1253-1267.

Soderlund, C., Haller, K., Pampanwar, V., Ebbole, D., Farman, M., Orbach, M., Wang, G.-L., Wing, R., Xu, J.-R., Brown, D., Mitchell, T., and Dean, R. (2006). MGOS: A Resource for Studying *Magnaporthe grisea* and *Oryza sativa* Interactions. Molecular Plant-Microbe Interactions 19, 1055-1061.

Song, F., and Goodman, R.M. (2001). Molecular biology of disease resistance in rice. Physiological and Molecular Plant Pathology 59, 1-11.

Sun, C.B., Suresh, A., Deng, Y.Z., and Naqvi, N.I. (2006). A Multidrug Resistance Transporter in Magnaporthe Is Required for Host Penetration and for Survival during Oxidative Stress. The Plant Cell 18, 3686-3705.

Sweigard, J.A., Carroll, A.M., Kang, S., Farrall, L., Chumley, F.G., and Valent, B. (1995). Identification, cloning, and characterization of *PWL2*, a gene for host species specificity in the rice blast fungus. The Plant Cell 7, 1221-1233.

Takano, Y., Choi, W., Mitchell, T.K., Okuno, T., and Dean, R.A. (2003). Large scale parallel analysis of gene expression during infection-related morphogenesis of *Magnaporthe grisea*. Molecular Plant Pathology 4, 337-346.

Talbot, N.J. (2003). On the trail of a cereal killer: exploring the biology of *Magnaporthe grisea*. Annual Review of Microbiology 57, 177-202.

Talbot, N.J., Ebbole, D.J., and Hamer, J.E. (1993). Identification and Characterization of *MPG1*, a Gene Involved in Pathogenicity from the Rice Blast Fungus *Magnaporthe grisea*. The Plant Cell 5, 1575-1590.

Talbot, N.J., Kershaw, M.J., Wakley, G.E., de Vries, O.M.H., Wessels, J.G.H., and Hamer, J.E. (1996). MPG1 Encodes a Fungal Hydrophobin Involved in Surface Interactions during Infection-Related Development of Magnaporthe grisea. The Plant Cell 8, 985-999.

Tang, W., Coughlan, S., Crane, E., Beatty, M., and Duvick, J. (2006). The application of laser capture microdissection to In Planta gene expression profiling of the maize anthracnose stalk rot fungus *Colletotrichum graminicola*. Molecular Plant-Microbe Interactions 19, 1240-1250.

Tao, Y., Xie, Z., Chen, W., Glazebrook, J., Chang, H.-S., Han, B., Zhu, T., Zou, G., and Katagiri, F. (2003). Quantitative Nature of Arabidopsis Responses during Compatible and Incompatible Interactions with the Bacterial Pathogen Pseudomonas syringae. The Plant Cell 15, 317-330.

Thomma, B., Bolton, M., Clergeot, P.H., and De Wit, P. (2006). Nitrogen controls in planta expression of *Cladosporium fulvum Avr9* but not other effector genes. Molecular Plant Pathology 7, 125-130.

Urban, M., Bhargava, T., and Hamer, J.E. (1999). An ATP - driven drug efflux pump is a novel pathogenicity factor in rice blast disease. EMBO Journal 18, 512-521.

Valent, B., Farrall, L., and Chumley, F.G. (1991). *Magnaporthe grisea* genes for pathogenicity and virulence identified through a series of backcrosses. Genetics 127, 87-101.

Van Damme, M., Andel, A., Huibers, R.P., Panstruga, R., Weisbeek, P.J., and Van den Ackerveken, G. (2005). Identification of *Arabidopsis* Loci Required for Susceptibility to the Downy Mildew Pathogen *Hyaloperonospora parasitica*. Molecular Plant-Microbe Interactions 18, 583-592.

Van den Ackerveken, G., Dunn, R., Cozijnsen, T., Vossen, P., Van den Broek, ., De Wit, P. (1994). Nitrogen limitation induces expression of the avirulence gene *Avr9* in the tomato pathogen *Cladosporium fulvum*. Molecular Gen Genetics 243, 277-285.

van der Does, H.C., and Rep, M. . (2007). Virulence Genes and the Evolution of Host Specificity in Plant-Pathogenic Fungi. Molecular Plant-Microbe Interactions 20, 1175-1182.

van Kan, J.A.L. (2006). Licensed to kill: the lifestyle of a necrotrophic plant pathogen. Trends in Plant Science 11, 247-253.

van Loon, L.C., Rep, M., and Pieterse, C.M.J. (2006). Significance of inducible defense-related proteins in infected plants. Annual Review of Phytopathology 44, 135-162.

Vergne, E., Ballini, E., Marques, S., Sidi Mammar, B., Droc, G., Gaillard, S., Bourot, S., DeRose, R., Tharreau, D., Notteghem, J.-L., and Morel, J.-B. (2007). Early and specific gene expression triggered by rice resistance gene *Pi33* in response to infection by *ACE1* avirulent blast fungus. New Phytologist 174, 159-171.

Vogel, J.P., Raab, T.K., Schiff, C., and Somerville, S. . (2002). PMR6, a Pectate Lyase-Like Gene Required for Powdery Mildew Susceptibility in Arabidopsis. The Plant Cell 14, 2095-2106.

Whisson, S.C., Boevink, P.C., Moleleki, L., Avrova, A., Morales, J.G., Gilroy, E.M., Armstrong, M.R., Grouffaud, S., van West, P., Chapman, S., Hein, I., Toth, I.K., Pritchard, L., and Birch, P. (2007). A translocation signal for delivery of oomycete effector proteins into host plant cells. Nature doi:10.1038, 1-4.

Wu, S.-C., Halley, J.E., Luttig, C., Fernekes, L.M., Gutiérrez-Sanchez, G., Darvill, A.G., and Albersheim, P. (2006). Identification of an *endo*-beta-1,4-D-xylanase from *Magnaporthe grisea* by gene knockout analysis, purification and heterologous expression. Applied and Environmental Microbiology 72, 986-993.

Xiong, L., and Yang, Y. (2003). Disease Resistance and Abiotic Stress Tolerance in Rice Are Inversely Modulated by an Abscisic Acid-Inducible Mitogen-Activated Protein Kinase. The Plant Cell 15, 745-759.

Xu, J.-R. (2000). MAP kinases in fungal pathogens. Fungal Genetics and Biology 31, 137-152.

Xu, J.-R., Urban, M., Sweigard, J.A., and Hamer, J.E. (1997). The CPKA Gene of Magnaporthe grisea Is Essential for Appressorial Penetration. Molecular Plant-Microbe Interactions 10, 187-194.

Xu, J.R., and Hamer, J.E. (1996). MAP kinase and cAMP signaling regulate infection structure formation and pathogenic growth in the rice blast fungus Magnaporthe grisea. Genes Dev. 10, 2696-2706.

Yang, B., Sugio, A., and White, F.F. (2006). Os8N3 is a host disease-susceptibility gene for bacterial blight of rice. Proceedings of the National Academy of Sciences U.S.A. 103, 10503-10508.

Zhao, X., Kim, Y., Park, G., and Xu, J.-R. (2005). A Mitogen-Activated Protein Kinase Cascade Regulating Infection-Related Morphogenesis in *Magnaporthe grisea*. The Plant Cell 17, 1317-1329.